PALAEOMAGNETIC ROTATIONS IN THE ABITIBI BELT

PALAEOMAGNETIC EVIDENCE FOR ANTI-CLOCKWISE ROTATION OF ROUYN-NORANDA STRUCTURAL BLOCK, QUEBEC, CANADA

By

MOHAMMAD TARIQ AMIN, M.Sc.,

A Thesis

Submitted to the School of Graduate Studies

in Partial Fulfillment of the Requirements

for the Degree

Master of Science

McMaster University

MASTER OF SCIENCE (1990) MCMASTER UNIVERSITY

(Geology) Hamilton, Ontario

TITLE: PALAEOMAGNETIC EVIDENCE FOR ANTI-CLOCKWISE ROTATION OF ROUYN-NORANDA STRUCTURAL BLOCK, QUEBEC, CANADA

AUTHOR: Mohammad Tariq Amin

M.Sc.,

SUPERVISOR: Professor Christopher J. Hale

NUMBER OF PAGES: viii, 136

Abstract

The Rouyn-Noranda area in the center of the Abitibi subprovince is composed of comparatively unmetamorphosed Archean volcanics of Blake River Group (BRG). Rouyn-Nornada is one of the lozenge shaped structural blocks in the area bounded by the Porcupine Destor Fault (PDF) zone and the Larder Lake Caddilac Fault (LCF) zone. 160 samples were collected from 23 different sites selected to lie in the center of the block, at or near the PDF zone and accross the PDF zone in the neighboring lozenge.

Stable magnetizations have been obtained from the central relatively unstrained parts of the lozenges. These magnetizations show some improvement in precision statistics after structural corrections implying that they are pre-folding and probably Archean in age. Sites along the PDF zone show scattered magnetizations, which do not agree at sample or site level.

The Zone I (Sites in the center of the Rouyn-Noranda block) structurally corrected mean direction (D=154.0, I=-35.0, k=13.0, α_{95}=19.0, N=6 sites) differ from the Zone III (Sites from the center of the adjacent block) mean direction (D=214.0, I=-43.0, k=16.0, α_{95}=32.0) by $60\pm37°$ implying that the Rouyn-Norand block have rotated anti-clockwise by $60\pm37°$ about a vertical axis relative to the adjacent structural block.

Acknowledgements

I thank Dr. C. J. Hale for helping and guiding me very patiently throughout the course for two years. Dr. P. M. Clifford who visited the field area with us and provided the structural notes.

I would also like to thank Peter Lloyd and Lisa Kellman, who helped with the laboratory preparation of samples.

This project was supported by Lithoprobe Grant to Dr. C. J. Hale.

Contents

Acknowledgements i

1 GENERAL INTRODUCTION 1

1.1 Object and Scope of the Project 1

1.2 Location of the Area 2

1.3 Introduction 2

1.4 Purpose of the Project 7

1.5 Previous Paleomagnetic Work in the Area 7

2 GEOLOGY OF THE AREA 10

2.1 Regional Geology of Abitibi Subprovince 10

2.2 Geology of Rouyn-Noranda Region 14

2.3 Regional Structure of the Abitibi Subprovince 15

2.4 Structure of the Rouyn-Noranda Region 15

3 METHODOLOGY 16

3.1 Sampling 16

3.2 Laboratory Work 17

3.3 Measurement of NRM 18
3.4 Demagnetization of Specimens 19
3.4.1 Alternating Field demagnetization 21
3.4.2 Thermal demagnetization 21
3.5 Presentation and Analysis of Data 22
3.6 Statistical Methods 26

4 PALAEOMAGNETIC RESULTS 28
4.1 NRM Intensities of Specimens 28
4.2 Stability of Specimens 34
4.3 Demagnetization Behavior of Specimens 44
4.4 NRM Directions 60
4.5 Demagnetization Results 65
4.5.1 Zone I 65
4.5.2 Zone II 74
4.5.3 Zone III 83
4.5.4 Zone IV 92
4.6 Characteristic Directions 101
4.7 Averaging of Directions 104
4.8 Structural Correction of Stable Directions 111
4.9 Palaeomagnetic Rotation 115

5 DISCUSSION AND CONCLUSIONS 119
5.1 General Discussion 119
5.2 Conclusions 125

5.3 Suggestions For Further Work 125

List of Tables

4.1 Summary of site average directions. 106

4.2 Summary of palaeomagnetic results. 111

4.3 Summary of structurally corrected palaeomagnetic results. 115

List of Figures

1.1 Geological map of the area. 3

2.2 Lithological subdivision of Abitibi Belt proposed by Ludden et al., 1986. 12

3.3 Orthogonal diagrams. 24

4.4 NRM intensity histograms for different zones. 29

4.5 NRM intensity histograms for different lithologies. 31

4.6 MDF histograms for different zones. 35

4.7 MDF histograms for different lithologies. 37

4.8 MDT histograms for different zones. 39

4.9 MDT histograms for different lithologies. 42

4.10 Zone I AF demagnetization curves. 45

4.11 Zone I thermal demagnetization curves. 47

4.12 Zone II AF demagnetization curves. 49

4.13 Zone II thermal demagnetization curves. 52

4.14 Zone III AF demagnetization curves. 54

4.15 Zone III thermal demagnetization curves. 56

4.16 Zone IV AF demagnetization curves. 58
4.17 Zone IV thermal demagnetization curves. 61
4.18 Stereographic plot of NRM directions. 63
4.19 Stereographic plots of magnetic directions during stepwise AF demagnetization of Zone I specimens. 66
4.20 Progressive orthogonal AF demagnetization plots of Zone I specimens. 68
4.21 Stereographic plots of magnetic directions during thermal demagnetization of Zone I specimens. 70
4.22 Progressive orthogonal thermal demagnetization plots of Zone I specimens. 72
4.23 Stereographic plots of magnetic directions during AF demagnetization of Zone II specimens. 75
4.24 Progressive orthogonal AF demagnetization plots of Zone II specimens. 77
4.25 Stereographic plots of magnetic directions during thermal demagnetization of Zone II specimens. 79
4.26 Progressive orthogonal thermal demagnetization plots of Zone II specimens. 81
4.27 Stereographic plots of magnetic directions during AF demagnetization of Zone III specimens. 84
4.28 Progressive orthogonal AF demagnetization plots of Zone III specimens. 86
4.29 Stereographic plots of magnetic directions during thermal demagnetization of Zone III specimens. 88
4.30 Progressive orthogonal thermal demagnetization plots of Zone III specimens. 90

4.31 Stereographic plots of magnetic directions during AF demagnetization of Zone IV specimens. 93
4.32 Progressive orthogonal AF demagnetization plots of Zone IV specimens. 95
4.33 Stereographic plots of magnetic directions during thermal demagnetization of Zone IV specimens. 97
4.34 Progressive orthogonal thermal demagnetization plots of Zone IV specimens. 99
4.35 Stereographic plot of stable directions. 102
4.36 Stereographic plot of site average directions. 107
4.37 Stereographic plot of zonal average directions. 109
4.38 Stereographic plot of structurally corrected zonal average directions. 113
4.39 Map showing the declinations of palaeomagnetic directions at various sites. 116

5.40 Wrench Fault Tectonics model for Abitibi (proposed by Hubert et al., 1984). 122

Chapter 1

GENERAL INTRODUCTION

1.1 Object and Scope of the Project

This report represents partial fulfillment of the requirements for the degree of M.Sc. Geology at the McMaster University, Hamilton, Ontario, Canada. Field work for this project was carried out from August 7, 1988 to August 12, 1988 in the Rouyn-Noranda area.

The main objective was to test the "Collage Hypothesis" in the Abitibi subprovince. The following procedures were adopted:

1. Paleomagnetic sampling.
2. Paleomagnetic measurements.
3. Identification of magnetic remanence in the rocks.
4. Identification of magnetic remanence carrier minerals.
5. Identification of difference in magnetic direction from different parts of the area.
6. Identification of block rotations and the role of major faults in the area.

1.2 Location of the Area

The project area shown in figure 1.1 comprise a small portion between 78°.00' - 79°.30' longitude and 48°.15'- 49°.30' latitude in the southern part of the Abitibi Greenstone Belt around Rouyn-Noranda. It is adjacent to the Quebec-Ontario boundary in the Western Quebec.

The sampled areas are covered by Ministry of Energy and Resources, Government of Quebec Geo-information maps number 32D/6- 0302, 32D/6-0204, 32D/7-0401, 32D/8-0402, 32D/8-0204, 32D/8-0401 and 32DE/6-0402. Area is accessible easily by roads. Most of the outcrops were exposed along road cuts. Only two sites were hidden in the bushes where we had to walk into them to get the samples.

1.3 Introduction

The Southern Volcanic Zone (Ludden et al., 1986) in the Abitibi subprovince is a region dominated by a series of east-west trending faults (Ludden et al, 1986), namely the Porcupine Destor Fault (PDF), the Larder Lake Cadillac Fault (LCF) and the Chicobi Lake Fault (CLF). These fault zones divide the region into several lozenge shaped blocks. Hubert et al (1984), Gelinas et al (1984) and Babineau (1983) carried out structural studies in the block between Rouyn-Noranda region and Val d'Or. Hubert et al, (1984) have recognized polyphase deformation in the area related to the E-W trending faults.

The Rouyn-Noranda area is one lozenge shaped block bounded by the Larder Lake fault (LCF) zone in the south and Porcupine Destor Fault (PDF) zone in the north. LCF and PDF are considered as strike slip faults (Hubert et al, 1984)

Figure 1.1: Geological map of the area (proposed by Ludden et al., 1986). The transparency shows the location of sampling sites.

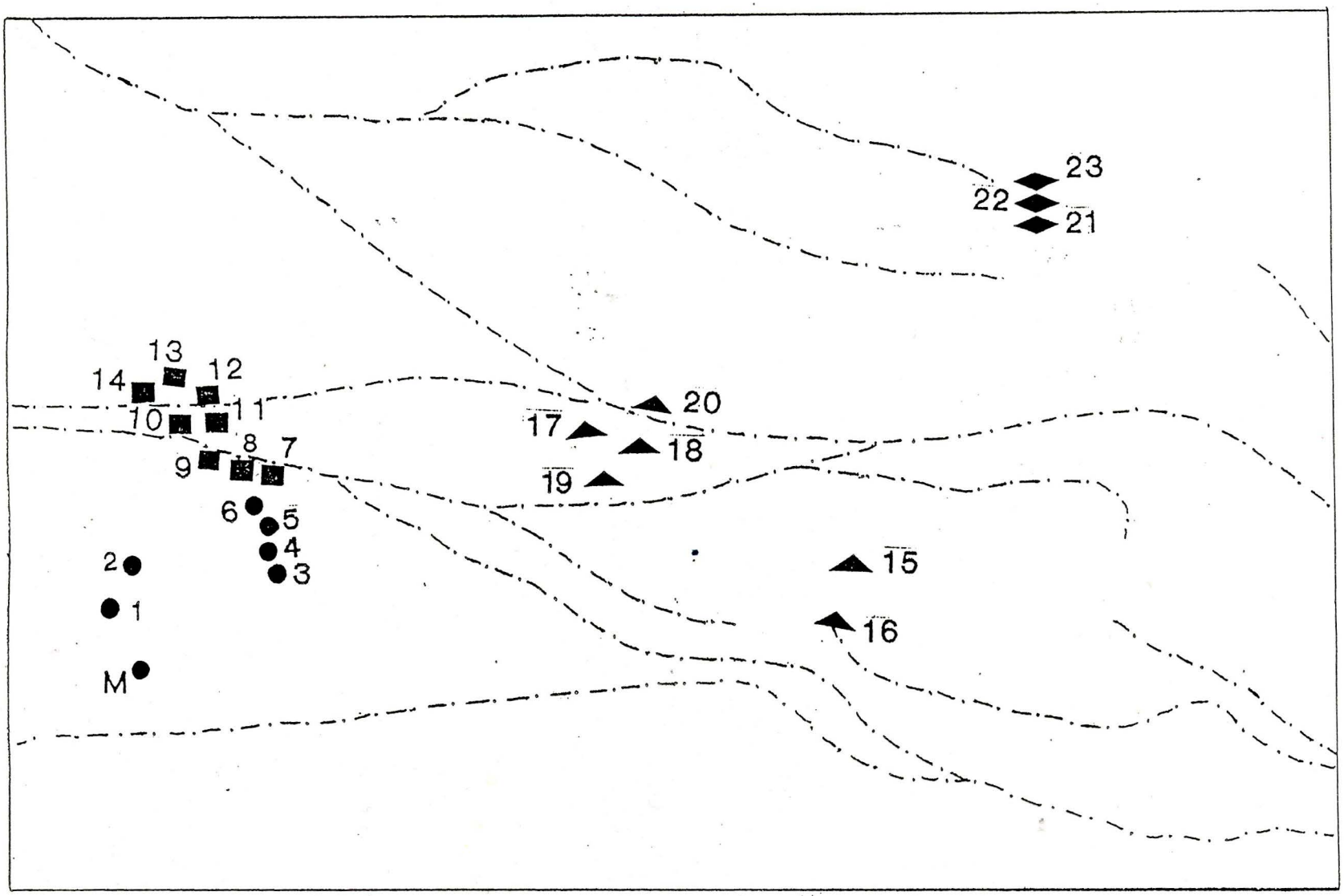
23
22
21
13
14
12
10
11
8
7
9
6
5
4
3
2
1
M
20
17
18
19
15
16

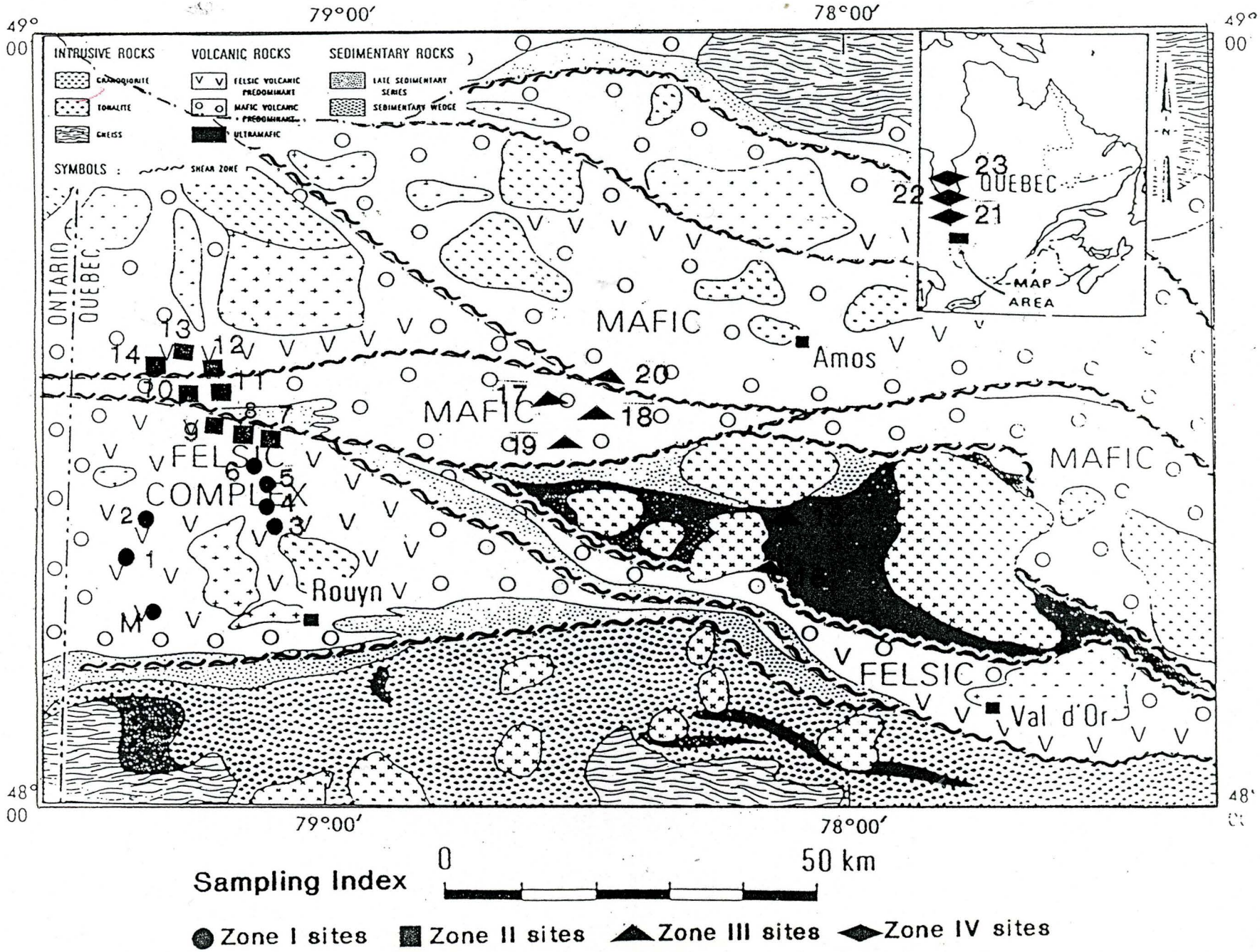
49° 00
79°00′
78°00′
INTRUSIVE ROCKS
GRANODIORITE
TONALITE
GNEISS
VOLCANIC ROCKS
FELSIC VOLCANIC PREDOMINANT
MAFIC VOLCANIC PREDOMINANT
ULTRAMAFIC
SEDIMENTARY ROCKS
LATE SEDIMENTARY SERIES
SEDIMENTARY WEDGE
SYMBOLS :
SHEAR ZONE
ONTARIO
QUEBEC
MAP AREA
23
22
21
MAFIC
Amos
FELSIC COMPLEX
MAFIC
Rouyn
FELSIC
Val d'Or
48° 00
0
50 km
Sampling Index
Zone I sites
Zone II sites
Zone III sites
Zone IV sites

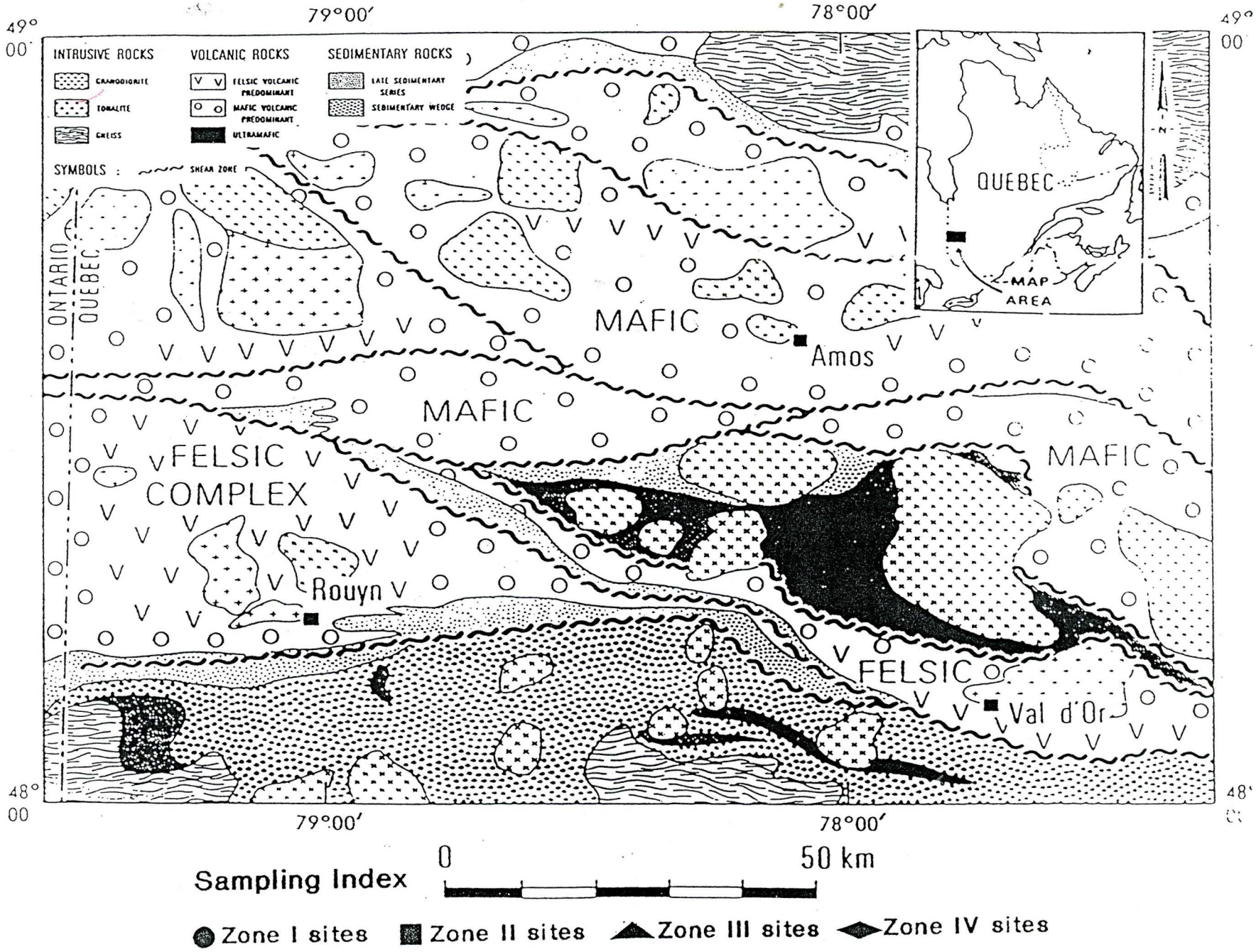
79°00′
78°00′
49° 00′
48° 00′
INTRUSIVE ROCKS
GRANODIORITE
TONALITE
GNEISS
VOLCANIC ROCKS
FELSIC VOLCANIC PREDOMINANT
MAFIC VOLCANIC PREDOMINANT
ULTRAMAFIC
SEDIMENTARY ROCKS
LATE SEDIMENTARY SERIES
SEDIMENTARY WEDGE
SYMBOLS :
SHEAR ZONE
ONTARIO
QUEBEC
QUEBEC
MAP AREA
MAFIC
Amos
MAFIC
FELSIC
COMPLEX
MAFIC
Rouyn
FELSIC
Val d'Or
0
50 km
Sampling Index
Zone I sites
Zone II sites
Zone III sites
Zone IV sites

continuing far beyond the Rouyn- Noranda area. Hubert et al (1984), after the detailed analysis of the structures of the Rouyn-Noranda area, suggested a mode of deformation in the area that resulted from oblique convergence and shortening along the strike slip faults as seen in the wrench fault tectonic regimes explained by Harland, (1971), Wilcox et al, (1973) and Beck (1976). They interpreted this area to be a mobile zone where terrains of very different properties converge obliquely, thus causing the block rotations about vertical axis. The amount and sense of displacement along strike slip faults and rotation of rigid blocks are different, but contemporaneous, consequences of a single deformation process and are related to each other (Ron et al, 1984). Therfore, the rotation of rigid blocks in the shear zones are detectable by structural and paleomagnetic methods.

Structural studies were undertaken in the field by Clifford, P. M. to mark the shear zones and to identify the sense of movement along the fault zones. The summary of his notes shows that there are no observable or measurable large faults with purely horizontal motion. Shear zones are not common in the outcrops. Mainly they strike E-W; dips are steep to vertical. Two are left-handed, one at a low plunge; one is right-handed; two are dip slip. He inferred that there is no obvious interpretation of the fault data in terms of a single stress field. There has been considerable discussion about the nature of the structures which accommodate the rotations about vertical axes and various models have been proposed by Beck (1976), Ron et al (1984) and McKenzie and Jackson (1983, 1986). It seems that the structures on block boundaries are likely to be complicated and hard to interpret and paleomagnetic observations remain the main method of mapping such rotations where structural information is constrained geologically (McKenzie and Jackson, 1989).

Paleomagnetism is being increasingly used to analyze the behavior of the continental crust in wide zones of deformation (Lamb, 1988). The declination and inclination of primary magnetizations obtained after thermal or alternating field demagnetization of samples from the different structural blocks can be used to determine a rotation of these blocks about vertical or horizontal axes. Recent work on the measurements of paleomagnetic declinations has shown that large rotations about vertical axes are common in regions of distributed continental deformation e.g., Iran (Freund, 1970), Western North America (Beck, 1976, Kamerling and Luyendyk, 1979, Luyendyk et al, 1980), Israel (Ron et al, 1984), and New Zealand (Lamb, 1988). For Paleomagnetic studies rotation is defined as;

$$R = D_o - D_x$$

where

D_o is the observed declination

D_x is the expected declination calculated from the APWP of the continent to which the rock is associated.

A term Block Rotation is applied when insitu or nearly insitu rotation of a crustal fragment about a nearly vertical axis occurs. Such rotations are expected in extensional and compressional regions (Harland, 1971), where rigid blocks are bounded by faults. Block rotation, also known as Tectonic Rotation, is that of a crustal block in which the internal deformation is negligible.

1.4 Purpose of the Project

The present study was carried out to test the "allochthonous collage" hypothesis of the evolution of Abitibi subprovince proposed by Hubert et al, (1984). Samples were collected from the central portion of the Rouyn-Noranda block which is relatively undeformed (Ludden et al., 1986) and preserves the classical primary volcanological features. Additionally samples were taken from the most deformed shear zones near PDF and outside the Rouyn-Noranda block from the easterly adjacent blocks. The Blake River Group was sampled from both of these adjacent blocks to compare the declinations of paleomagnetic remanence. Any diffrence in declinations was expected to show the post Blake River Group emplacement rotations in the area. Some sites were sampled from an area approximately 100 Km North of the Rouyn-Noranda across the Chicobi Lake Fault to see if there exists a difference in paleomagnetic declinations of the specimens from these different regions.

1.5 Previous Paleomagnetic Work in the Area

There are many previous contributions to the Paleomagnetic studies of the Archean rocks. Most of the previous work in the area emphasized the identification of paleomagnetic remanence, the positions of the paleopoles, the establishment of APWP and the paleomagnetic dating of the thermal events. The principal previous contributions on the paleomagnetism of the Archean rocks from the Rouyn-Noranda area and the adjacent regions are as follows:

1. Pesonen, L. J., (1973) in M.Sc. Thesis at the University Of Toronto reported a southwesterly direction from the Matachewan diabase dikes (D=205.6°, I=-7.4°,

k=42, α_{95} = 10.5°, N=6 number of samples).

2. Pullaiah and Irving, (1975) reported a direction (D=330°, I=71°, k=139, α_{95} =3°) from the Otto Stock situated in the Structural Province near Kirkland Lake, Ontario. It is now dated 2.6 Ga. They also reported a southerly magnetic direction (D=205°, I=-30°, k=68, α_{95} =15°).

3. Irving and Naldrett (1977) reported that the magnetization of the Archean country rock is reset by the intrusions of the diabase up to distances of 80 meters. They reported an Archean directions obtained from the Archean Gabbro (D=189°, I=-23°, α_{95}=17°, n=8 oriented cores), from Kamiskotia Gabbro (D=289°, I=23°, k=144, α_{95}=5°) and from Dundonald Sill (D=269°, I=32°, k=19, α_{95}=18°). They reported Abitibi dike direction (D=267°, I=63°, k=117, α_{95}=4°) and Matachewan dike direction (D=207°, I=-16°, k=54, α_{95}=7°). They also provided an APW curve for the late Archean based on the above mentioned magnetizations in the form of Track six.

4. Schutts and Dunlop, (1981) of the University of Toronto studying the mafic extrusive and intrusive rocks from the Abitibi subprovince obtained an Archean magnetic direction (D=114°, I=-32°, k=15, α_{95} =11°, n=13 site averages) and three other direction corresponding to the post archean overprinting episodes. A direction (D=21°, I=13°, k=44, α_{95} =6°, n=14 site averages) corresponding to the Metachewan diabase dike intrusion episode dated approximately 2600 MYBP, another direction (D=277°, I=70°, k=52, α_{95} =8°, n=8 site averages) corresponding to Abitibi Diabase Dike intrusion episode dated approximately 2100 MYBP, and a third direction (D=166°, I=56°, k=14, α_{95} =8°, n=28 site averages) corresponding to the 1900-1700 MYBP Hudsonian orogeny in the Churchill and Bear Provinces

and the Penokean orogeny in the Southern Province. They also mentioned that Archean characteristic direction was found in basalts far removed from intrusions and most of the post Abitibi directions were obtained in samples taken near the intrusive in the region 1700-1900 Myr ago, facilitated by hot fluid transport through faults and contact zones of weakness had occurred.

5. Geissman et al, (1982) obtained a characteristic remanence of the Ghost Range intrusive complex, Central Abitibi Belt (D=280°, I=2°, k=5.5 and α_{95} = 11.8°, VGP=13° E,7° S). They reported both high-coercivity, high blocking temperature remanence residing in magnetite and low coercivity, low blocking temperature remanence residing in pyrrhotite. Their data too did not agree on site, geographic location or rock types.

6. Tasillo-Hirt et al, (1982) of the Department of Geology, University of Toronto, Canada reported an Archean magnetization direction (D=190°, I=-29.2°, k=1.5 and α_{95} = 25.0°, n=21 specimens from 21 samples) from the Blake River Group dated $2703^{+}_{-}2$ Ma in the Kirkland area. Their data had poor consistency of directions linearly decaying to the origin in vector analysis on site, sample and subsample levels, but they described an important evidence supporting preservation of primary magnetization in some parts of the central Abitibi Belt by performing a conglomerate test on the cobbles derived from Blake River Volcanics. They also suggested 80° clockwise rotation and 80° tilt of Holtyre Fault Block.

and the Penokean orogeny in the Southern Province. They also mentioned that Archean characteristic direction was found in basalts far removed from intrusions and most of the post Abitibi directions were obtained in samples taken near the intrusive in the region 1700-1900 Myr ago, facilitated by hot fluid transport through faults and contact zones of weakness had occurred.

5. Geissman et al, (1982) obtained a characteristic remanence of the Ghost Range intrusive complex, Central Abitibi Belt (D=280°, I=2°, k=5.5 and α_{95} = 11.8°, VGP=13° E,7° S). They reported both high-coercivity, high blocking temperature remanence residing in magnetite and low coercivity, low blocking temperature remanence residing in pyrrhotite. Their data too did not agree on site, geographic location or rock types.

6. Tasillo-Hirt et al, (1982) of the Department of Geology, University of Toronto, Canada reported an Archean magnetization direction (D=190°, I=-29.2°, k=1.5 and α_{95} = 25.0°, n=21 specimens from 21 samples) from the Blake River Group dated 2703$\pm$2 Ma in the Kirkland area. Their data had poor consistency of directions linearly decaying to the origin in vector analysis on site, sample and subsample levels, but they described an important evidence supporting preservation of primary magnetization in some parts of the central Abitibi Belt by performing a conglomerate test on the cobbles derived from Blake River Volcanics. They also suggested 80° clockwise rotation and 80° tilt of Holtyre Fault Block.

Chapter 2

GEOLOGY OF THE AREA

2.1 Regional Geology of Abitibi Subprovince

The Archean Abitibi Greenstone Belt of the Superior Province, Canada is crudely a parallelogram-shaped structure (Goodwin and Ridler, 1970). It extends from the Grenville Front in the east and southeast through Noranda and Timmins to the Kapuskasing Structural Zone in the west. It is bounded in the north by the Opatica subprovince (Ludden et al. 1986) and in the south by the sedimentary sequence of the Bellecombe gneiss belt (Dimroth et al., 1982).

The Abitibi Belt, composed of volcanic, plutonic and sedimentary rocks is sandwiched between the Grenville Front and the Kapuskasing Structural Zone. These two are the younger tectonic structures in the area and seem to play an important role in the structural evolution of the Abitibi subprovince. These two structures has placed high metamorphic grade terrains and low metamorphic grade Archean supracrustal rocks side by side (Ludden et al., 1986) in the Abitibi belt.

The Grenville Front have placed Archean grey-gneisses of upper amphibolite grade side by side with Archean metavolcanic rocks in the Chibougamau region (Frith and Doig, 1975) and "reworked" Archean granulites side by side with the Pontiac metasediments and migmatites in the southeastern extremities of the Abitibi subprovince (Martignole, 1984; Frith and Doig, 1975). The Opatica granite-gneiss terrain is also Archean in age and associated with the structural evolution of Abitibi belt, but its exact structural relationships with the Abitibi belt are poorly understood (Ludden et al. 1986).

Ludden et al, (1986) subdivided the Abitibi belt from north to south into a northern volcanic zone (NVZ), a central granite-gneiss zone (CGZ), a southern volcanic zone (SVZ) and a southern granite-gneiss zone (SGZ) (Figure 2.2). The volcanic complexes in the Chibougamau, Chapais and Matagami areas make up the NVZ and the volcanics of the Val d'Or, Rouyn-Noranda, Porcupine and Timmins areas make up the SVZ. The central Granodiorite-gneiss terrain divides the NVZ and SVZ and the southern granite-gneiss zone comprises the Pontiac metasediments, monzonitic plutons and migmatites. The NVZ and SVZ are different in volcanism, plutonic rocks, structural evolution, sedimentary evolution and age relationships. The volcanoes of the NVZ were characterized by emergent activity and cored by tonalitic to granodioritic plutons (Pitcher, 1983) which were emplaced in a continental crust whereas the SVZ is characterized by the presence of komatiite-tholeiite plateaux of subaqueous volcanics (Gelinas et al. 1984 and Dimroth et al. 1982).

The volcanism in SVZ is centered on ring fractures and formed in rift basins located between major shear zones (Ludden et al., 1986). Ludden et al., (1986) interpreted that the volcanic and sedimentary rocks of the SVZ now represent a collage

Figure 2.2: Subdivision of Abitibi subprovince into 4 different lithological zones (proposed by Ludden et al., 1986).

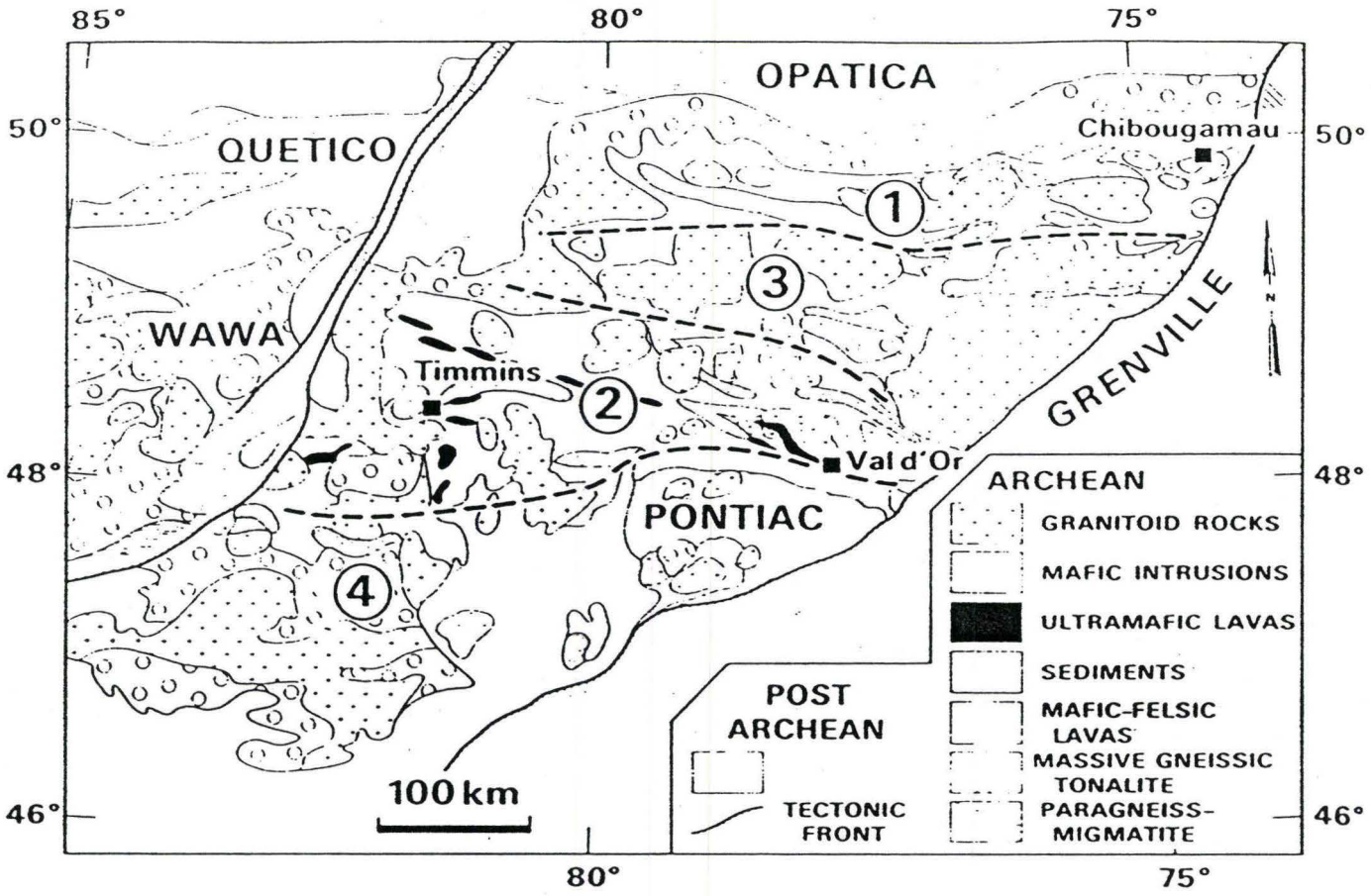

(1) NORTHERN VOLCANIC ZONE

(2) SOUTHERN VOLCANIC ZONE

(3) CENTRAL GRANITE-GNEISS ZONE

(4) SOUTHERN GRANITE-GNEISS ZONE

of blocks. These blocks have contrasting lithologies and metamorphic grades and have been subjected to different degrees of uplift and erosion. They also suggested that the blocks of volcanic terrain in the SVZ were allochthonous relative to the NVZ and were rotated, uplifted and eroded during the wrench faulting prevalent in the region.

2.2 Geology of Rouyn-Noranda Region

Rouyn-Noranda region lies in the SVZ defined by Ludden et al, (1986) and comprises Blake River Group (BRG) lithologies which are a complex assemblage of basalt, andesite, dacite, rhyolite flows and minor pyroclastic rocks (Jensen, 1975a, b). The ages of these units are constrained between 2710 $\pm$ 2 and 2703 $\pm$ 2 Ma. (Nunes and Jensen, 1980) by U-Pb zircon dating. Two major east-west trending fractures, the PDF and the LCF represent the northern and southern limits of the Blake River Group (BRG). The Kinojevis Group, comprising a series of volcanic units lies to the north of PDF and metasedimentary rocks of the Timiskaming Group lie to the south of LCF (Hubert et al. 1984). The region has undergone prehnite-pumpellyite to lowermost green schist facies of burial or regional metamorphism (Jolly, 1974; Jensen, 1978a, b, 1981). Rocks sampled for the present study are mostly massive basalt, lava flows, gabbro, dacite and diorite. Komatiites were sampled at one site.

2.3 Regional Structure of the Abitibi Subprovince

Porcupine Destor Fault and Larder Lake Fault which are the most significant structural features of the Abitibi subprovince represent zones of high ductility. The PDF described by Bannerman (1939, 1940), Ambrose (1941), Graham (1954), Boivin (1974) consists of a ductile fault zone 20-100 m wide that branches into several secondary faults. It follows a general east-west trend and dips steeply toward the south in the eastern part of the area. Minor strike slip faults are observed adjacent to the PDF zone (Boivin, 1974; Trudel, 1979). Most of them are right handed vertical faults, whereas, a few of them are left-handed.

The LCF described by Gunning (1937,1941), Wilson (1962) and Goulet (1978) also consists of a ductile fault zone of width varying between 20 and 250 m.

2.4 Structure of the Rouyn-Noranda Region

According to Hubert et al., 1984 the folded structures in the Rouyn-Noranda region and the planar and linear elements associated with them are divided into three generations of deformation. In addition to the PDF and LCF there are other faults in the area which remain inside the Rouyn-Noranda block. These faults correspond to a system of normal and reverse faults compatible with the geometry of a system of wrench fault tectonics (Harland, 1971; Wilcox et al., 1973). Hubert, Gelinas and Trudel, (1984) have defined structural patterns in the Rouyn-Noranda region which are interpreted to result from left lateral wrench fault movements between the LCF and the PDF.

Chapter 3

METHODOLOGY

3.1 Sampling

Sampling was an important factor in order to study the block rotations in the Rouyn-Noranda area. Sites were to be situated in different parts of the area so that the magnetic directions obtained could be compared and their systematic differences, if any, could be determined. The area was divided into four structurally different zones (figure 2.2) for the sampling purposes: Seven sites were sampled from Zone I i.e., the area in center of the Rouyn-Noranda block, seven from Zone II i.e., the area along PDF, five from Zone III i.e.,the area adjacent to the PDF outside the Rouyn-Noranda block and four sites from Zone IV i.e., the area near Casa Berardi approximately 80 Km away from the Rouyn-Noranda block across the Porcupine Destor Fault and the Chicobi Lake Fault. 5 to 8 oriented samples were collected from each site. These were block samples approximately 1000 cm^3 in volume. The outcrop in the area was scarce so often the samples from a site were not more than

5 meters apart. All the samples were oriented in the field by marking on them the Strike and Dip directions determined with a Brunton Compass.

Altogether 160 samples were collected from 24 sites. Sites AB1 to AB6 and ABM lie in Zone I , sites AB7 to AB14 lie in Zone II, sites AB15 to AB20 lie in Zone III and sites AB21 to AB23 lie in Zone IV.

3.2 Laboratory Work

In the laboratory, additional reference lines were drawn on the samples with the waterproof ink. The blocks were fixed in concrete such that their surfaces marked with the strike and dip were horizontal. Cores of 2.1-2.3 cm diameter were drilled from the samples. These cores were then sawn into cylinders of 2.1-2.2 cm length that were used as specimens for the measurement of NRM of the rocks. Palaeomagnetic measurements were carried out in the laboratory using the Schonstedt SSM-2 Spinner Magnetometer which could successfully measure NRM intensities as low as 10^{-3} A/m. A Schonstedt Geophysical Specimen Demagnetizer was used for Alternating Field demagnetizations. A large batch furnace capable of heating up to 60 specimens was used for thermal demagnetizations. A field of 0 ± 12 nT was maintained in the center of a 3 axis Helmholtz coil system. Most of the specimens were demagnetized in 6 coil set, whereas some of the specimens were demagnetized in a 12 coil set.

3.3 Measurement of NRM

The Schonstedt SSM-2 Spinner Magnetometer was used for palaeomagnetic measurements. It comprises a Fluxgate system enclosed in a cylindrical magnetic shield and a sample holding arm attached to an electric motor to facilitate spinning. It has a micro-processor attached to the spinner magnetometer for processing the fluxgate output. After each spin this micro-processor calculates values for two of the three orthogonal components of specimen's magnetization. The whole assembly is interfaced to a Texas Instrument micro-computer for further data processing and operation of the spinner magnetometer.

The cylindrical specimens are fitted into a cubic specimen holder made of plastic, which is conveniently fixed in the chuck of the magnetometer's spinning arm. The continuous spin of the magnetic specimen generates the fluctuating magnetic field. The component of the magnetic moment perpendicular to the rotation axis is compared with a reference signal which is generated from the rotating system. Fourier analysis of an alternating voltage proportional to the magnetization vector is done to find the phase difference between the reference and signal voltages. The phase difference between the reference and signal voltages is proportional to the angle between the direction of the measured component and a fixed direction across the sample holder, oriented such that when component of magnetic moment perpendicular to the rotation axis and fiducial direction are parallel the phase difference is zero (Collinson, 1983).

Each specimen was spun in six mutually orthogonal orientations such that each of the six faces of the cubical sample holder were in turn presented to the fluxgate

and any two of the X, Y and Z axes were in turn perpendicular to the spin axis. Two orthogonal components of magnetization were obtained from each spin. Six orientations thus provided four determinations each of the X,Y and Z components, two of each sign. The Intensity, Declination and Inclination of the magnetization was then obtained from the average values of the X, Y and Z components.

The specimens were demagnetized in steps either by alternating field or by heating and their residual magnetization was measured after every step.

3.4 Demagnetization of Specimens

A magnetic sample may contain two or more types of magnetizations. The rock acquires a primary remanent magnetization at the time of its formation which is parallel to the ambient magnetic field direction. The primary magnetization can be Thermo-remanent magnetization (TRM) in igneous rocks (Neel,1955. Verhoogen, 1959. Stacey, 1962,1963.), Depositional remanent magnetization (DRM) in sedimentary rocks (Griffiths et al,1960. Irving and Major, 1964. Collinson, 1965a,. Lovelie, 1974. Nagata, 1961. Stacey, 1962). Chemical remanent magnetization (CRM) may be present as primary remanent magnetization in sedimentary and igneous rocks (Kobayashi, 1959. Larson and Walker, 1975. Stacey,1963.

The rock may then acquire a secondary magnetization between the time of its formation and the present time. Viscous remanent magnetization (VRM) is acquired if there are magnetic grains in a rock in which thermal fluctuations cause metastable changes in domain alignment or domain wall positions (Collinson,1983. Neel, 1955. Stacey, 1963). Partial thermoremanent magnetization (PTRM) is acquired by rocks

whose temperature is raised by burial under deposits or by intrusions. If the temperature of the rock exceeds the blocking temperature of any magnetic grains present in the rock they will acquire a PTRM when the rock subsequently cools (Briden, 1965. Irving & Opdyke, 1965). Lightening strikes on the exposed rocks may produce a local magnetization (Cox, 1961., Purucker, 1974). The vector sum of primary and secondary magnetizations as they exist at present in the rock is called the Natural Remanent Magnetization (NRM).

The rocks in the present study are volcanic lava flows which have been affected by prehnite-pumpellyite to lowermost greenschist facies of burial or regional metamorphism (Jolly 1974, 1977; Jensen 1978a,b, 1981). Pullaiah et al, 1975 showed that magnetization of single-domain pure magnetite and hematite should survive the prehnite-pumpellyite and low greenschist facies metamorphism provided there has been no chemical change of the iron minerals. In this case the expected NRM contained in the rocks under study may be TRM. On the other hand it is also expected that regional geological events involving deep erosion and various generations of burial and intrusion may have resulted in thermal and/or chemical resetting of part of the pre-existing NRM (Schutts & Dunlop, 1981). Since it is the primary NRM or the NRM acquired by the rocks prior to rotation of the blocks which is important for this study. To compare the declinations of magnetization in various zones, it is first necessary to remove any secondary magnetizations acquired by the rocks after rotation, leaving the primary or the pre-rotation NRM intact as much as possible .

3.5 Presentation and Analysis of Data

The basic data obtained are directions and intensities of magnetization measured in rock specimens from various sites. After magnetic cleaning a well defined stable direction remained in some specimens. The stable directions obtained from these samples were averaged to obtained the sample average directions. The sample average directions obtained from each site were averaged to obtain a site average direction. Site Average directions obtained from each zone were averaged to obtain zonal average directions. At sample level the number of specimens used was 1-3, at site level the number of samples averaged was 3-5, and at zonal level the number of sites averaged was 3-6.

A Basic language computer program "Spimag" written in the McMaster University Palaeomagnetism Laboratory was used to operate the spinner magnetometer and to obtain values of the X, Y and Z magnetization components from the magneto-meter's processing unit. The program used the X, Y and Z components to calculate the Intensity of Magnetization, Declination and Inclination after each demagnetization step. It also performed the spherical trigonometric calculations for converting directions of NRM derived from the magnetometer to directions referred to the regional system.

The changes in NRM that occurred during demagnetization were displayed on stereographic plots, demagnetization curves (plots of normalized NRM verses the applied AF peak field or the temperature) and Zijderveld diagrams (Zijderveld, 1967).

Declinations and inclinations calculated after NRM measurements were plotted

on a Wulff's Net using the Spimag program. The stable end points reached during demagnetizations of specimens were interpreted to represent the primary (stable) NRM directions of the specimens. These directions were then used for sample averaging.

The changes in the Intensity with demagnetization were plotted against the peak AF or Temperature. The AF decay curves were used to determine the Median Demagnetization Field and coercivity distribution of the magnetic grains whereas the Thermal decay curves indicate the blocking temperatures of the magnetic minerals.

Zijderveld diagrams were made using a computer program written in Basic language for principal component analysis (Kirschvink, 1980) . These diagrams combine Intensity and Directional changes on the same diagram. The end of the total magnetization vector is projected as points on two orthogonal planes. The horizontal plane containing the vector $(X^2 + Y^2)^{1/2}$ and either the vertical and $X(X^2 + Z^2)^{1/2}$ or vertical and $Y(Y^2 + Z^2)^{1/2}$ plane, where X, Y and Z are magnetization components referred to the diagram axes. These planes are shown as super-imposing areas with a common axis on the diagram and the axes are scaled in suitable intensity units. The intensity of each projected NRM component after each demagnetization step is proportional to the distance from the origin to the corresponding point. As demagnetization proceeds the points on each plane will trace out paths according to the changes in D, I and Intensity see figure 3.3. A straight line was fitted to the component of NRM decaying to the origin (Kirschvink, 1980) and its D and I were calculated. This direction was considered to be the characteristic (primary) NRM of the specimen and was further used for sample averaging.

Figure 3.3: Orthogonal diagrams. (a) Representation of a magnetization vector as orthogonal components and the projection on a horizontal plane "H" and a vertical plane "V", (b) Zijderveld (1967) plots showing the projection of the vectors on to the horizontal "h" and vertical "v" planes. Intensity of NRM is shown on EW axis in suitable scales. After Piper, J. D. A., (1988).

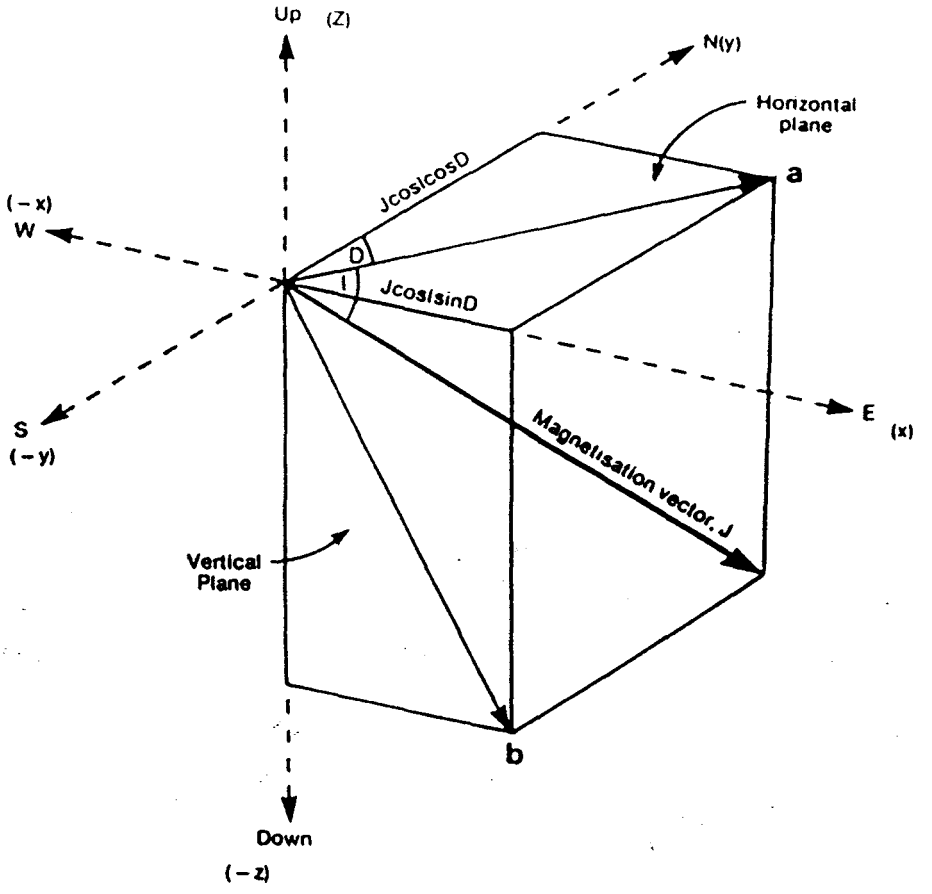
Up (Z)
N(y)
Horizontal plane
a
JcosIcosD
D
I
JcosIsinD
(-x)
W
S
(-y)
E
(x)
Magnetisation vector, J
Vertical Plane
b
Down
(-z)

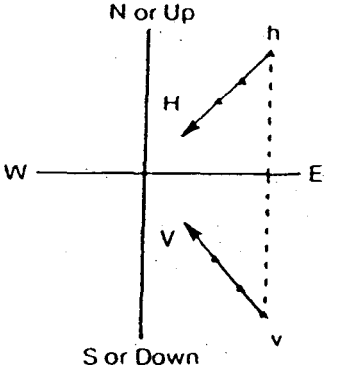
N or Up
h
H
W
E
V
v
S or Down

3.6 Statistical Methods

Scatter and dispersion in the NRM directions obtained from the specimens may be due to systematic or random errors arising from magnetometer noise, inaccuracies in sample orientation, and imperfections in demagnetizing procedures. There may be dispersion in NRM directions among a group of specimens from a sample, site or zone due to the secular variation of geomagnetic field and variation in the strength of residual secondary magnetization.

Statistical methods were applied to describe the dispersion in the NRM directions while averaging was done to calculate the sample mean, site mean, and zonal mean directions (Fisher, 1953).

For N number of unit vectors a mean direction of resultant vector R was calculated by first expressing the individual directions in their direction cosines l,m,n where

l=cos D cos I

m=sin D cos I

n=sin I

D=Declination

I=Inclination

Then direction cosines of the resultant l_r,m_r and n_r were found by the following equation:

$$l_r = 1/R\ (l_1 + l_2 \ldots\ldots l_N)$$

$$m_r = 1/R\ (m_1 + m_2 \ldots\ldots m_N)$$

$n_r = 1/R\ (n_1 + n_2 \ldots\ldots n_N)$

and the resultant R was calculated by equation

$R^2 = (l_1 + l_2 \ldots\ldots l_N)^2 + (m_1 + m_2 \ldots\ldots m_N)^2 + (n_1 + n_2 \ldots\ldots n_N)^2$

The declination and inclination of the mean were found by the following relations.

$\text{Tan } D_r = (m_1 + m_2 \ldots\ldots m_N)/(l_1 + l_2 \ldots\ldots l_N)$

$\text{Sin } I_r = (n_1 + n_2 \ldots\ldots n_N)/R$

The probability distribution proposed by Fisher for points on a sphere is of the form

$$P = \frac{K}{4Sinhk} e^{KCos\phi}$$

where

ϕ = angle between the true mean direction and one of the N vectors

K = Precision parameter

The best estimate k of the Fisherian precision parameter K (Fisher Kappa) is given for k>3 by Fisher as;

$$k = \frac{N-1}{N-R}$$

k was calculated by using the above relation. k may be in the range of 10-1000, the higher the value the more tightly grouped the directions.

The accuracy of the mean direction derived from N vectors with resultant R is expressed as the semi-angle α of a cone about the observed mean within which the true mean lies with 95% probability. α_{95} the circle of 95% confidence was calculated by the equation:

$$Cos\alpha_{(1-P)} = 1 - \frac{N-R}{R}[\frac{1}{P}^{1/N-1} - 1]$$

where

P = 0.05

Smaller values of α_{95} imply that the directions are more tightly grouped.

Chapter 4

PALAEOMAGNETIC RESULTS

4.1 NRM Intensities of Specimens

Intensities of natural remanent magnetization (NRM) of 303 specimens measured are shown in figure 4.4 and figure 4.5. These figures are histograms of intensities. In figure 4.4 the specimens are divided into 4 structurally different zones. The NRM intensities of specimens from all the zones range between 0.0001 A/m and 10 A/m. Most of the specimens have intensities between 0.01 A/m and 10 A/m. Few specimens have intensities greater than 10 A/m.

Intensities of Zone I specimens are unimodal ranging between 0.01 A/m and 10 A/m (Fig. 4.4a). Intensities of Zone II specimens can be divided into 3 groups i.e., less than 0.01 A/m, between 0.01 and 1.0 A/m and greater than 1.0 A/m (Fig. 4.4b). There are relatively more specimens in Zone II which have intensities higher than 1 A/m. Zone III specimens have most intensities between 0.01 A/m and 10 A/m (Fig. 4.4c). The distribution of intensities in Zone III is similar to the distribution

Figure 4.4: Histograms of the intensity of natural remanent magnetization (a) Zone I, (b) Zone II, (c) Zone III and (d) Zone IV.

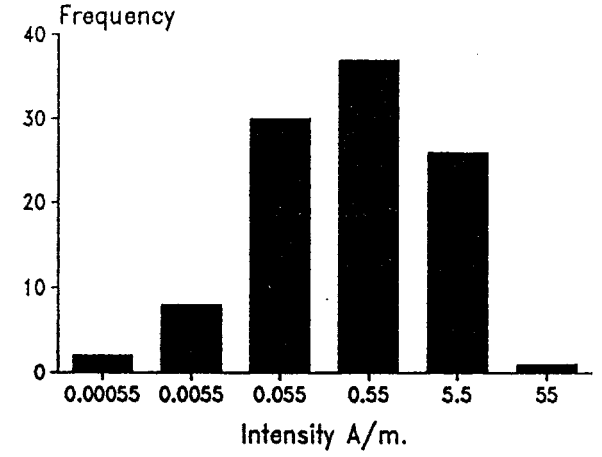
Frequency
40
30
20
10
0
0.00055
0.0055
0.055
0.55
5.5
55
Intensity A/m.

(a)

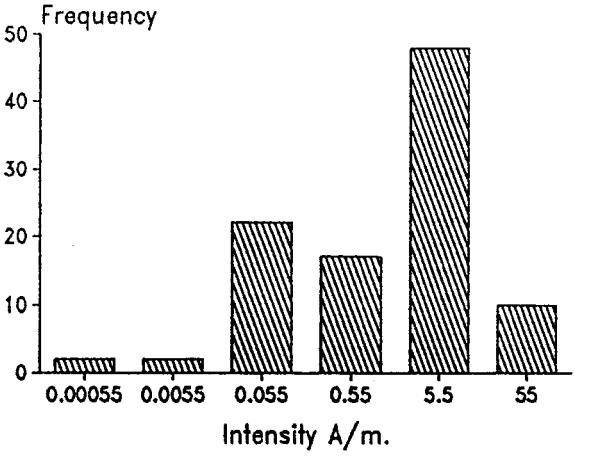
Frequency
50
40
30
20
10
0
0.00055
0.0055
0.055
0.55
5.5
55
Intensity A/m.

(b)

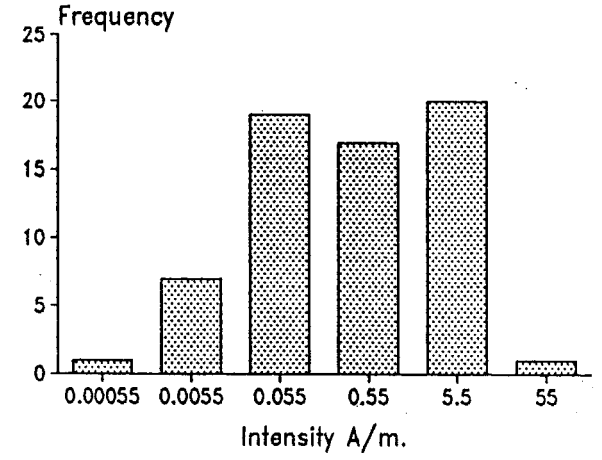
Frequency
25
20
15
10
5
0
0.00055
0.0055
0.055
0.55
5.5
55
Intensity A/m.

(c)

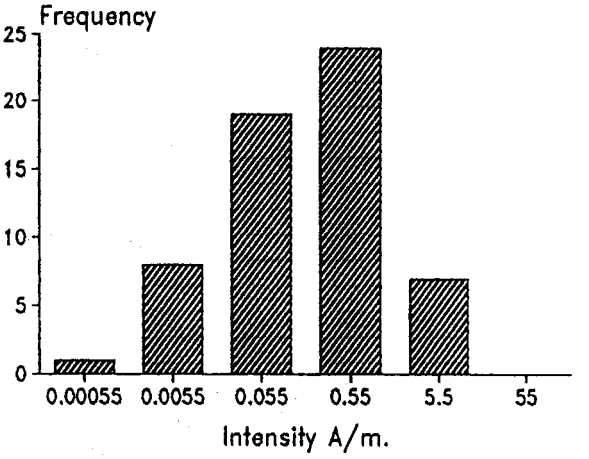
Frequency
25
20
15
10
5
0
0.00055
0.0055
0.055
0.55
5.5
55
Intensity A/m.

(d)

Figure 4.5: Histograms of the intensity of natural remanent magnetization (a) Basalt, (b) Dacite, (c) Gabbro and (d) Diorite.

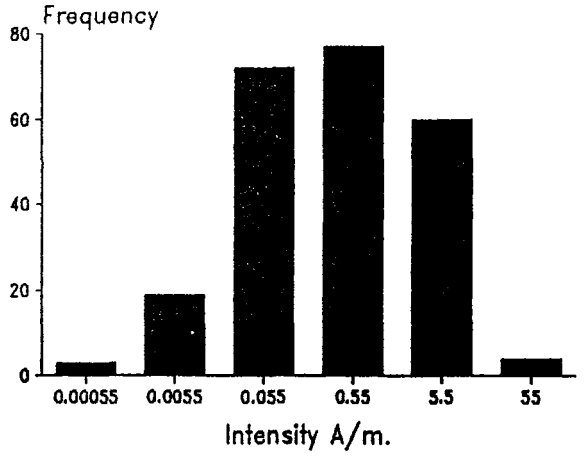
Frequency
80
60
40
20
0
0.00055
0.0055
0.055
0.55
5.5
55
Intensity A/m.

(a)

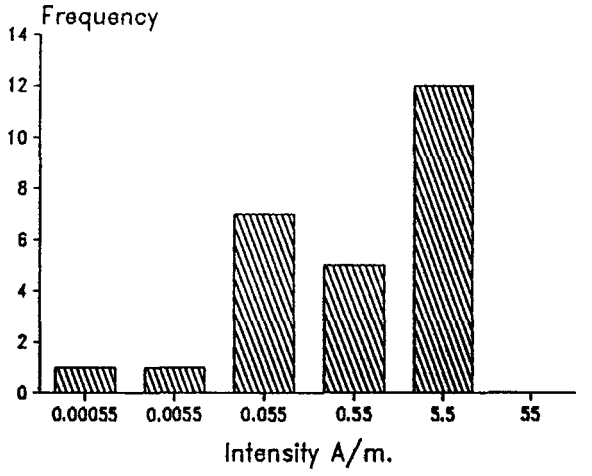
Frequency
14
12
10
8
6
4
2
0
0.00055
0.0055
0.055
0.55
5.5
55
Intensity A/m.

(b)

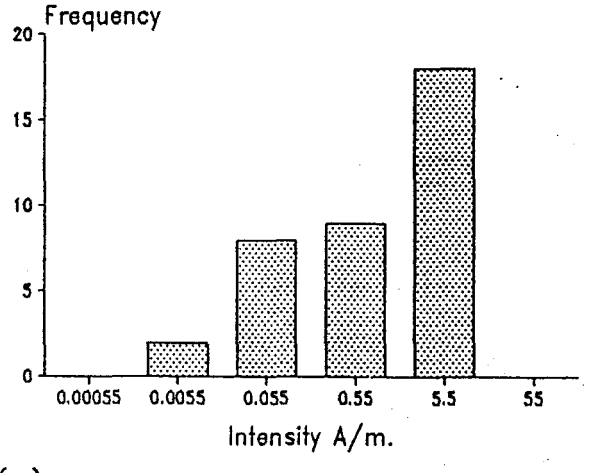
Frequency
20
15
10
5
0
0.00055
0.0055
0.055
0.55
5.5
55
Intensity A/m.

(c)

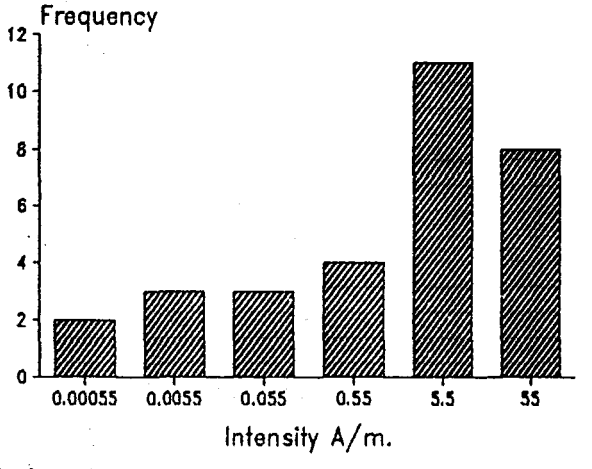
Frequency
12
10
8
6
4
2
0
0.00055
0.0055
0.055
0.55
5.5
55
Intensity A/m.

(d)

of intensities in Zone I. Most of the Zone IV intensities range between 0.001 A/m and 1.0 A/m (Fig. 4.4d) showing that this zone has relatively lower intensities than the other zones.

In figure 4.5 the specimens have been divided into different lithology types that were sampled. Mainly Basalt was sampled from all the zones. Dacite was sampled from 2 sites in Zone II only. Gabbro was sampled from 1 site each in zones I, II and III. Diorite was sampled from 1 site in zone I and from 1 site in zone II.

Intensities of Basalts mainly lie between 0.01 A/m and 10 A/m (Fig. 4.5a), however, a few specimens have values lesser or greater than this range. Intensities of Dacite specimens can be divided into 3 groups i.e., less than 0.01 A/m, between 0.01 and 1.0 A/m and greater than 1.0 A/m (Fig. 4.5b). Gabbro specimens have intensities distributed between 0.001 A/m and 10 A/m with most specimens having values between 0.01 A/m and 10 A/m (Fig. refint:rokc). Intensities of the Diorite specimens are distributed between 0.0001 A/m and 100 A/m with most intensities greater than 1.0 A/m (Fig. 4.5d).

It is apparent from figure 4.5 that the intensities of basalt and gabbro specimens are similarly grouped, whereas, the intensities of dacite and diorite specimens are distributed. This distribution of intensities may be due to the varying amounts of primary opaques present in the dacite and diorite specimens. Some Basalt and Diorite specimens possess very high intensities (>10 A/m), which may reflect the abundance of primary opaques in the them. The presence of more Diorite samples in zone II is the cause of increased number of higher intensities in this zone II and their distribution over all the ranges (Fig. 4.4b).

4.2 Stability of Specimens

The magnetic stability of the specimens is shown in figure 4.6 and figure 4.7. Figure 4.6 is a histogram of median demagnetization field (MDF) determined in alternating field demagnetization procedures. In this figure the specimens have been differentiated into 4 zones. All the MDF's can be divided into 3 groups, soft coercivities (MDF< 10 mT) seen in all the zones, medium coercivities (MDF=10-40 mT) present mostly in zones II and Iv, and hard coercivities (MDF=40-60 mT) seen in zones I and IV. Although these 3 groups of coercivities are present in all the zones but their amount varies.

Zone I specimens show two types of coercivities (Fig. 4.6a), soft and hard. Zone II specimens also show two types of coercivities (Fig. 4.6b), soft and medium. Most of the Zone III specimens have soft coercivities. Some specimens have medium and a few have hard coercivities (Fig. 4.6c). Zone IV specimens have all the 3 types of coercivities (Fig. 4.6d).

In figure 4.7 the specimens have been divided into dif- ferent lithologies. Basalt specimens show all the 3 types of coercivities (Fig. 4.7a). Dacite specimens show only soft and medium coercivities (Fig. 4.7b). Gabbro specimens show all the 3 types of coercivities (Fig. 4.7c) like the basalt specimens. Diorite specimens show soft coercivities with a very few specimens of medium and hard coercivities (Fig. 4.7d).

It is apparent from figure 4.7 that most of the specimens from all the lithologies have soft coercivity with smaller number of medium and hard coercivities. Dacite specimens have no hard coercivities. Figure 4.8 is a histogram of the tempera-

Figure 4.6: Histograms of the median demagnetization fields (MDF) (a) Zone I, (b) Zone II, (c) Zone III and (d) Zone IV.

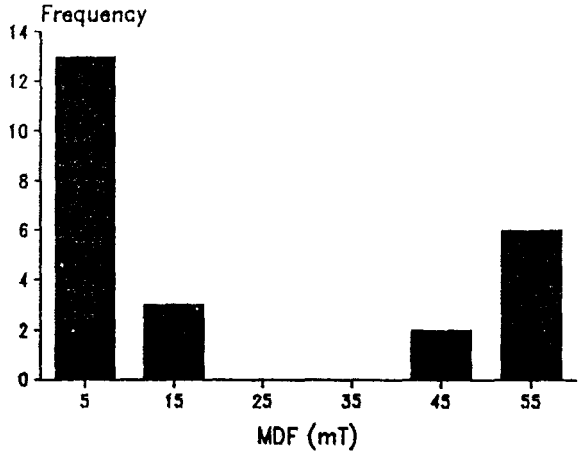
Frequency
14
12
10
8
6
4
2
0
5
15
25
35
45
55
MDF (mT)

(a)

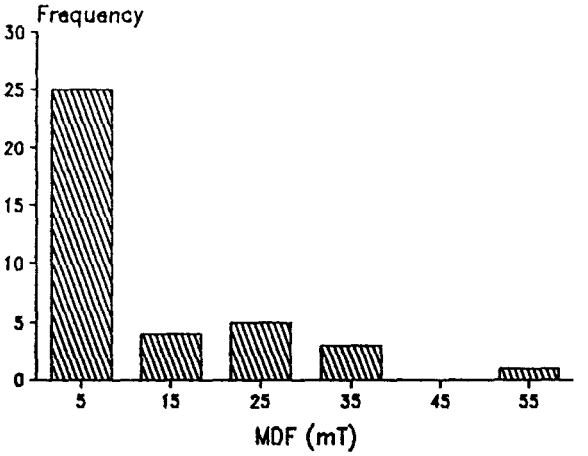
Frequency
30
25
20
15
10
5
0
5
15
25
35
45
55
MDF (mT)

(b)

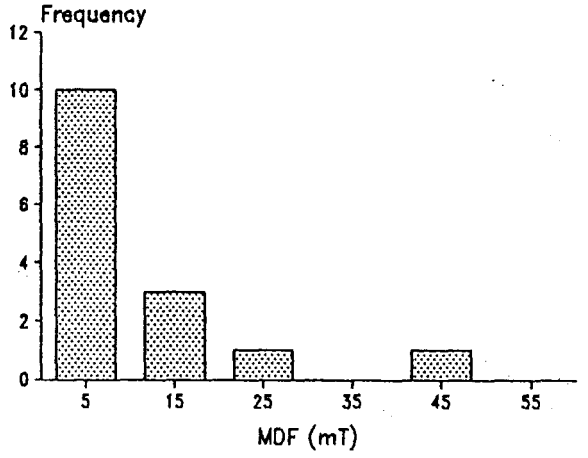
Frequency
12
10
8
6
4
2
0
5
15
25
35
45
55
MDF (mT)

(c)

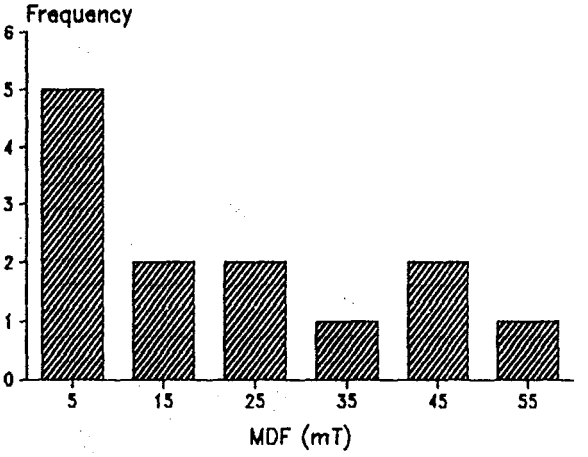
Frequency
6
5
4
3
2
1
0
5
15
25
35
45
55
MDF (mT)

(d)

Figure 4.7: Histograms of the median demagneti fields (MDF) (a) Basalt, (b) Dacite, (c) Gabbro and (d) Diorite.

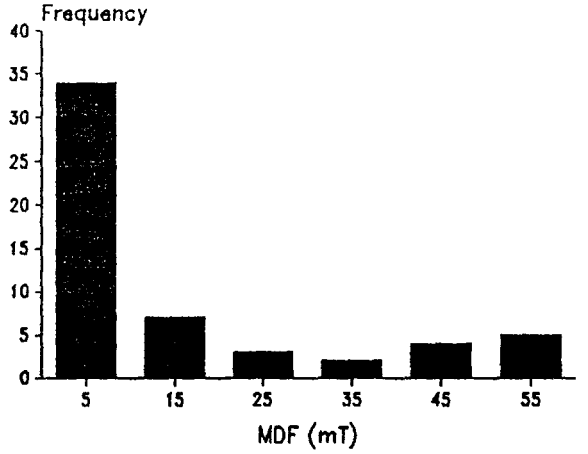
Frequency
40
35
30
25
20
15
10
5
0
5
15
25
35
45
55
MDF (mT)

(a)

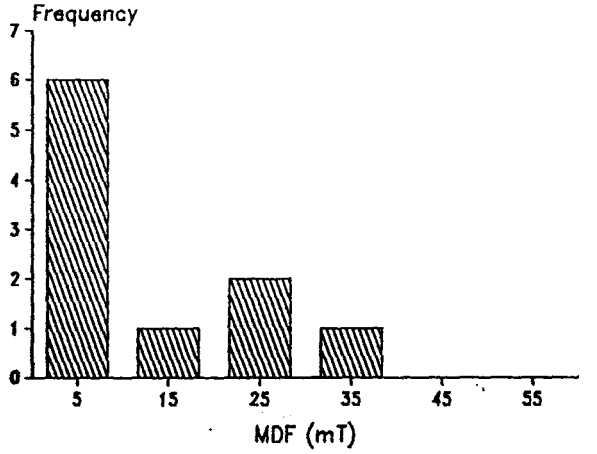
Frequency
7
6
5
4
3
2
1
0
5
15
25
35
45
55
MDF (mT)

(b)

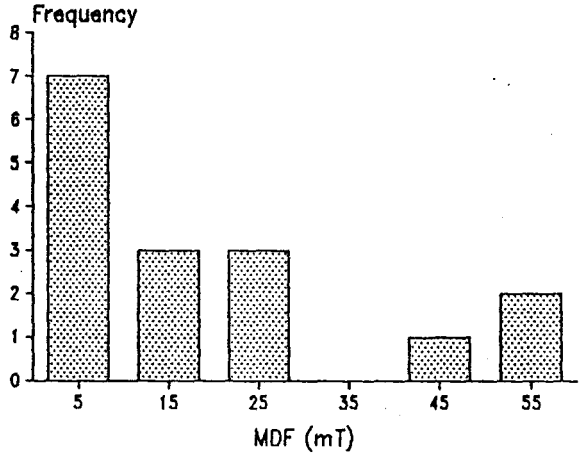
Frequency
8
7
6
5
4
3
2
1
0
5
15
25
35
45
55
MDF (mT)

(c)

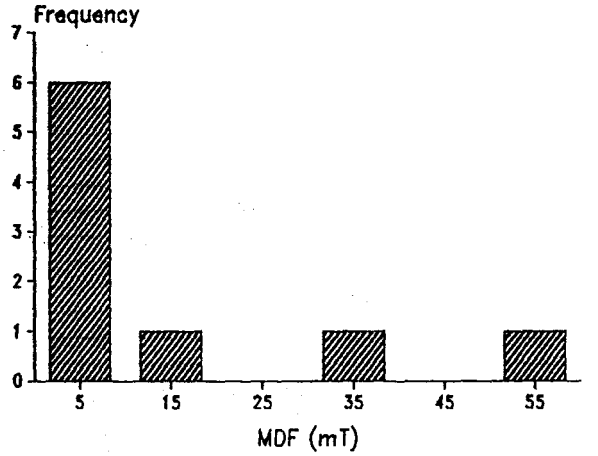
Frequency
7
6
5
4
3
2
1
0
5
15
25
35
45
55
MDF (mT)

(d)

Figure 4.8: Histograms of the temperatures at 50% NRM of the specimens is removed (MDT) in thermal demagnetization (a) Zone I, (b) Zone II, (c) Zone III and (d) Zone IV.

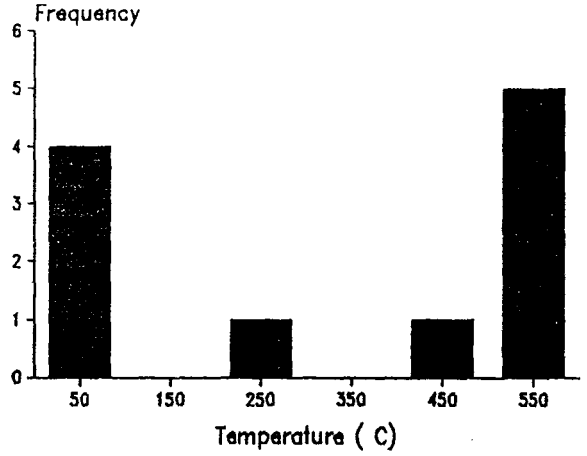
Frequency
6
5
4
3
2
1
0
50
150
250
350
450
550
Temperature (C)

(a)

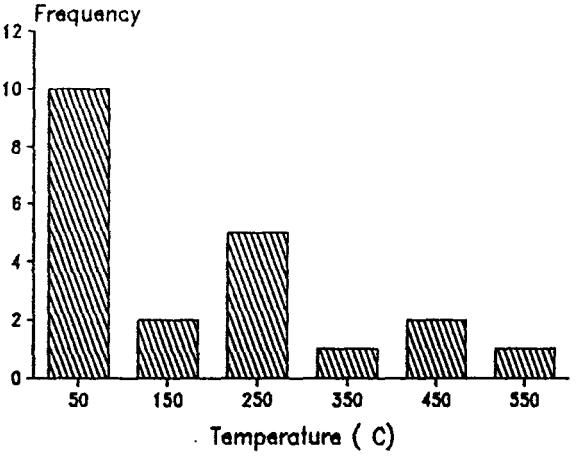
Frequency
12
10
8
6
4
2
0
50
150
250
350
450
550
Temperature (C)

(b)

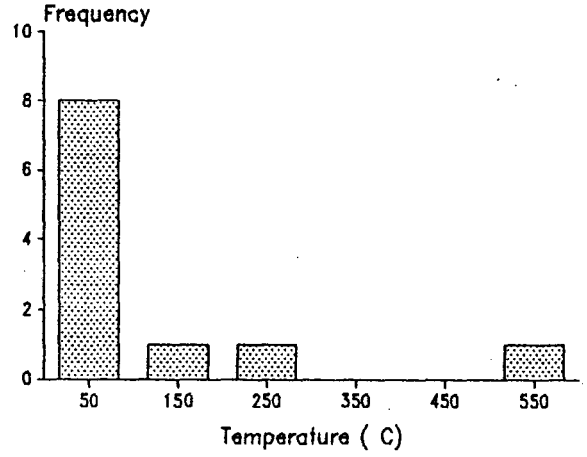
Frequency
10
8
6
4
2
0
50
150
250
350
450
550
Temperature (C)

(c)

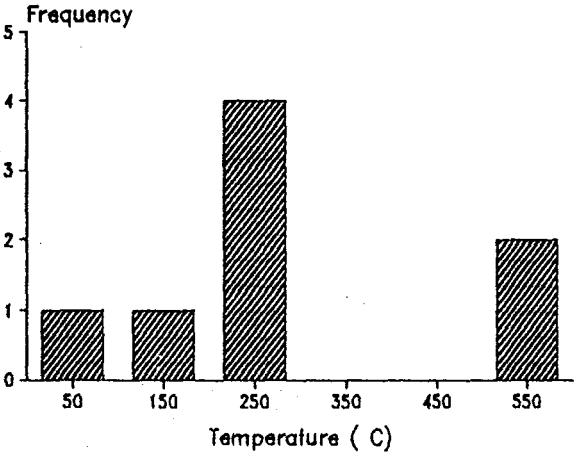
Frequency
5
4
3
2
1
0
50
150
250
350
450
550
Temperature (C)

(d)

tures at which 50% NRM of the specimens is removed (MDT). The specimens are divided into different zones. There are three types of NRM stabilities, low stabilities (MDT<100°C) present in all the zones, medium stabilities (MDT=100-400°C) present mostly in zones II and IV, and high stabilities (MDT>400°C) present mostly in zones I and IV. Zone I specimens (Fig. 4.8a) have low and high stabilities with a few specimens with medium stabilities. Zone II specimens have low and medium stabilities (Fig. 4.8b). Zone III specimens have low stabilities with a few specimens showing medium and high stabilities (Fig. 4.8c). Zone IV specimens have medium and high stabilities (Fig. 4.8d). In figure 4.9 the specimens are divided into different lithologies. Basalt specimens have all the 3 types of NRM stabilities (Fig. 4.9a). Dacite specimens have dominantly low NRM stabilities (Fig. 4.9b). Gabbro specimens also have all the 3 types of NRM stabilities (Fig. 4.9c). Diorite specimens have only low and high NRM stabilities (Fig. 4.9d).

In multidomain grains and near the singledomain-multidomain grain size boundary i.e., $3.0x10^{-5}$ mm for magnetite and 0.15 cm for hematite (McEllhiny, 1973), the magnetic hardness increases with decrease in grain size (Stacey, 1962) or the difference in oxidation states, which with the decrease in grain size causes the magnetic hardness to increase (Watkins and Haggerty, 1967) .

Since the coercivities and the types of NRM stabilities are not strictly dependent on the zones or the lithologies they may be a function of oxidation state of the rocks or the grain size of the opaque minerals.

Figure 4.9: Histograms of the temperatures at 50% NRM of the specimens is removed (MDT) in thermal demagnetization (a) Basalt, (b) Dacite, (c) Gabbro and (d) Diorite.

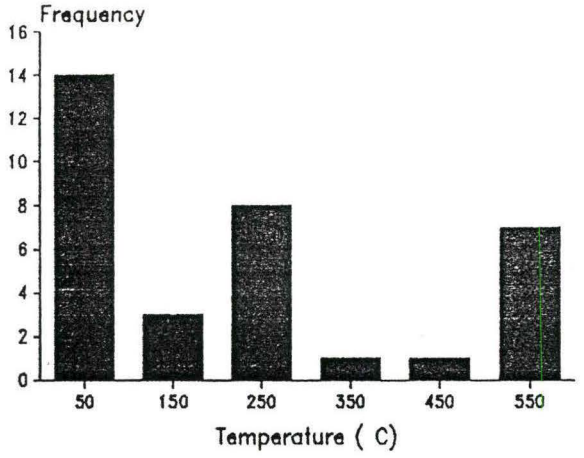
Frequency
16
14
12
10
8
6
4
2
0
50
150
250
350
450
550
Temperature (C)

(a)

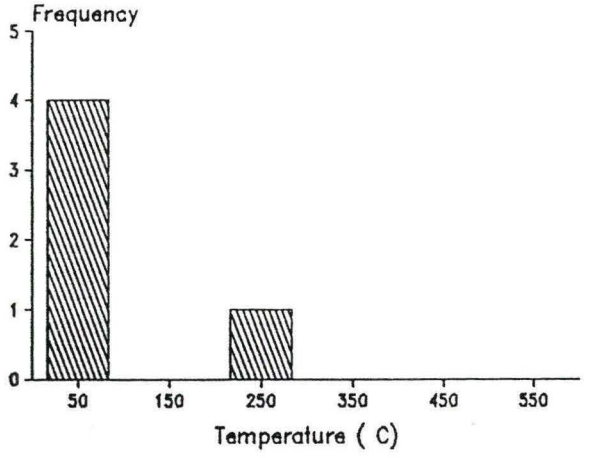
Frequency
5
4
3
2
1
0
50
150
250
350
450
550
Temperature (C)

(b)

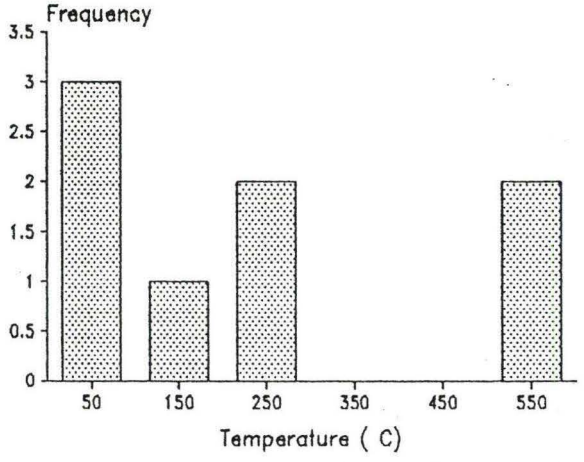
Frequency
3.5
3
2.5
2
1.5
1
0.5
0
50
150
250
350
450
550
Temperature (C)

(c)

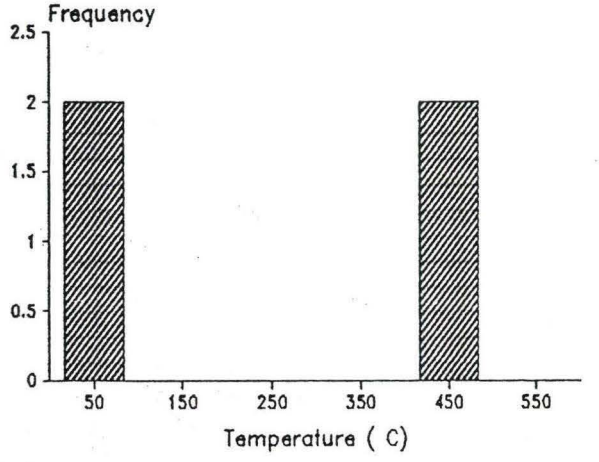
Frequency
2.5
2
1.5
1
0.5
0
50
150
250
350
450
550
Temperature (C)

(d)

4.3 Demagnetization Behavior of Specimens

Zone I specimens show two types of demagnetization curves i.e., Low and High coercivity curves (Fig. 4.10). In low coercivity specimens MDF's range between 50-80 Oe.(5-8 mT) as shown in figure 4.10a. In high coercivity specimens the MDF's range between 500-600 Oe.(50-60 mT) as shown in figure 4.10b. Both types of curves are found from samples from sites AB3 and AB5. Thermal demagnetization of specimens from this zone also reveals two type of behavior (Fig. 4.11). One is the rapidly decreasing intensity curve with blocking temperatures distributed between 100 and 550°C (Fig. 4.11a). 50% of the NRM in this type of behavior is removed between 100 and 350°C. The second type of curve observed in zone I specimens is a square shouldered curve with discreet blocking temperatures between 520° 580°C with a small component retained at 640°C (Fig. 4.11b). The coercivities and blocking temperatures of these specimens indicate that the remanence is carried by magnetite. Specimens with low coercivities and distributed blocking temperatures may be carried by magnetites or titanomagnetites of relatively large grain size. The specimens with high coercivities and discreet blocking temperatures may be carried by magnetites of relatively small grain size. Specimens showing these curves are from sites AB4 and AB5 which show well grouped southerly steep negative directions.

Zone II specimens show three type of coercivity curves (Fig. 4.12) Low coercivity curves with MDF's ranging between 40- 125 Oe.(4-12.5 mT) as shown in figure 4.12a, medium coercivity curves with MDF ranging between 500-900 Oe., (50-90 mT), remanent coercivities exceeding 1000 Oe (100 mT) as shown in figure 4.12b, and unstable demagnetization curves showing zig-zag unstable behavior as shown in

Figure 4.10: Alternating Field demagnetization of rocks in zone I (a), Low coercivity behavior and (b) high coercivity behavior.

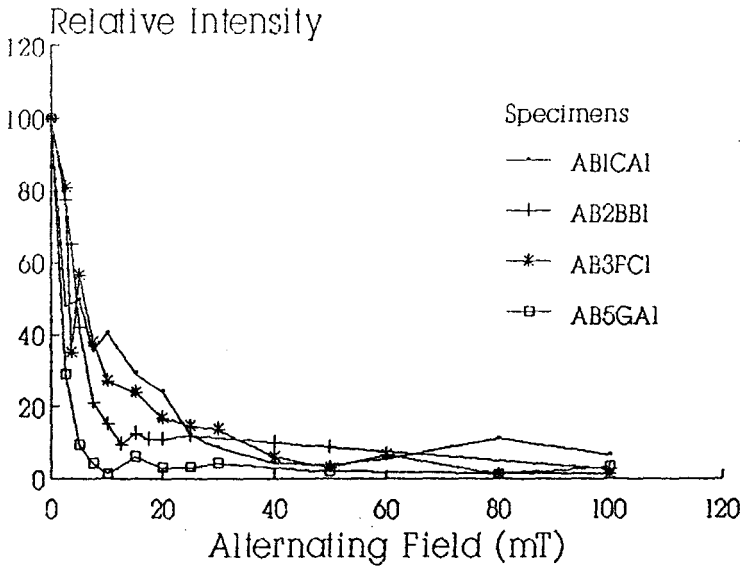
Relative Intensity
120
100
80
60
40
20
0
0
20
40
60
80
100
120
Alternating Field (mT)
Specimens
AB1CA1
AB2BB1
AB3FC1
AB5GA1

a

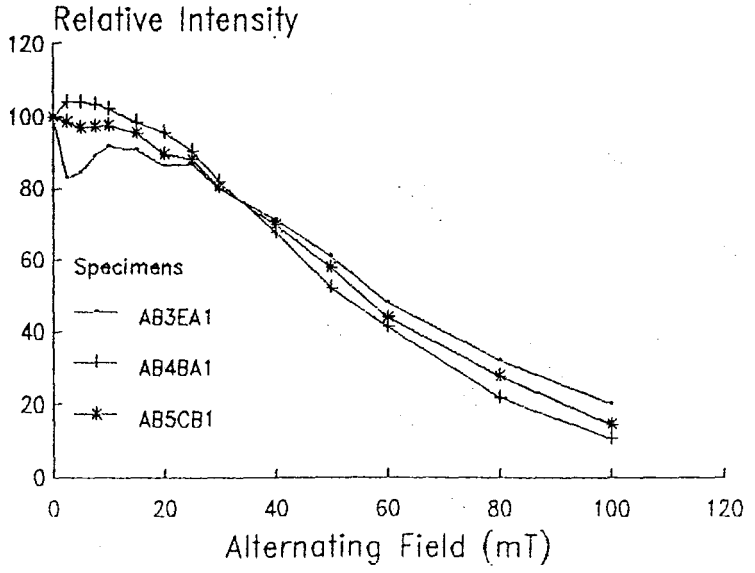
Relative Intensity
120
100
80
60
40
20
0
0
20
40
60
80
100
120
Alternating Field (mT)
Specimens
AB3EA1
AB4BA1
AB5CB1

b

Figure 4.11: Thermal demagnetization of zone I rocks (a) distributed blocking temperatures and (b) discreet blocking temperatures.

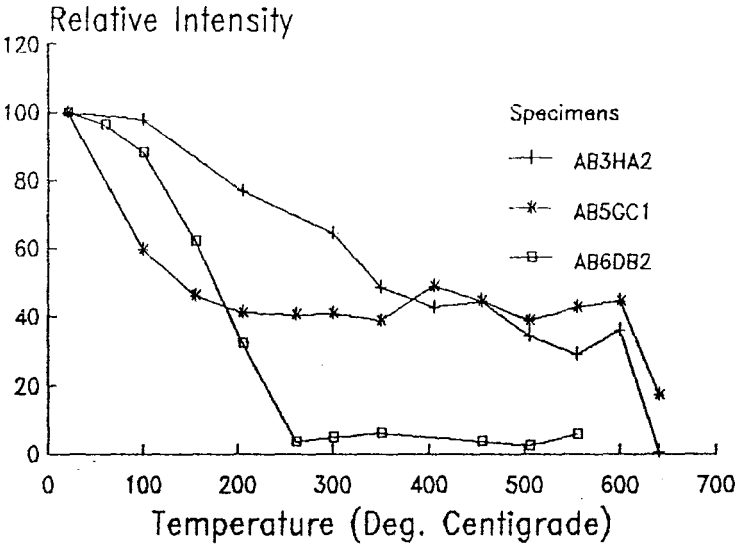
Relative Intensity
120
100
80
60
40
20
0
0
100
200
300
400
500
600
700
Temperature (Deg. Centigrade)
Specimens
AB3HA2
AB5GC1
AB6DB2

a

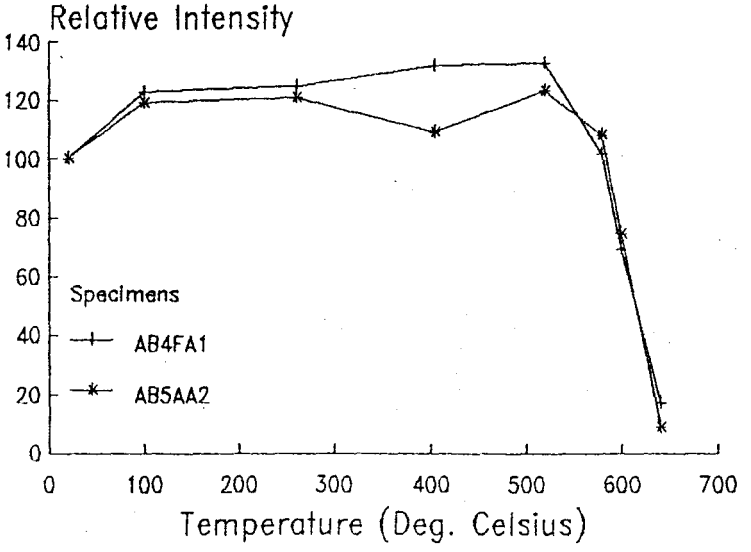
Relative Intensity
140
120
100
80
60
40
20
0
0
100
200
300
400
500
600
700
Temperature (Deg. Celsius)
Specimens
AB4FA1
AB5AA2

b

Figure 4.12: Alternating Field demagnetization of rocks in zone II (a) Low coercivity behavior, (b) high coercivity behavior and (c) unstable coercivity behavior.

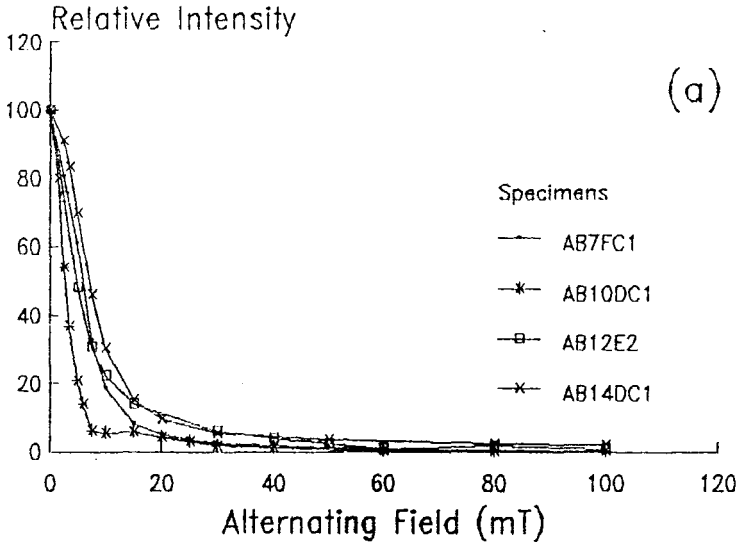
Relative Intensity
(a)
Specimens
AB7FC1
AB10DC1
AB12E2
AB14DC1
Alternating Field (mT)

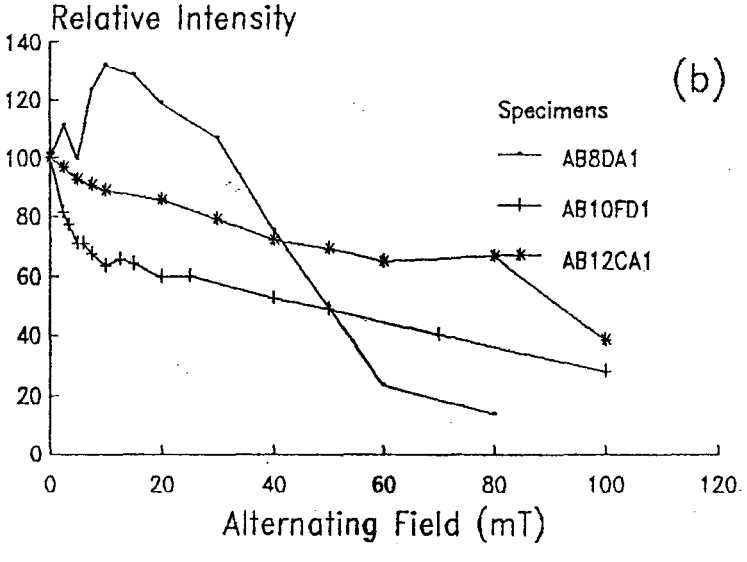
Relative Intensity
(b)
Specimens
AB8DA1
AB10FD1
AB12CA1
Alternating Field (mT)

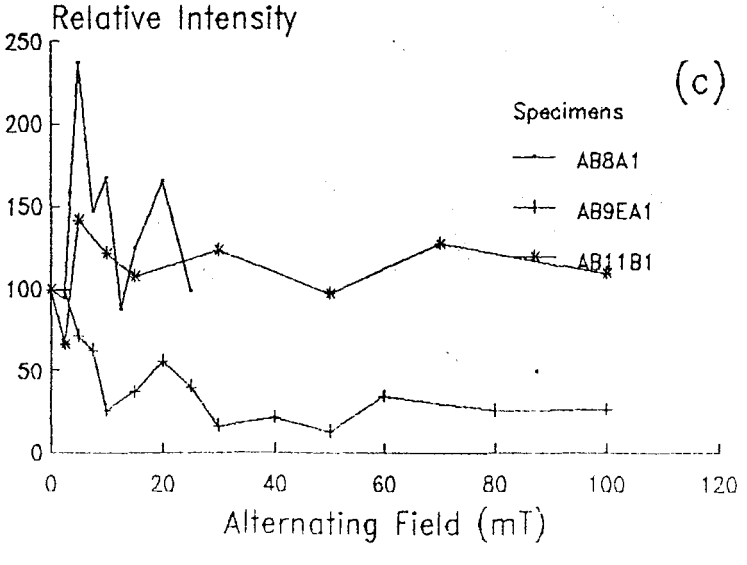
Relative Intensity
(c)
Specimens
AB8A1
AB9EA1
AB11B1
Alternating Field (mT)

figure 4.12c. Thermal demagnetization curves are of two types (Fig. 4.13). Gradually decreasing intensity curves with blocking temperatures distributed between 100-580°C (Fig. 4.13a). 50% of the remnance of these specimens is removed between 200-450°C. The second type of curves show zig-zag unstable behavior (Fig. 4.13b).

The soft (low coercivity) remanences with blocking temperatures ranging between 100-580°C may be carried by large magnetite or titanomagnetite grains. The hard (high coercivity) remanences with blocking temperatures ranging between 100-580°C may be carried by very fine grained magnetites or titanomagnetites.

Zone III specimens show three types of behavior in AF demagnetization (Fig. 4.14). Low coercivity curves with MDF's between 20 and 50 Oe. (2-5 mT) as in figure 4.14a. Medium coercivity curves with MDF's between 200-500 Oe. (20-50 mT) as in Figure 4.14b, and zig-zag unstable behavior as in Figure 4.14c. Thermal demagnetization curves show two types of behavior (Fig. 4.15). One is characterized by rapidly decreasing remnance curves with blocking temperatures distributed between 100-500°C (Fig. 4.15a). Their 50% remnance is removed between 200 and 300°C. The second is characterized by zig-zag curves showing unstable behavior as shown in figure 4.15b. The low coercivity remanence with blocking temperatures distributed between 100-500°C may be carried by magnetite grains of very large grain size seen at in site AB15 thin sections. The presence of different coercivities in specimens from same site (low, medium and unstable coercivities in site AB18 specimens. Low and unstable coercivities in site AB16 specimens) reflect the variation in opaque abundances and their grain sizes in the rock.

Zone IV specimens show two types of AF demagnetization behavior (Fig. 4.16). Specimens from sites AB20, AB21 and AB22 show zig-zag unstable curves as shown

Figure 4.13: Thermal demagnetization of zone II rocks (a) distributed blocking temperatures and (b) unstable demagnetization behavior.

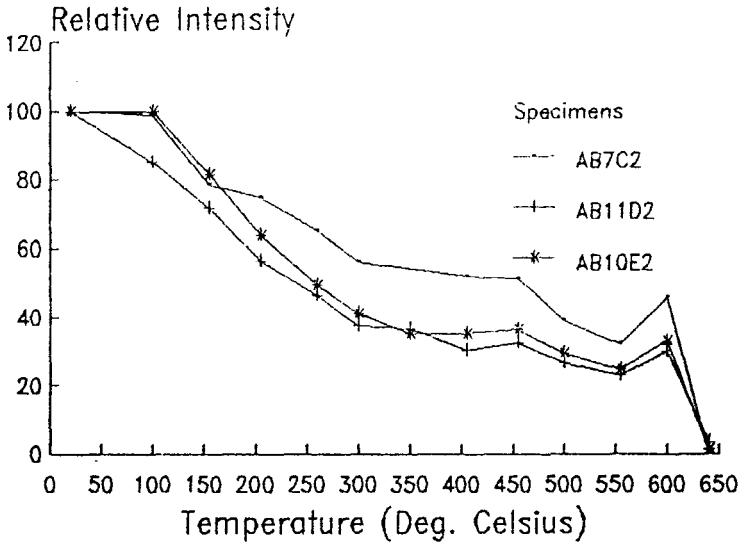
Relative Intensity
120
100
80
60
40
20
0
Specimens
AB7C2
AB11D2
AB10E2
0 50 100 150 200 250 300 350 400 450 500 550 600 650
Temperature (Deg. Celsius)

a

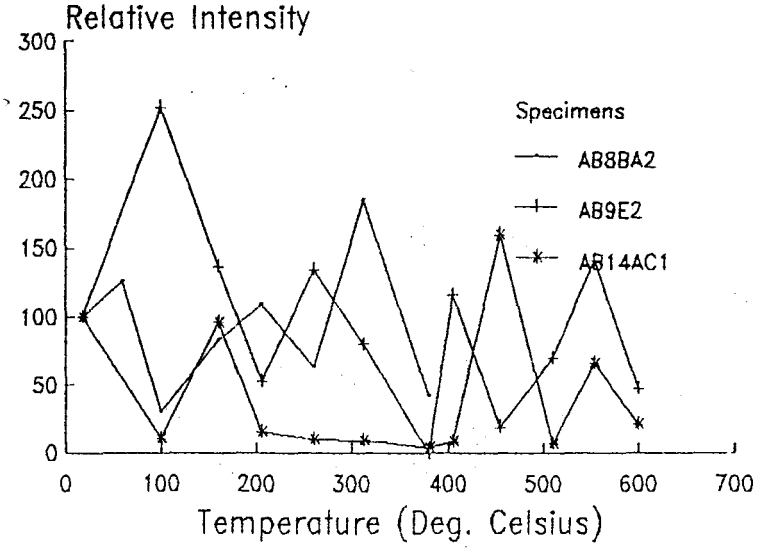
Relative Intensity
300
250
200
150
100
50
0
Specimens
AB8BA2
AB9E2
AB14AC1
0 100 200 300 400 500 600 700
Temperature (Deg. Celsius)

b

Figure 4.14: Alternating Field demagnetization of rocks in zone III (a) Low coercivity behavior, (b) high coercivity behavior and (c) unstable coercivity behavior.

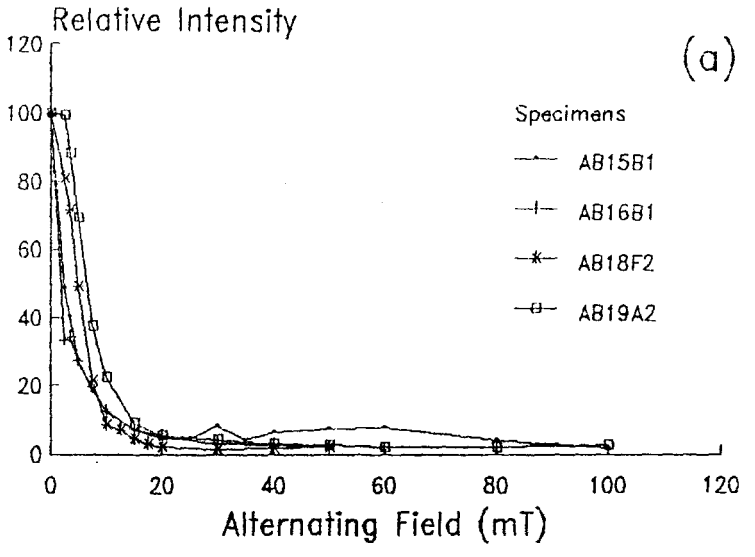
Relative Intensity
(a)
Specimens
AB15B1
AB16B1
AB18F2
AB19A2
120
100
80
60
40
20
0
0
20
40
60
80
100
120
Alternating Field (mT)

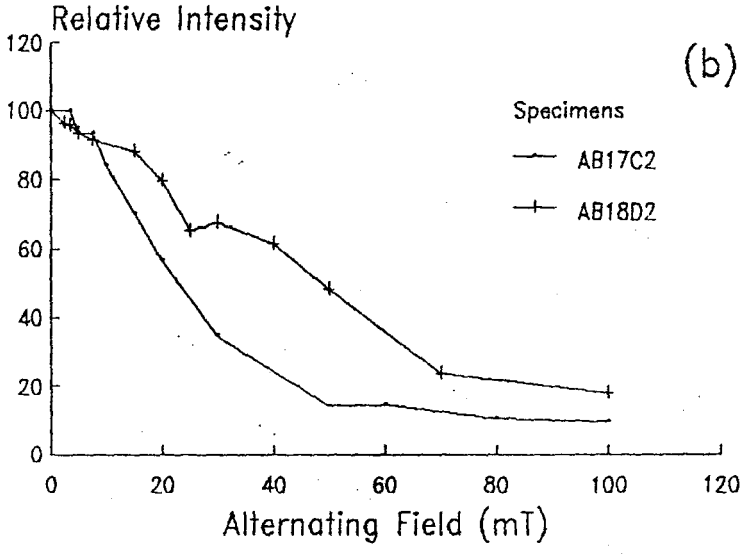
Relative Intensity
(b)
Specimens
AB17C2
AB18D2
120
100
80
60
40
20
0
0
20
40
60
80
100
120
Alternating Field (mT)

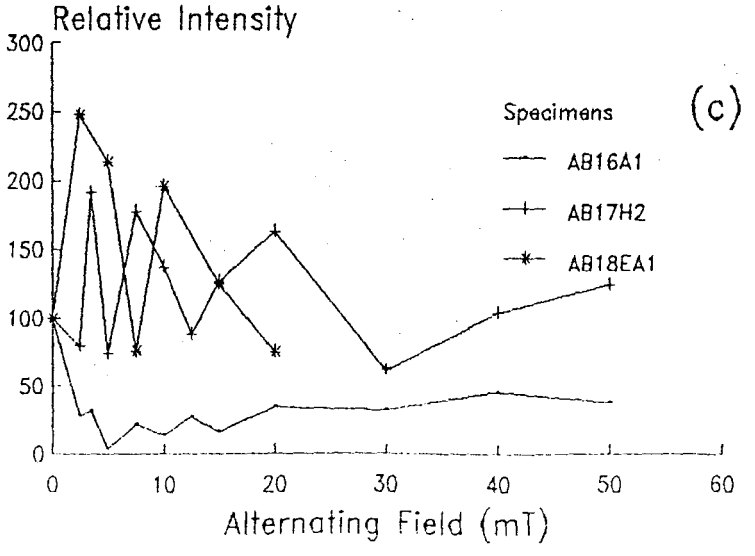
Relative Intensity
(c)
Specimens
AB16A1
AB17H2
AB18EA1
300
250
200
150
100
50
0
0
10
20
30
40
50
60
Alternating Field (mT)

Figure 4.15: Thermal demagnetization of zone III rocks (a) distributed blocking temperatures and (b) unstable demagnetization behavior.

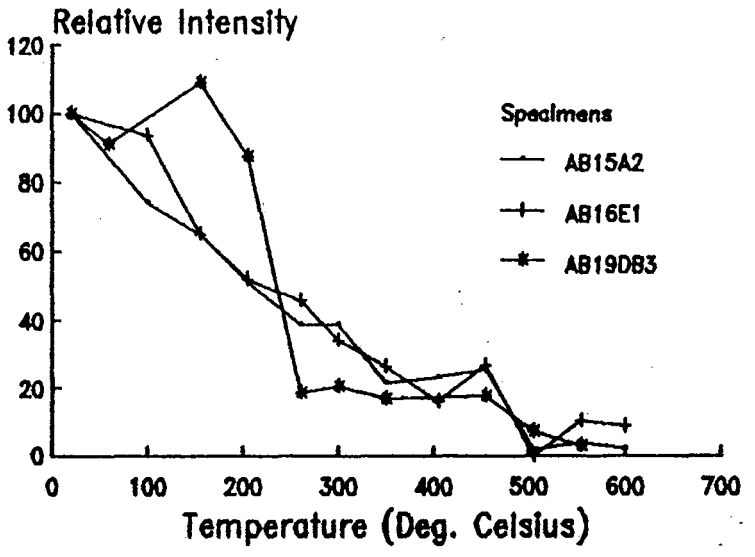
Relative Intensity
120
100
80
60
40
20
0
0
100
200
300
400
500
600
700
Temperature (Deg. Celsius)
Specimens
AB15A2
AB16E1
AB19D83

a

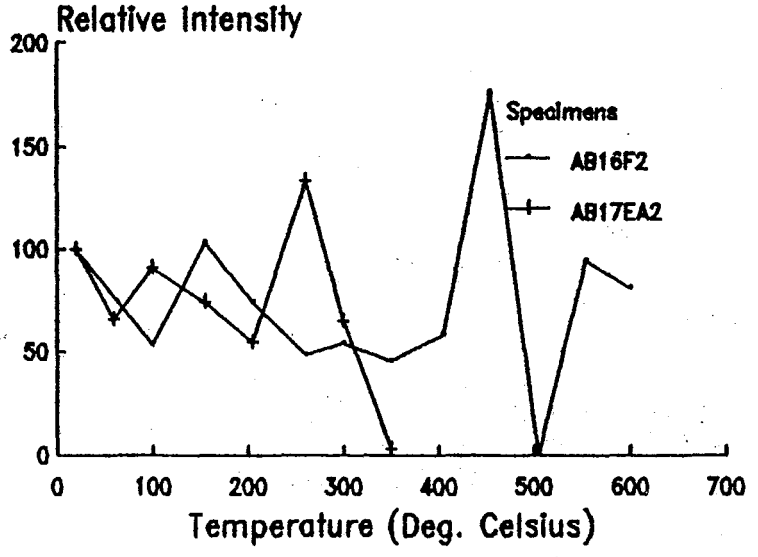
Relative Intensity
200
150
100
50
0
0
100
200
300
400
500
600
700
Temperature (Deg. Celsius)
Specimens
AB16F2
AB17EA2

b

Figure 4.16: Alternating Field demagnetization of rocks in zone IV (a) unstable coercivity behavior and (b) high coercivity behavior.

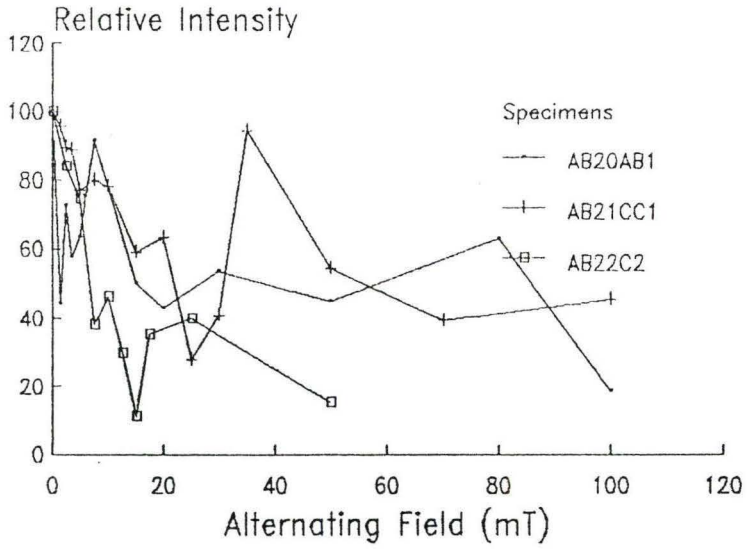
Relative Intensity
120
100
80
60
40
20
0
0
20
40
60
80
100
120
Alternating Field (mT)
Specimens
AB20AB1
AB21CC1
AB22C2

a

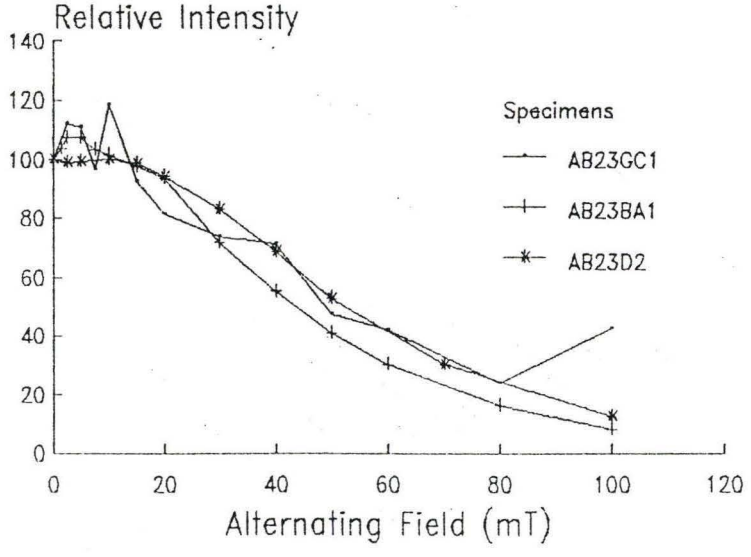
Relative Intensity
140
120
100
80
60
40
20
0
0
20
40
60
80
100
120
Alternating Field (mT)
Specimens
AB23GC1
AB23BA1
AB23D2

b

in figure 4.16a. Specimens from site AB23 show high coercivity curves (Fig. 4.16b) with MDF's between 400-600 Oe. (40-60 mT). Some of this remanence is retained at 100 mT applied peak field. Thermal demagnetization curves also show two types of behavior (Fig. 4.17). Sites AB20, AB21 and AB22 show zig-zag unstable curves (Fig. 4.17a). Specimens from site AB23 show square shouldered thermal demagnetization curves (Fig. 4.17b) with discreet blocking temperatures between 400-550°C. These high blocking temperatures and the hard remanence behavior characterized by high coercivity reflect that the magnetization may be carried by magnetite. It is present only in site AB23 specimens, which show well grouped northeasterly directed intermediate inclination magnetization.

4.4 NRM Directions

The Natural Remanent Magnetization (NRM) directions and stable ultimate directions from all the specimens were analyzed and are described as follows. The NRM directions of 309 specimens from 24 sites divided into 4 zones are plotted on separate equal area nets in figure 4.18. Figure 4.18a is a plot of zone I (sites AB1-AB6 & ABM) specimens. These specimens have a cluster of southerly, negative and steep directions. NRM directions of specimens from Zone II (sites AB7-AB14) are plotted in figure 4.18b. These directions are scattered all over the stereonet and do not agree at sample, site or zone level. The directions of specimens from Zone III (sites AB15-AB19) form a cluster of Northwesterly steep directions as shown in figure 4.18c and the specimens from Zone IV (sites AB20-AB23) plotted in figure 4.18d form a group of North-easterly intermediate inclination directions. Both

Figure 4.17: Thermal demagnetization of zone IV rocks (a) unstable demagnetization behavior and (b) discreet blocking temperatures.

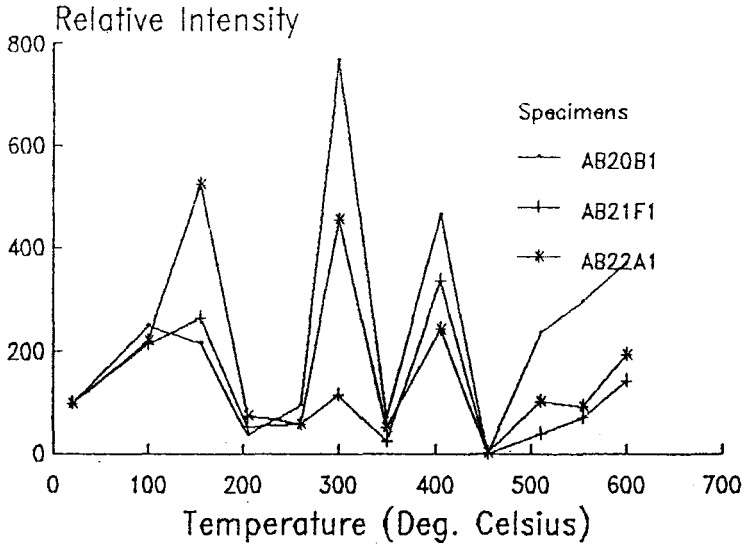
Relative Intensity
800
600
400
200
0
Specimens
AB20B1
AB21F1
AB22A1
0
100
200
300
400
500
600
700
Temperature (Deg. Celsius)

a

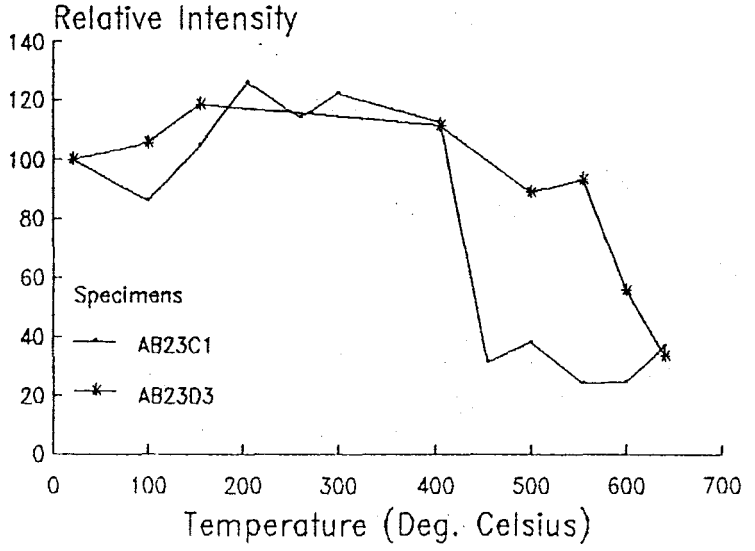
Relative Intensity
140
120
100
80
60
40
20
0
Specimens
AB23C1
AB23D3
0
100
200
300
400
500
600
700
Temperature (Deg. Celsius)

b

Figure 4.18: Equal area stereographic projections of natural remanent magnetization (NRM) directions obtained from specimens of (a) Zone I, (b) Zone II, (c) Zone III, and (d) Zone IV. Open circles indicate upward directions and solid circles indicate downward directions.

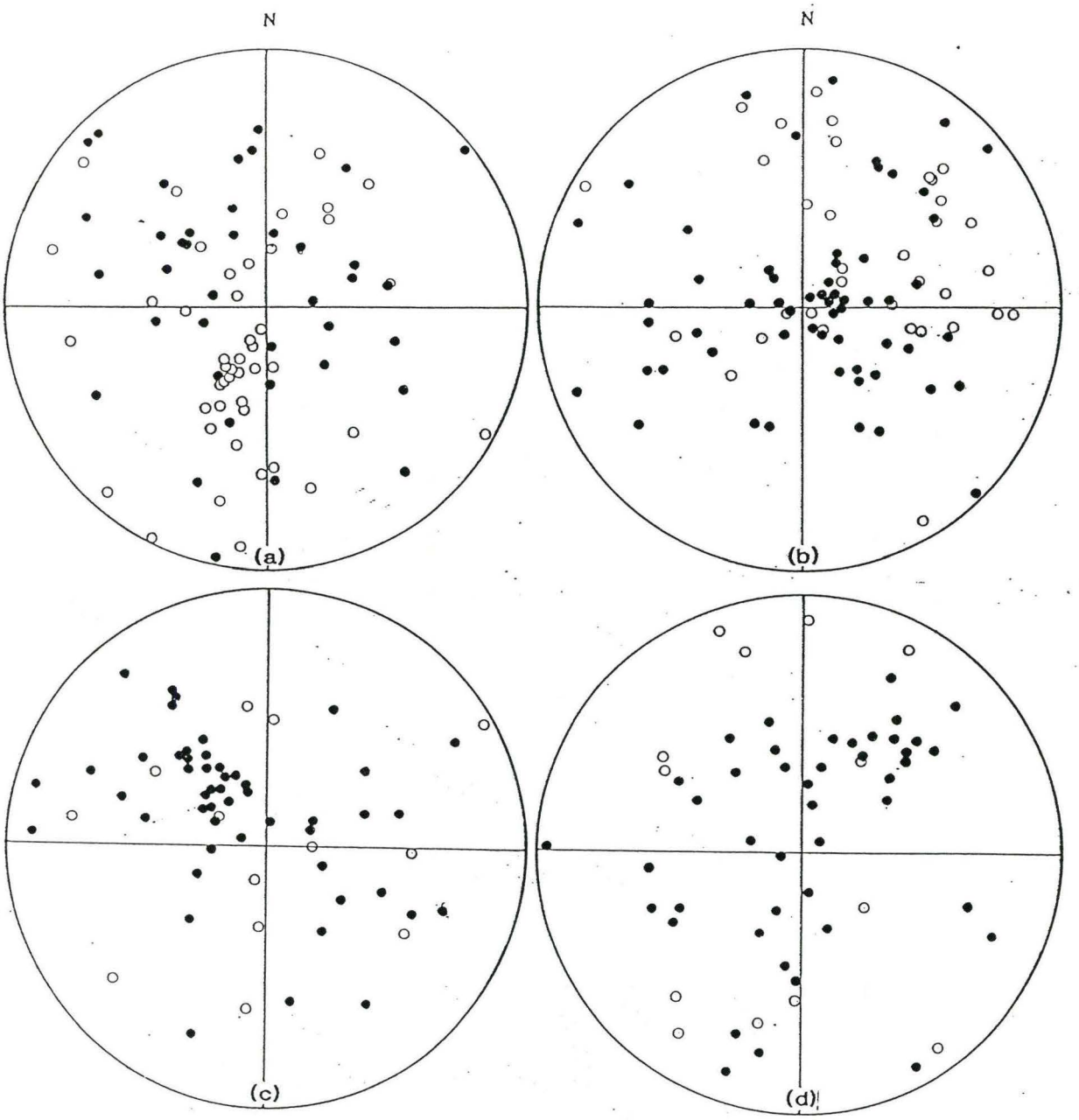
N
N
(a)
(b)
(c)
(d)

positive and negative directions are present in all the zones.

4.5 Demagnetization Results

Directional changes in the NRM of specimens were analyzed by Stereographic Plots and Zijderveld Diagrams after demagnetization by AF or Thermal methods.

4.5.1 Zone I

51 specimens from zone I were demagnetized by alternating field out of which only 30 specimens show some stable directions while the rest show unstable randomized demagnetization behavior. Typical examples of stable end points from this zone are shown in figure 4.19, and typical examples of Zijderveld diagrams are shown in figure 4.20

42 specimens were demagnetized by heating upto 600°C. Of these 18 specimens gave stable end points with southerly, steep, negative directions. Typical examples are shown in figure 4.21. 15 specimens gave Zijderveld diagrams with single component magnetization. 6 of them decay to the origin univectorilly (Fig. 4.22). and 9 stay stable upto 400°C and then quickly decay to the origin.

Most of the stable directions from zone I are southerly steep and negative. These directions agree reasonably well on sample and site level. They are mostly single component showing very little change in direction even after demagnetization upto 1000 Oe (100 mT) applied peak field or a temperature of 600°C. Magnetizations obtained from this zone are more stable than other zones, have higher coercivity and MDF's. Their 50% NRM is removed at higher temperatures than the other two

Figure 4.19: Typical examples of equal area stereographic projection of residual magnetic directions of Zone I specimens during step wise AF demagnetization.

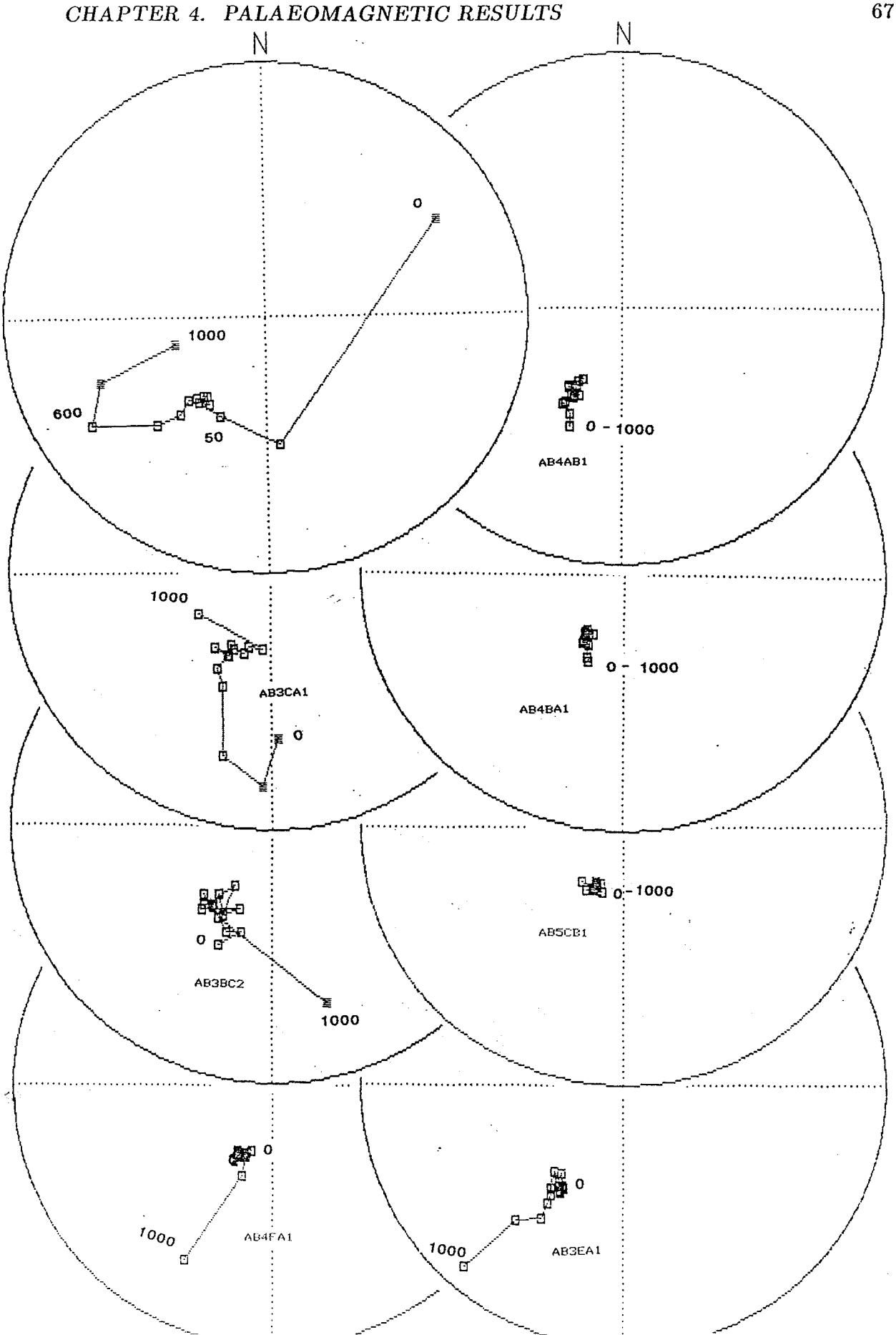
N
0
1000
600
50
N
0 - 1000
AB4AB1
1000
AB3CA1
0
0 - 1000
AB4BA1
0
AB3BC2
1000
0 - 1000
AB5CB1
0
1000
AB4FA1
0
1000
AB3EA1

Figure 4.20: Typical examples of progressive orthogonal AF demagnetization diagrams of Zone I specimens.

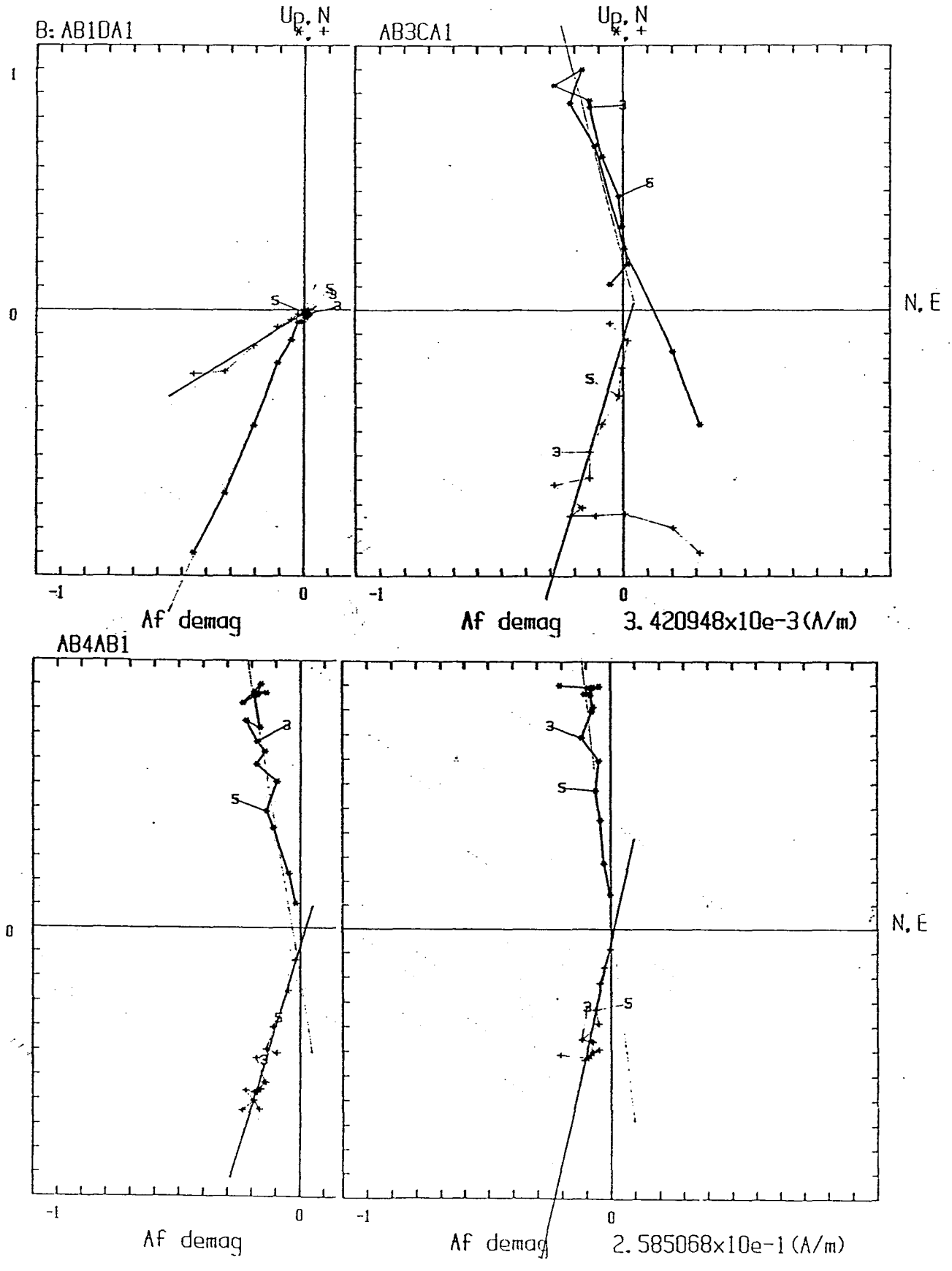
B: AB1DA1
Up, N
AB3CA1
Up, N
N, E
Af demag
Af demag
3.420948x10e-3(A/m)
AB4AB1
N, E
Af demag
Af demag
2.585068x10e-1(A/m)

Figure 4.21: Typical examples of equal area stereographic projection of residual magnetic directions of Zone I specimens during step wise Thermal demagnetization.

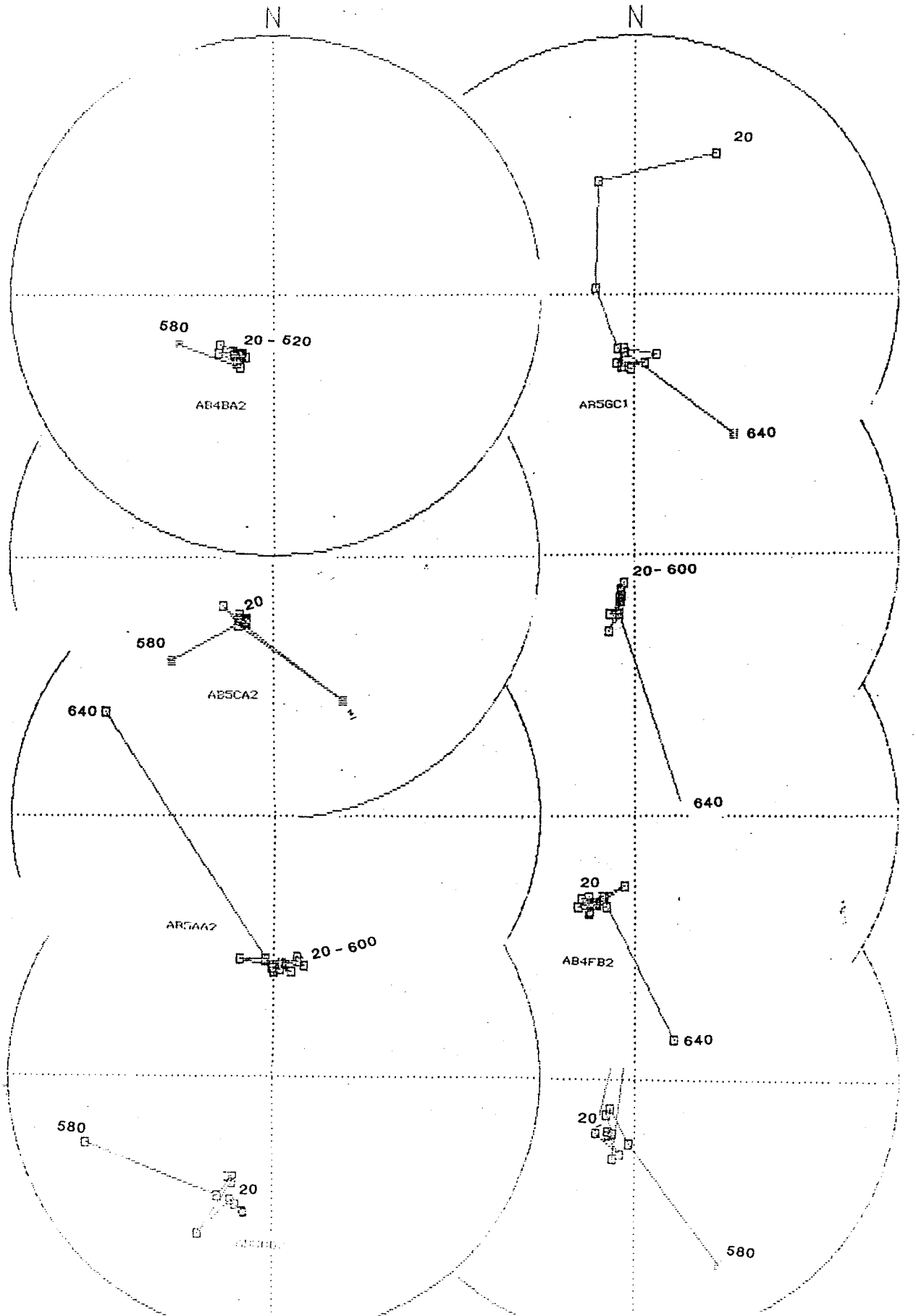
N
580
20 - 620
AB4BA2
N
20
AB5GC1
640
20- 600
20
580
AB5CA2
640
AB5AA2
20 - 600
20
AB4FB2
640
580
20
20
580

Figure 4.22: Typical examples of progressive orthogonal Thermal demagnetization diagrams of Zone I specimens.

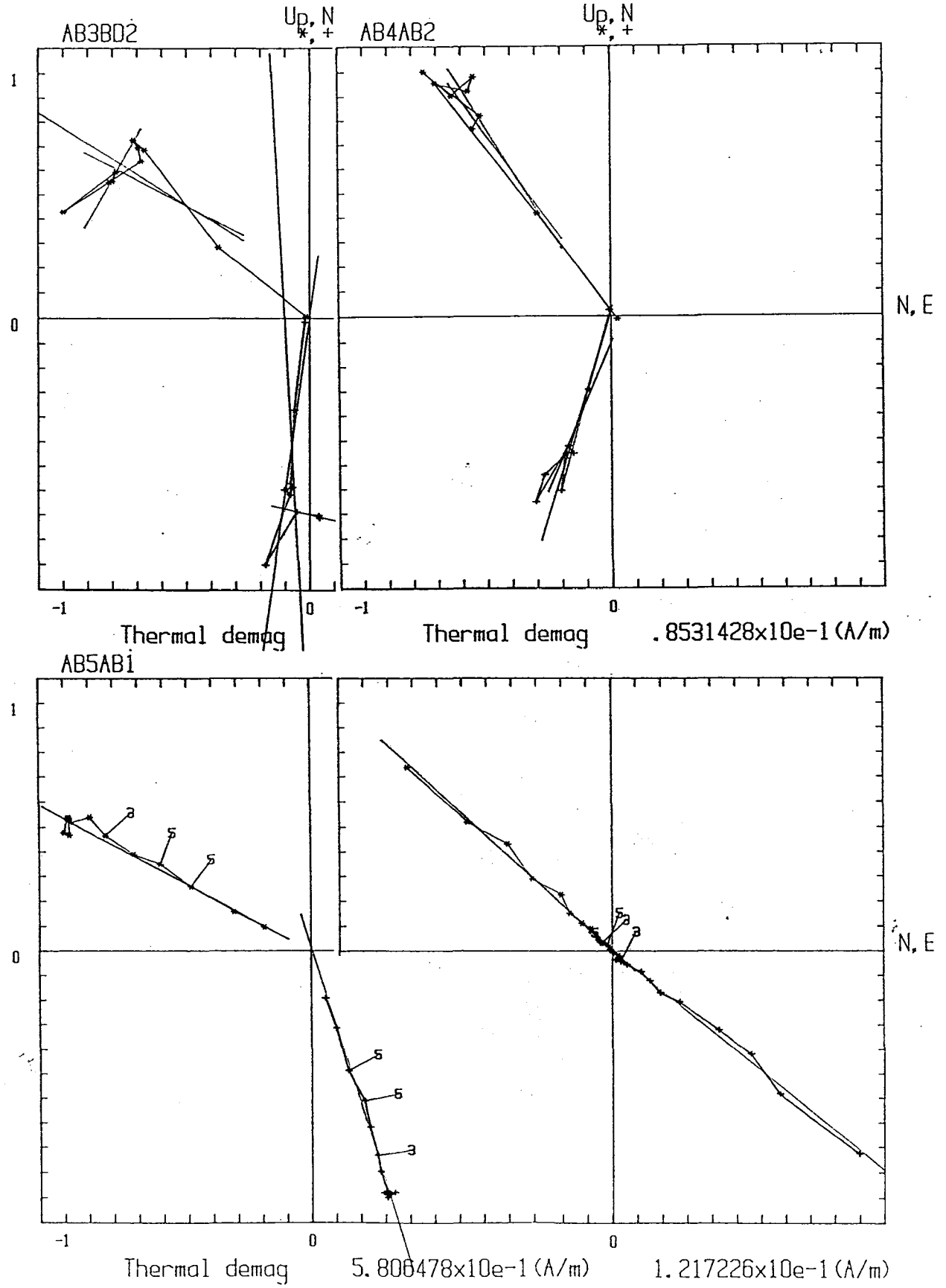
AB3BD2
Up, N
*, +
AB4AB2
Up, N
*, +
1
0
-1
0
N, E
Thermal demag
-1
0
Thermal demag .8531428x10e-1(A/m)
AB5AB1
1
0
N, E
-1
0
0
Thermal demag
5.808478x10e-1(A/m)
1.217226x10e-1(A/m)

magnetizations found in the region and is present in different type of rock suites in the zone i.e., Basalts, Gabbro and Diorite.

4.5.2 Zone II

47 specimens were AF demagnetized from this zone out of which only 17 specimens show stable end points. 11 of these show positive, steep directions and 6 specimens show negative shallow to intermediate directions either easterly or westerly (Fig. 4.23). Both negative and positive polarities are present, but they are scattered.

24 specimens show single component magnetization decaying univectorilly to the origin (Figure 4.24). These directions do not agree at sample or site level.

46 specimens were demagnetized by Thermal Methods. 21 specimens show stable end points shown in figure 4.25). 15 of these have positive steep directions which are dispersed and 6 specimens have NRM directions which are negative steep and easterly . 5 specimens show swinging demagnetization pattern.

Zijderveld diagrams show that 18 specimens have single component magnetization decaying univectorilly to the origin and 6 specimens show two component magnetization. Typical examples from this zone are shown in figure 4.26. The specimens from this zone show stable end points in stereo plots and linear segments in Zijderveld diagrams but their directions do not agree on sample or site level.

Most of the stable directions from this zone are scattered and do not agree on sample or site level. Most of these directions are single component showing very little change in direction during demagnetization (Fig. 4.23). They do not show any grouping and appear to be scattered. Both normal and reversed polarities are

Figure 4.23: Typical examples of equal area stereographic projection of residual magnetic directions of Zone II specimens during step wise AF demagnetization.

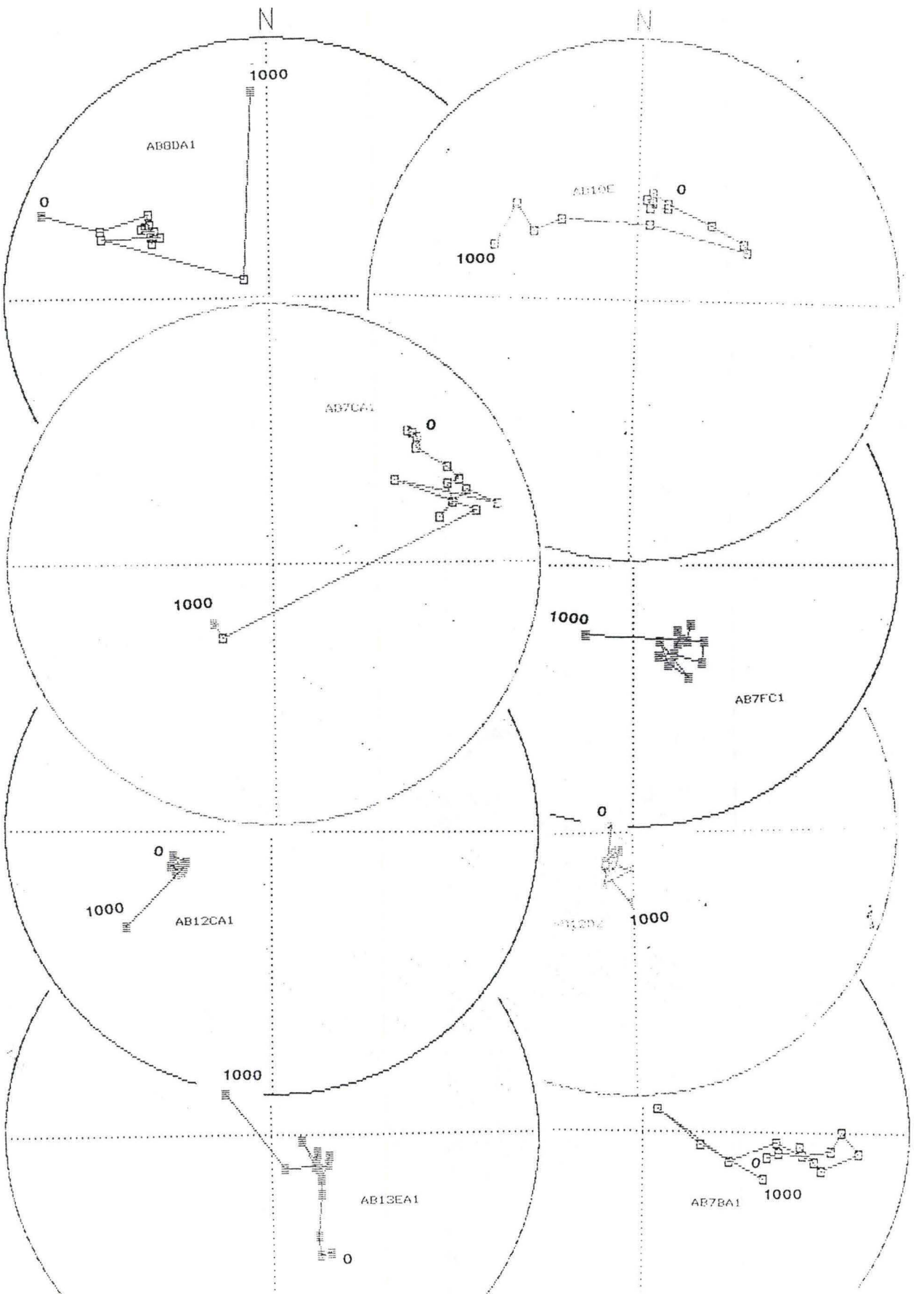
N
1000
AB8DA1
0
N
AB10E
0
1000
AB7CA1
0
1000
1000
AB7FC1
0
AB12CA1
0
1000
1000
1000
AB13EA1
0
AB7BA1
0
1000

Figure 4.24: Typical examples of progressive orthogonal AF demagnetization diagrams of Zone II specimens.

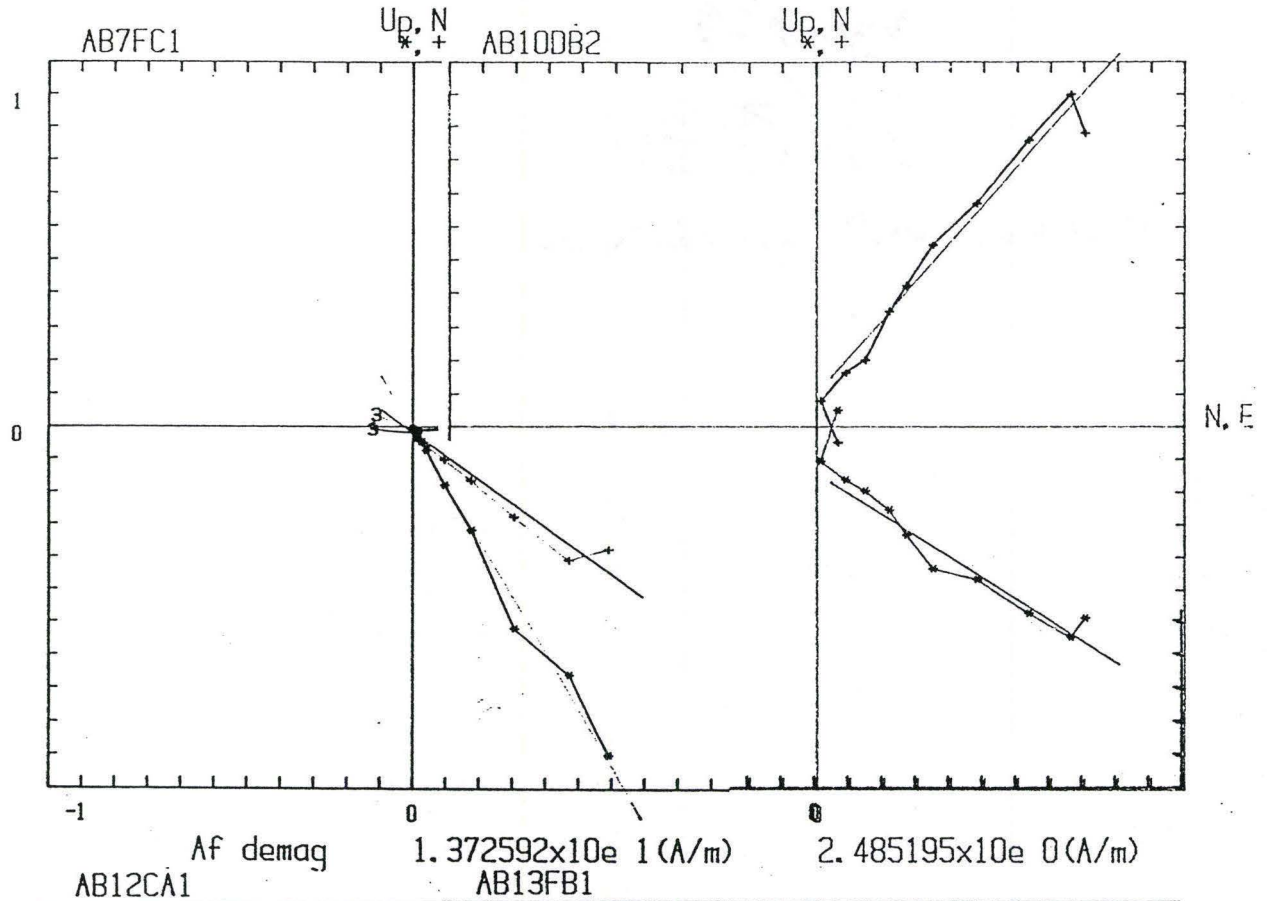
AB7FC1
Up, N
AB10DB2
Up, N
1
0
N, E
-1
0
0
Af demag
1.372592x10e 1(A/m)
2.485195x10e 0(A/m)

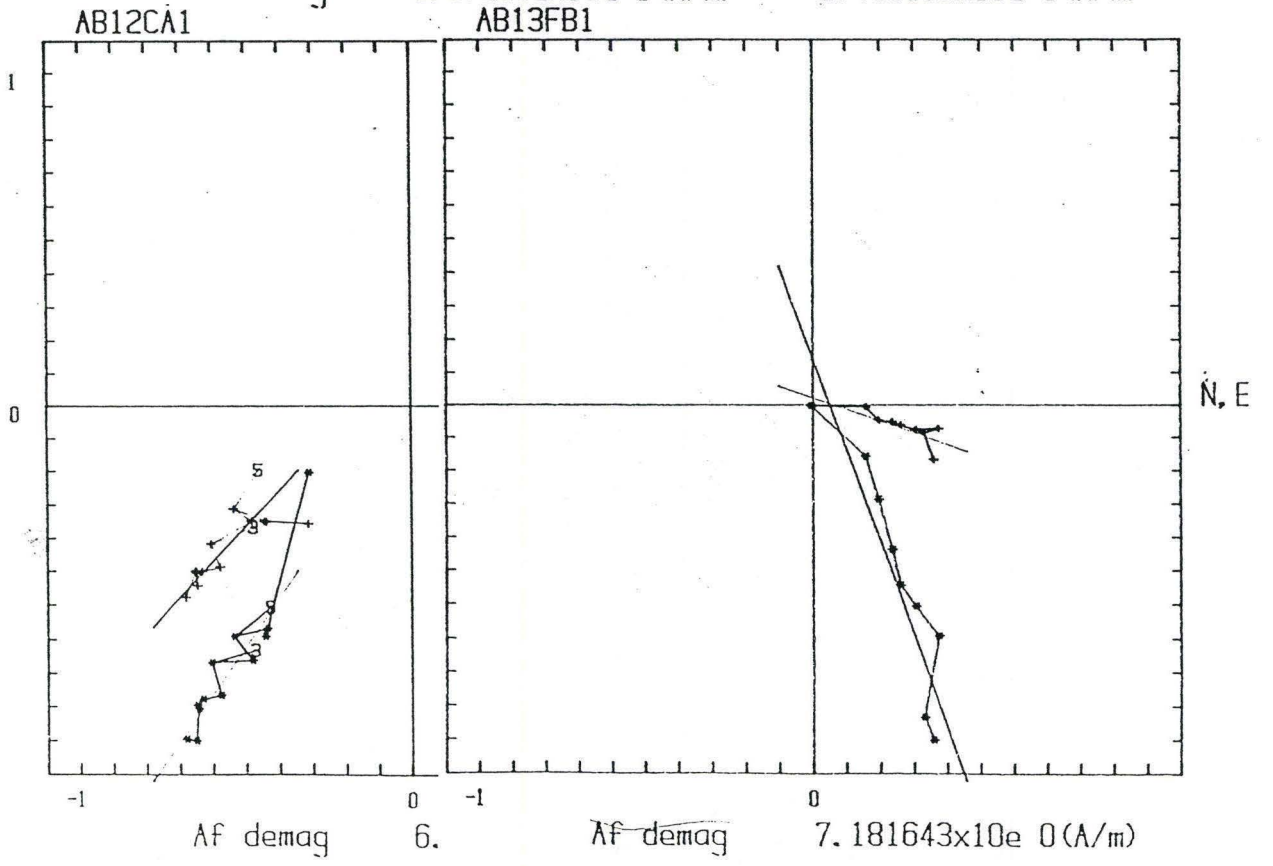
AB12CA1
AB13FB1
1
0
N, E
-1
0
-1
0
Af demag
6.
Af demag
7.181643x10e 0(A/m)

Figure 4.25: Typical examples of equal area stereographic projection of residual magnetic directions of Zone II specimens during step wise Thermal demagnetization.

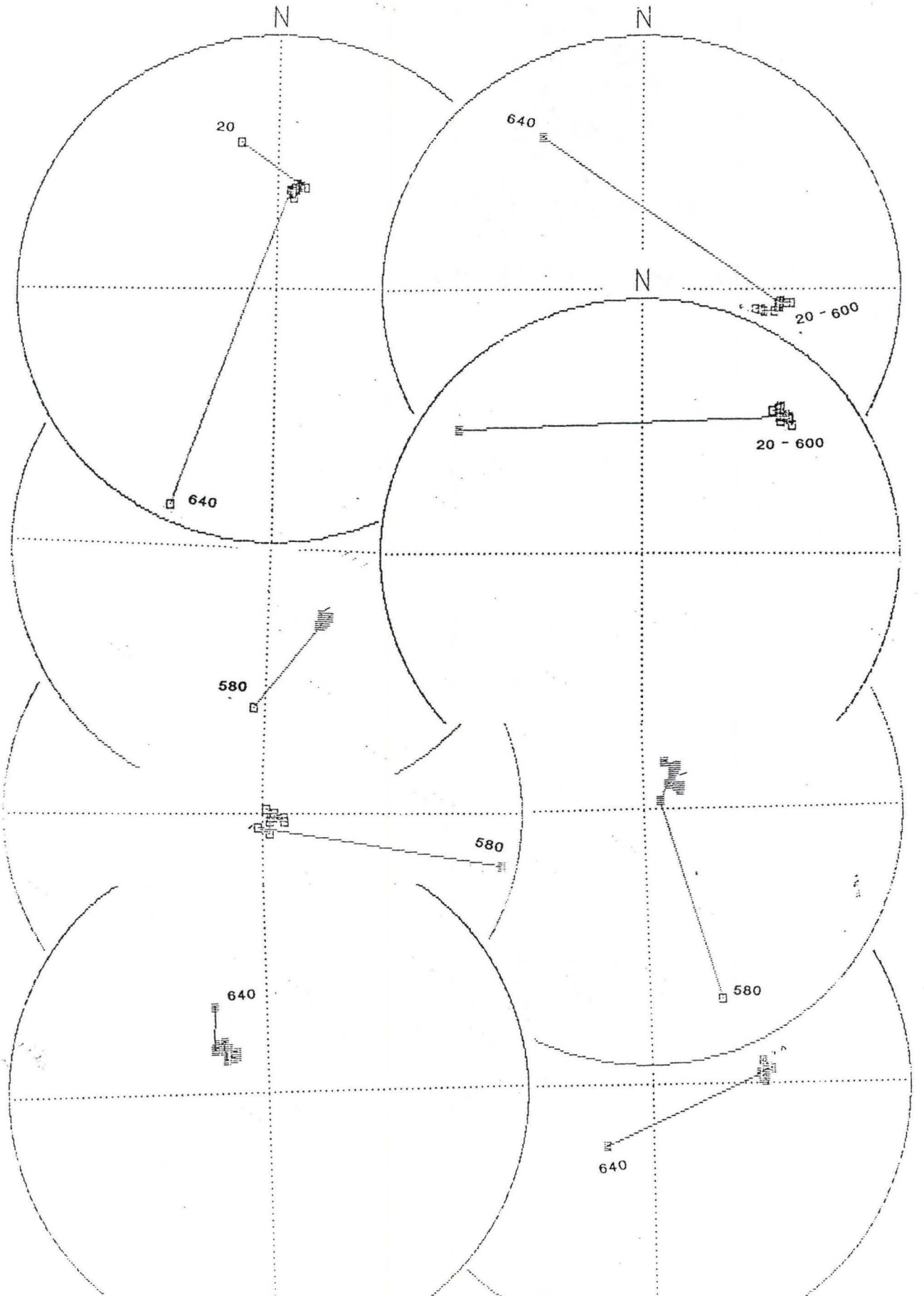
N
20
640
N
640
20 - 600
N
20 - 600
580
580
640
580
640

Figure 4.26: Typical examples of progressive orthogonal Thermal demagnetization diagrams of Zone II specimens.

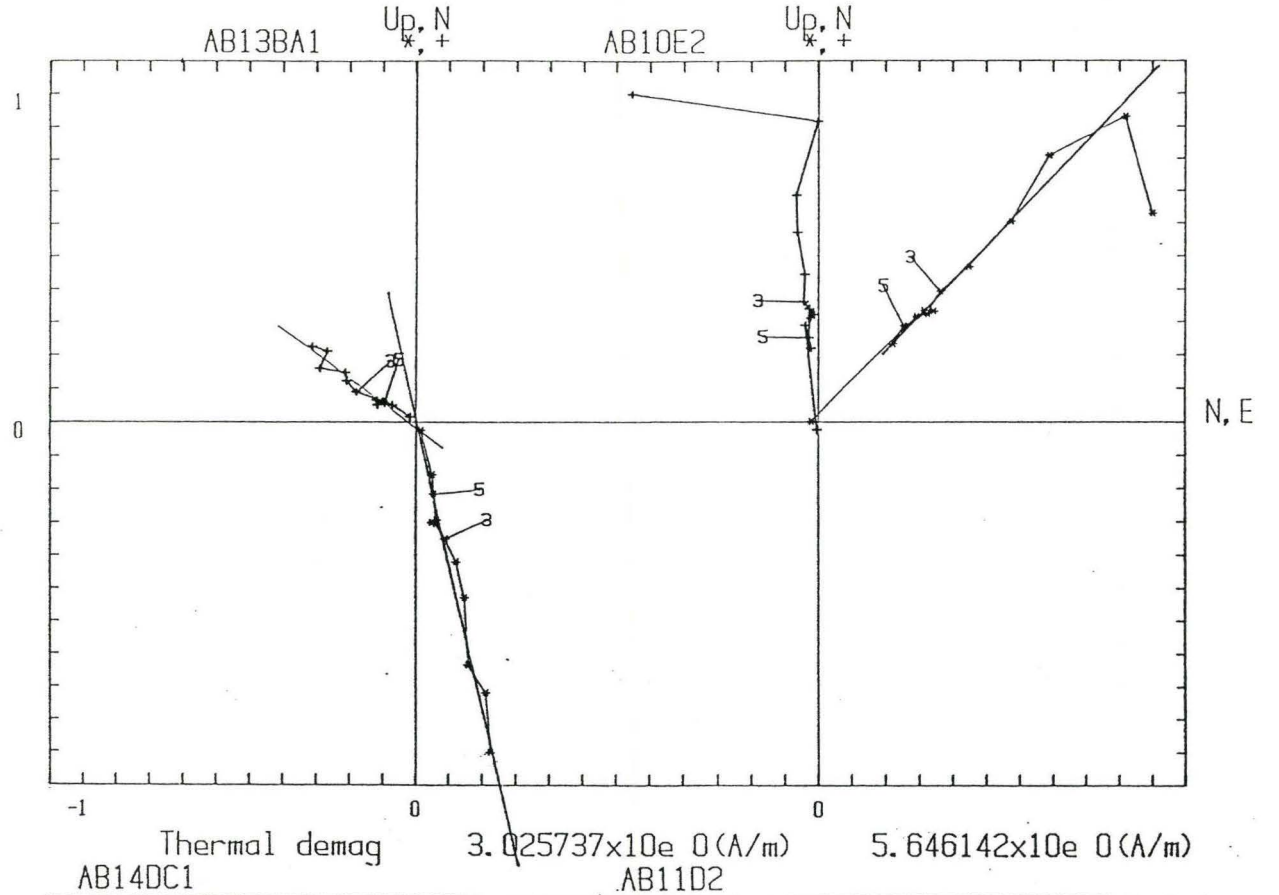
AB13BA1
Up, N
*, +
AB10E2
Up, N
*, +
1
0
-1
0
0
N, E
3
5
Thermal demag
3.025737x10e 0(A/m)
5.646142x10e 0(A/m)

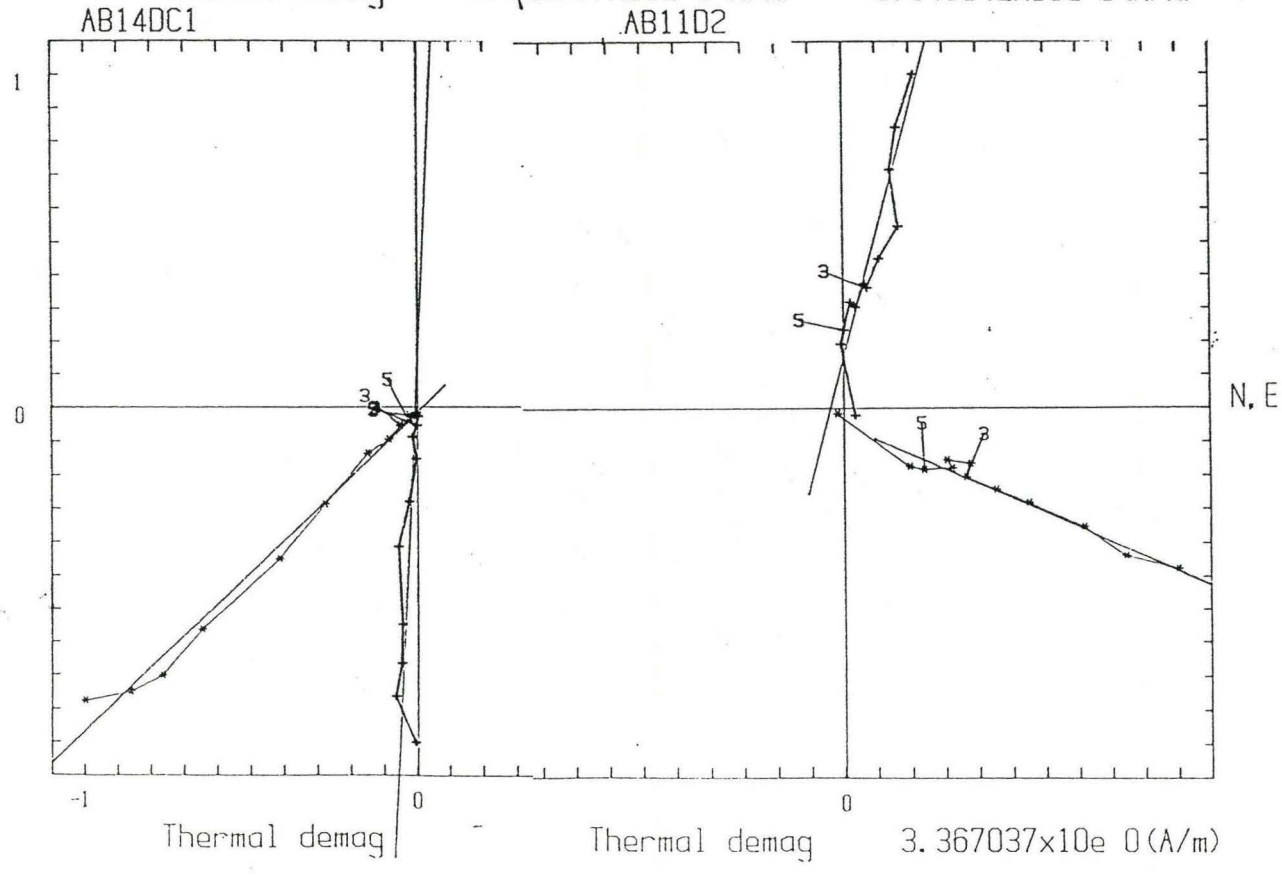
AB14DC1
AB11D2
1
0
-1
0
0
N, E
3
5
Thermal demag
Thermal demag
3.367037x10e 0(A/m)

present. Although these magnetizations are stable, their MDF's and 50% NRM removal temperatures are lower than the Zone I specimens. Some specimens show unstable moving behavior during AF demagnetization (Fig. 4.23a).

4.5.3 Zone III

31 specimens were demagnetized by AF method from this zone. 18 specimens show stable end points. 12 of these have positive steep westerly directions (Fig. 4.27). Zijderveld diagrams show that 10 specimens possess single component magnetizations decaying smoothly to the origin. Typical examples are shown in figure 4.28.

33 specimens were demagnetized by Thermal methods from this zone. 13 specimens exhibit Westerly steep positive directions as shown in figure 4.29 and 20 specimens possess scattered random magnetization. Zijderveld diagrams show that 9 specimens have single component magnetization which decays to the origin making a straight line and 3 specimens show two component magnetization. Typical examples are shown in figure 4.30.

Most of the stable directions from this zone are Westerly steep and positive. Some directions with intermediate negative and steep positive polarities are present in northeastern quadrant. These directions agree on sample and site level. They are mostly single component showing very little change in direction even after demagnetization upto 1000 Oe. (100 mT) applied peak field or 600°C temperature. These magnetizations have comparatively low MDF's (mostly below 10 mT) and their 50% NRM removal temperatures are below 300°C.

Figure 4.27: Typical examples of equal area stereographic projection of residual magnetic directions of Zone III specimens during step wise AF demagnetization.

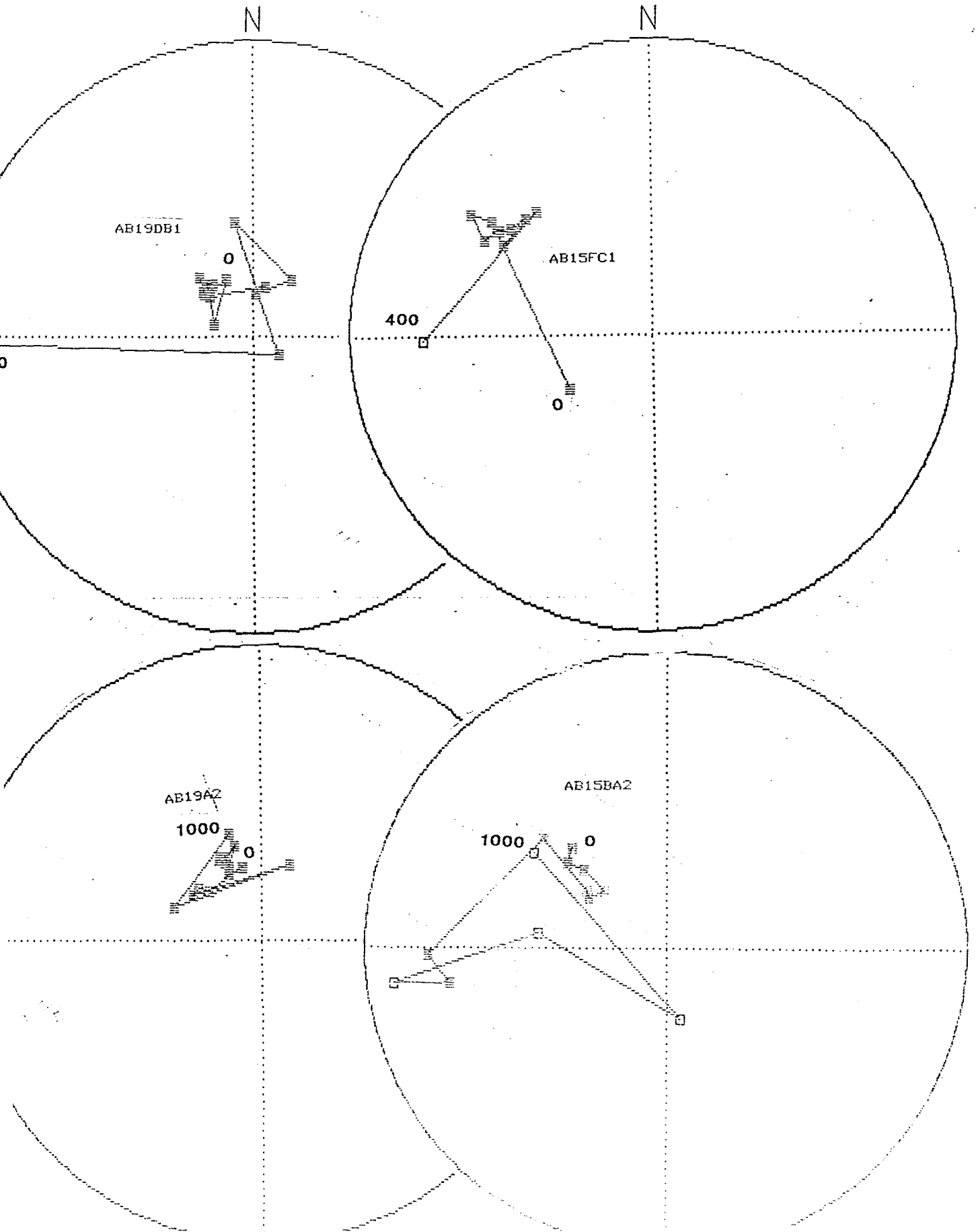
N
AB19DB1
0
0
N
AB15FC1
400
0
AB19A2
1000
0
AB15BA2
1000
0

Figure 4.28: Typical examples of progressive orthogonal AF demagnetization diagrams of Zone III specimens.

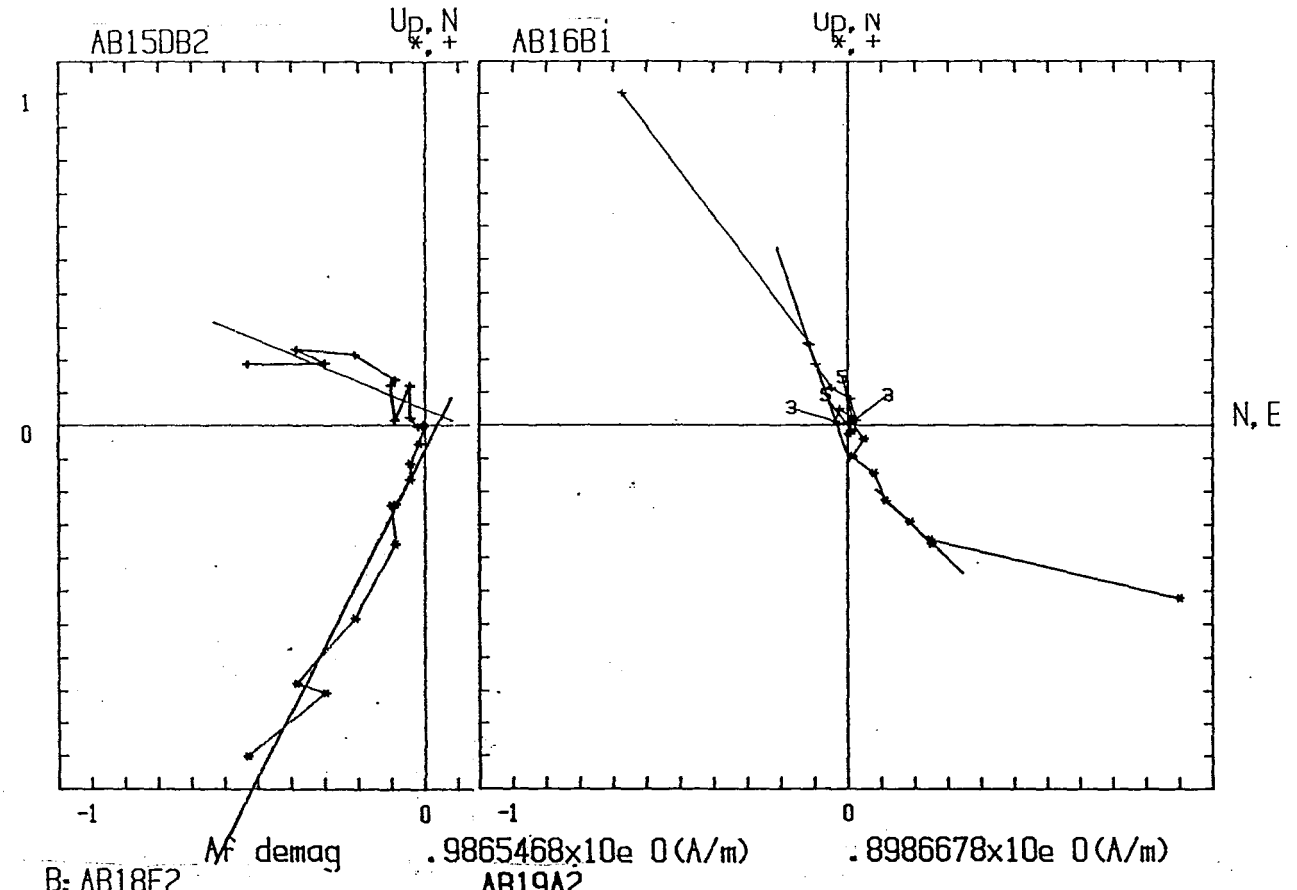
AB15DB2
Up, N
AB16B1
Up, N
1
0
-1
0
-1
0
N, E
Af demag
.9865468x10e 0(A/m)
.8986678x10e 0(A/m)

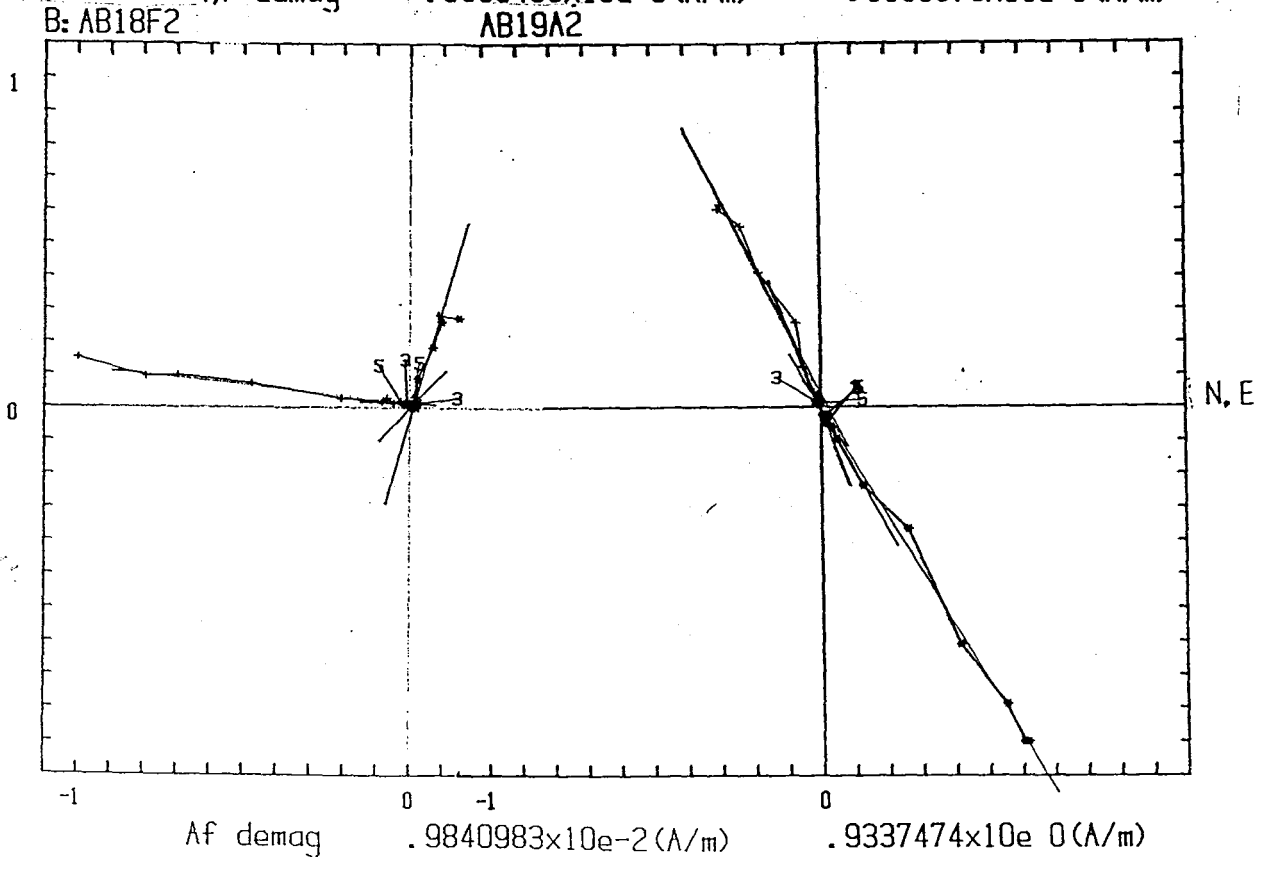
B: AB18F2
AB19A2
1
0
-1
0
-1
0
N, E
Af demag
.9840983x10e-2(A/m)
.9337474x10e 0(A/m)

Figure 4.29: Typical examples of equal area stereographic projection of residual magnetic directions of Zone III specimens during step wise Thermal demagnetization.

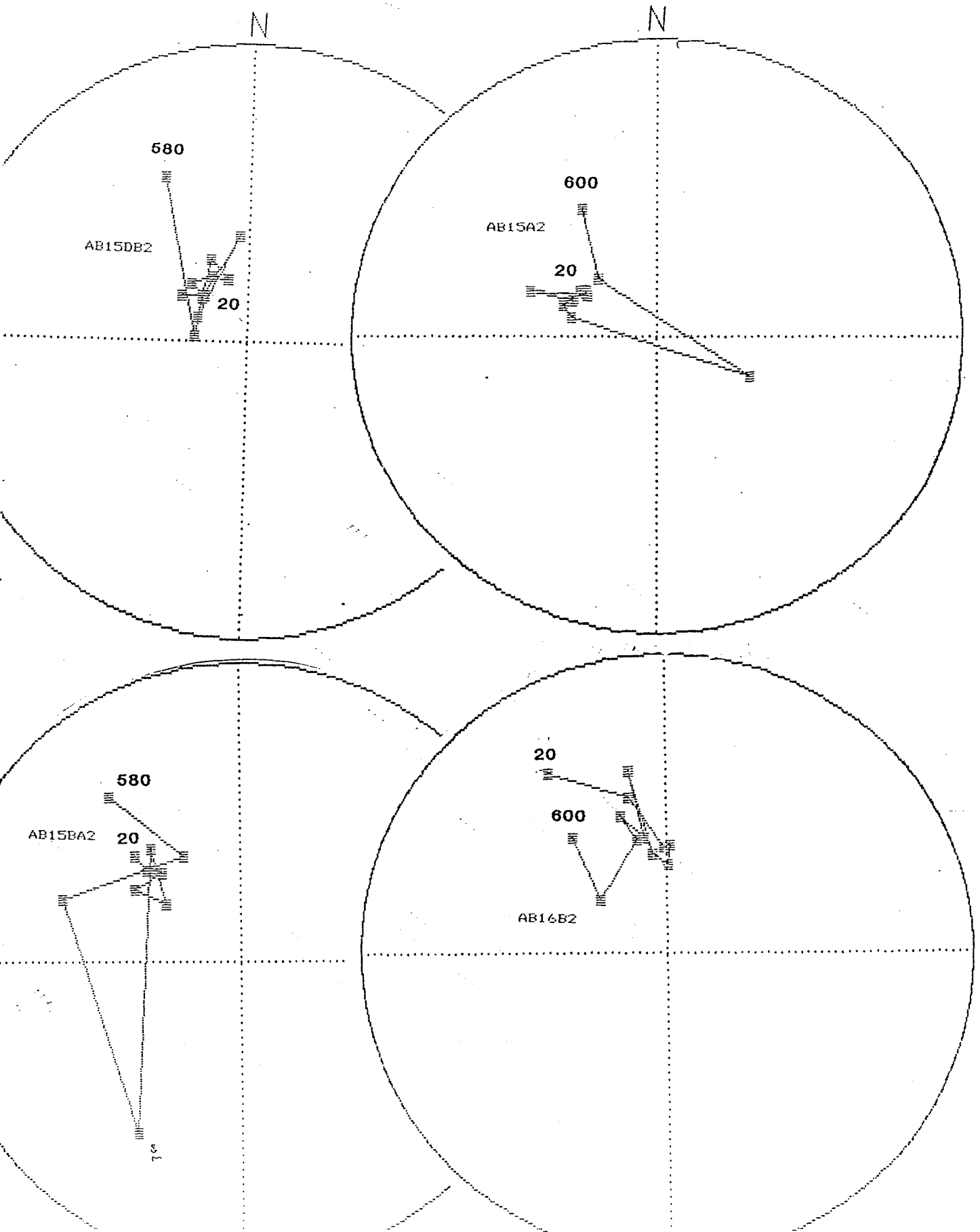
N
580
AB15DB2
20
N
600
AB15A2
20
580
AB15BA2
20
20
600
AB16B2

Figure 4.30: Typical examples of progressive orthogonal Thermal demagnetization diagrams of Zone III specimens.

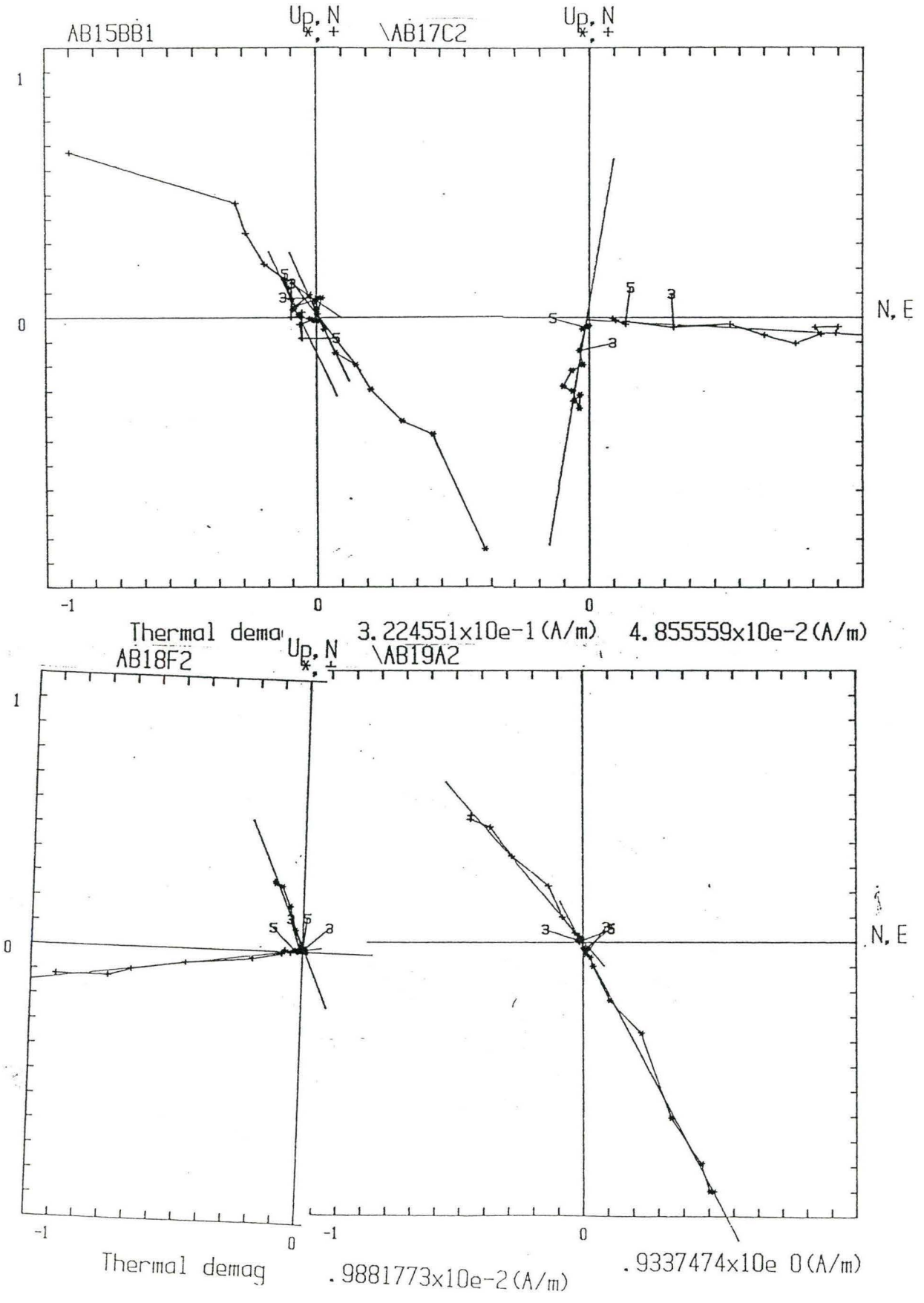
AB15BB1
Up, N
\AB17C2
Up, N
N, E
Thermal dema
3.224551x10e-1(A/m)
4.855559x10e-2(A/m)
AB18F2
Up, N
\AB19A2
N, E
Thermal demag
.9881773x10e-2(A/m)
.9337474x10e 0(A/m)

4.5.4 Zone IV

26 specimens were demagnetized by AF methods. 11 specimens show stable end points. 7 of them possess north-easterly intermediate positive directions, and 2 specimens show swinging end points. Typical examples are shown in figure 4.31. Zijderveld diagrams show that 3 specimens possess single component magnetization decaying to the origin univectorilly and 5 specimens show two or more component magnetization. Typical examples are shown in figure 4.32.

27 specimens were demagnetized by thermal methods from this zone. 5 specimens possess easterly positive intermediate stable direction as shown in figure 4.33 and 21 specimens show randomly scattered directions. Zijderveld diagrams show 2 specimens possessing single component magnetization and 8 specimens possessing two or more components of magnetization as shown in figure 4.34.

Most of the stable directions from this zone come from the site AB21 and AB23 specimens. These directions agree well on sample and site level. Site AB23 directions are northeasterly, intermediate and positive and the site AB21 directions are westerly, positive and steep, similar to the zone III directions. They are mostly single component showing very little change in direction even after demagnetization upto 1000 Oe. (100 mT) applied peak field or 600°C temperature. The magnetizations found in site AB23 specimens have high MDF's and High 50% NRM removal temperatures.

Figure 4.31: Typical examples of equal area stereographic projection of residual magnetic directions of Zone IV specimens during step wise AF demagnetization.

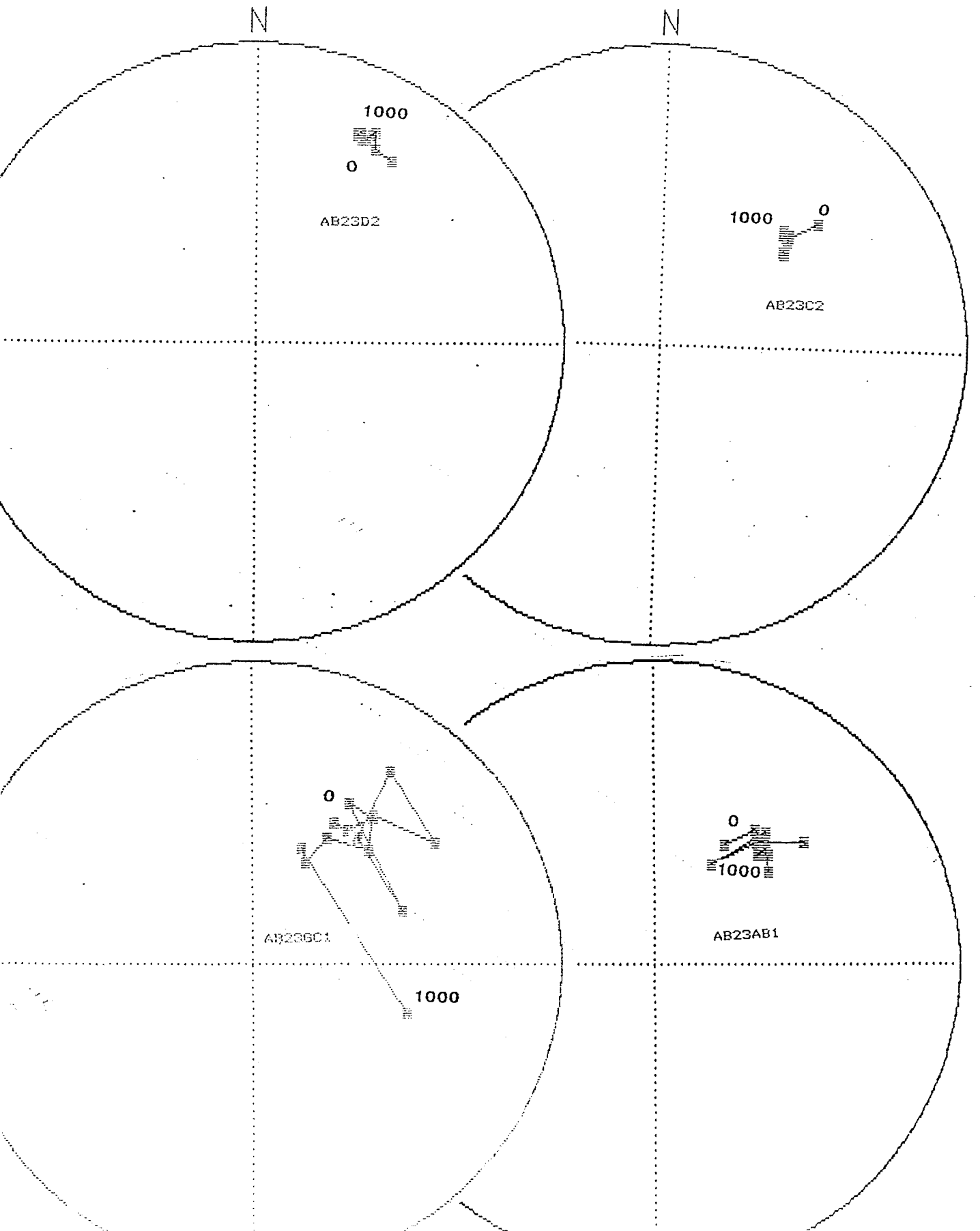
N
1000
0
AB23D2
N
1000
0
AB23C2
0
AB23C1
1000
0
1000
AB23AB1

Figure 4.32: Typical examples of progressive orthogonal AF demagnetization diagrams of Zone IV specimens.

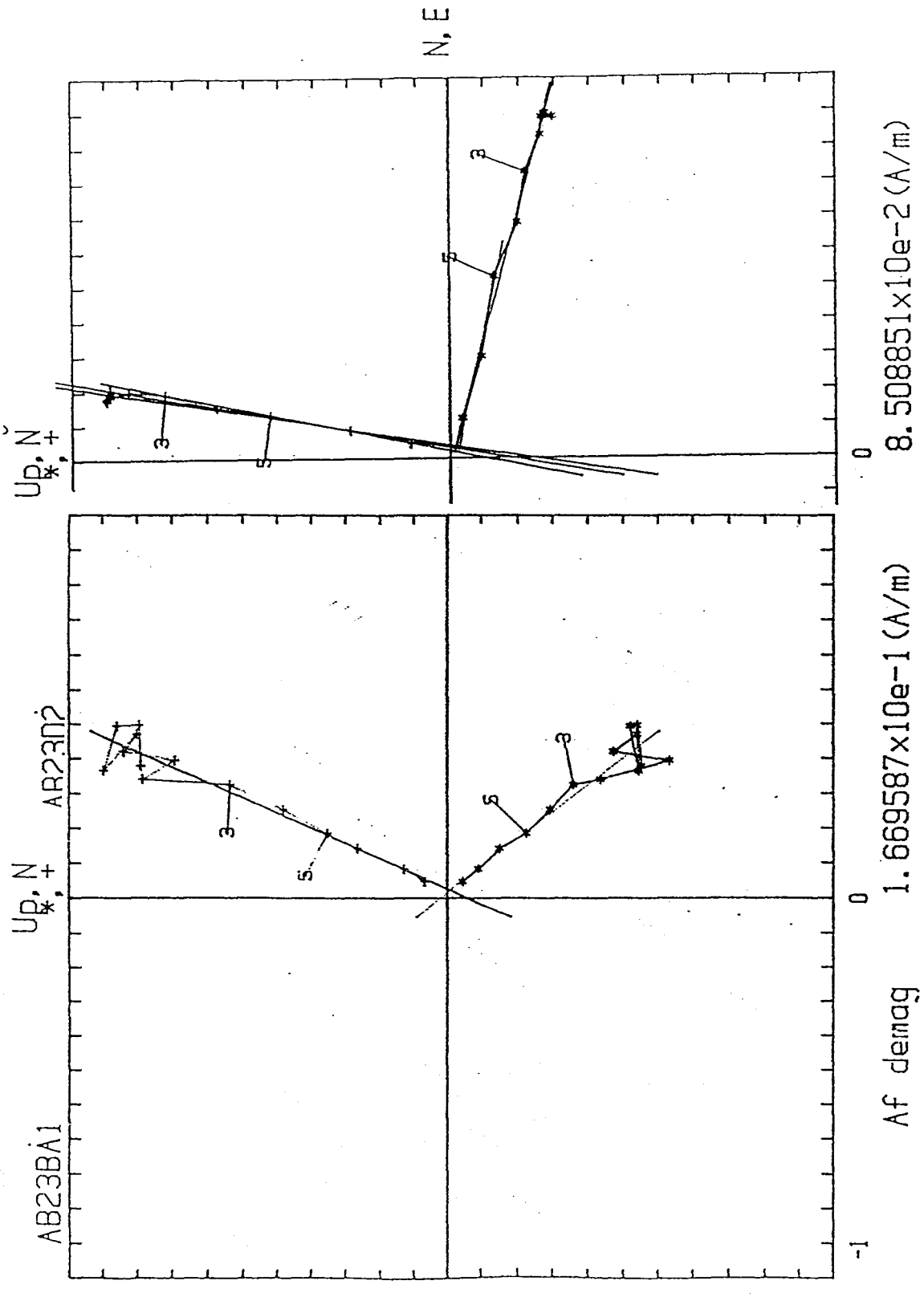
N, E
Up, N
8.508851x10e-2 (A/m)
AB23BA1
AR23D2
1.669587x10e-1 (A/m)
Af demag
0
-1
3
5

Figure 4.33: Typical examples of equal area stereographic projection of residual magnetic directions of Zone IV specimens during step wise Thermal demagnetization.

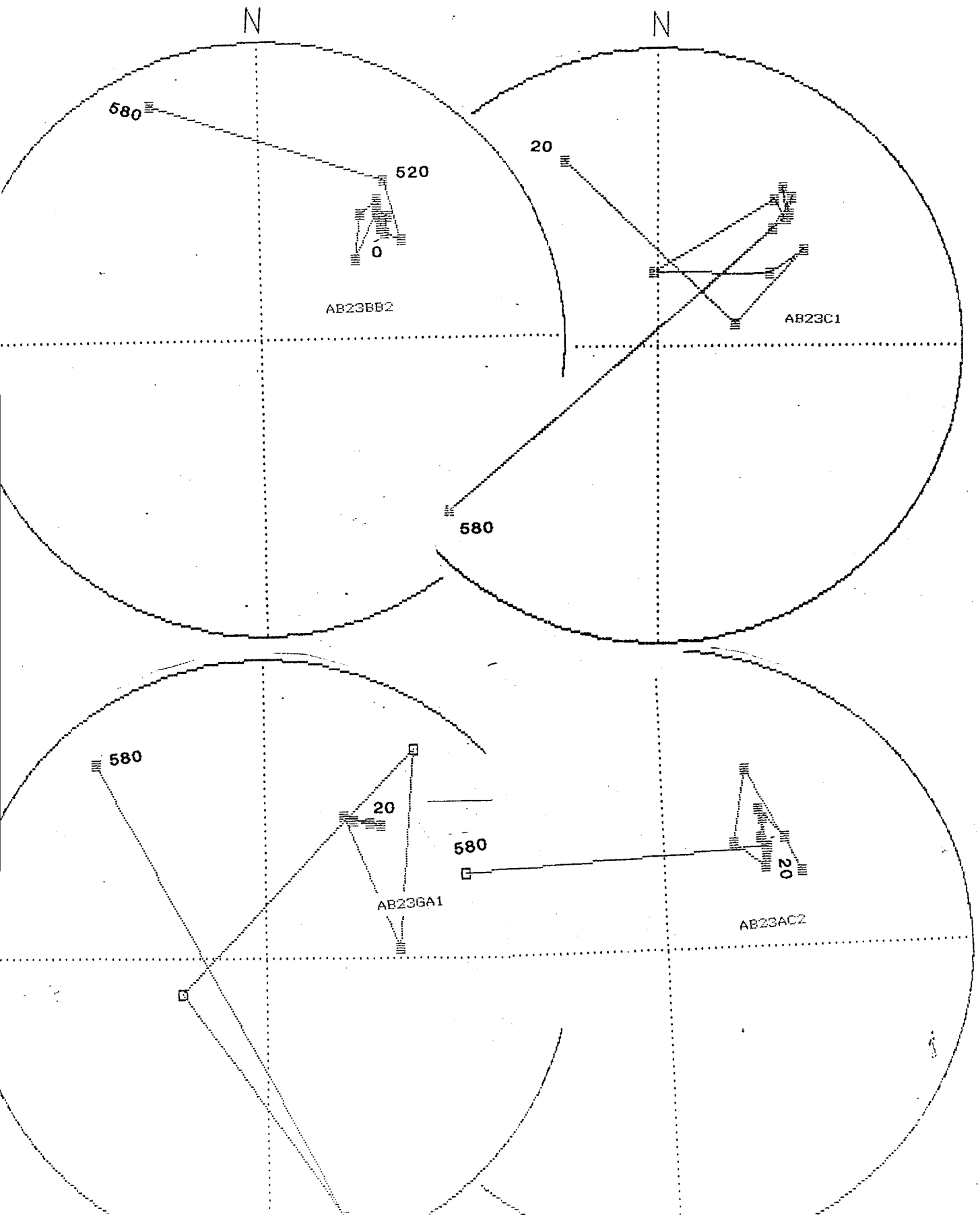
N
580
520
0
AB23BB2
N
20
AB23C1
580
580
20
580
AB23GA1
20
AB23AC2

Figure 4.34: Typical examples of progressive orthogonal Thermal demagnetization diagrams of Zone IV specimens.

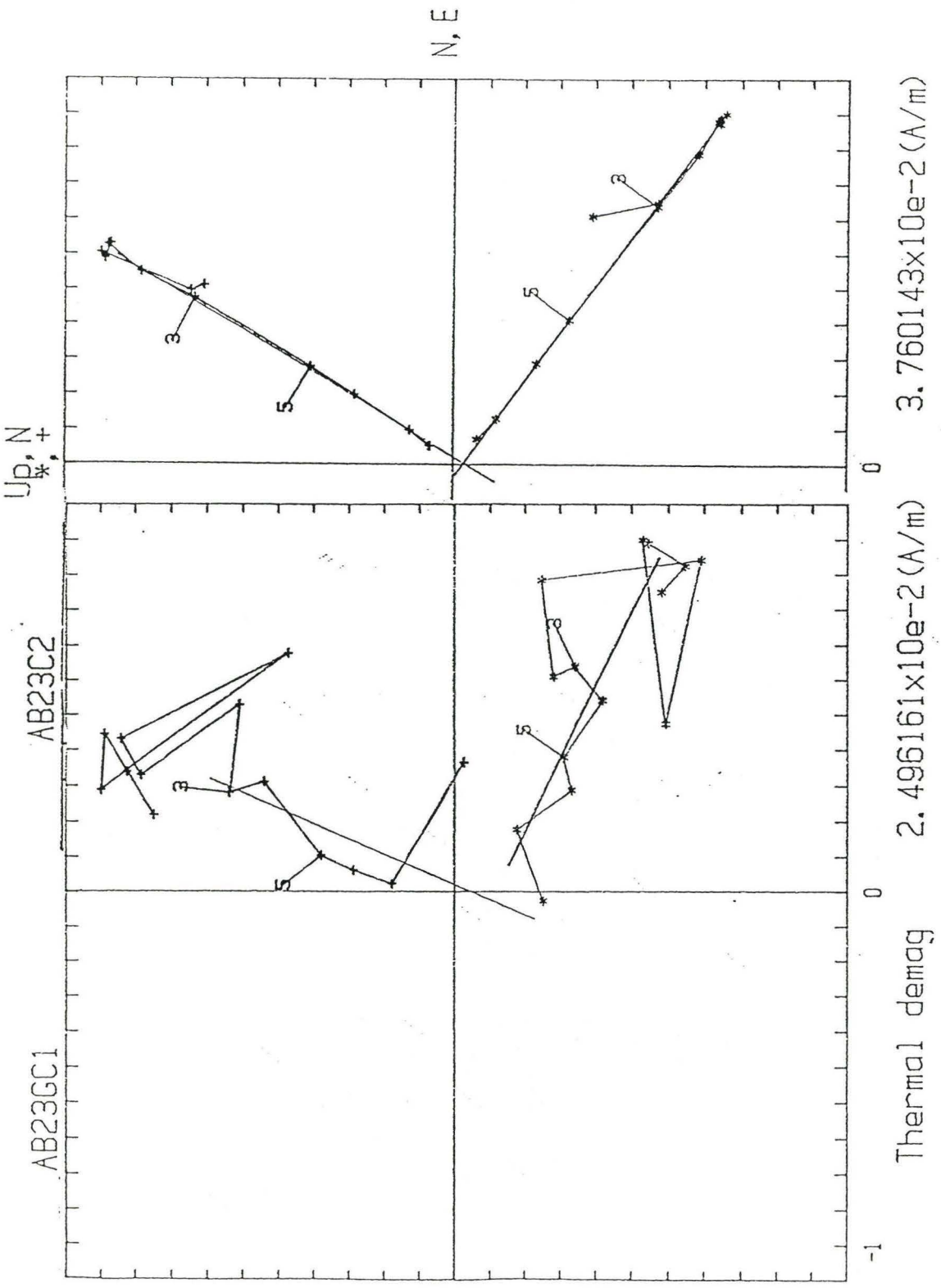
N, E
Up, N
*, +
AB23C2
AB23GC1
3
5
0
-1
Thermal demag
2.496161x10e-2(A/m)
3.760143x10e-2(A/m)

4.6 Characteristic Directions

Characteristic directions were analyzed by visual inspection of Zijderveld diagrams (Zijderveld 1967) for straight line segments, stereonet plots for stable end points, and the principal component analysis by the use of a Basic language computer program (Kirschvink 1980), by linear least square fitting of the linear segments obtained on orthogonal vector plots. If the error in least square fitting was greater than $\pm 12°$ then stable end points on stereonet plots were selected by visual inspection.

Stable end points of the 188 specimens obtained by the above mentioned criteria from four zones after progressive demagnetization upto 100 mT or 600°C are plotted on separate equal area stereonets in Figure 4.35. 38specimens did not yield any stable directions. It can be seen from the figure 4.35 that the directions obtained from the four zones are different and can be distinguished. Zone I specimens (Fig. 4.35a) show dominantly negative directions. There are few specimens that give positive directions. These positive directions lie in the southern and north-western parts of the stereonet. There is a well grouped southerly, steep and negative polarity cluster. This group of directions is the characteristic direction of zone I specimens. The stable directions obtained from zone II specimens (Fig. 4.35b) are scattered all over the stereonet. Both normal and reversed polarities are present. Only sites AB10, AB11 and AB13 from this zone show easterly intermediate to steep positive directions that are very poorly grouped. Zone III specimens (Fig. 4.35c) show dominantly positive, north-westerly steep directions. Very few reversed polarities are present, but they are not grouped at sample or site level. The northwesterly, steep positive group of directions is characteristic of zone III specimens. The directions obtained

Figure 4.35: Equal area stereographic projections of characteristic magnetization directions obtained from specimens of (a) Zone I, (b) Zone II, (c) Zone III, and (d) Zone IV. Open circles indicate upward directions and solid circles indicate downward directions.

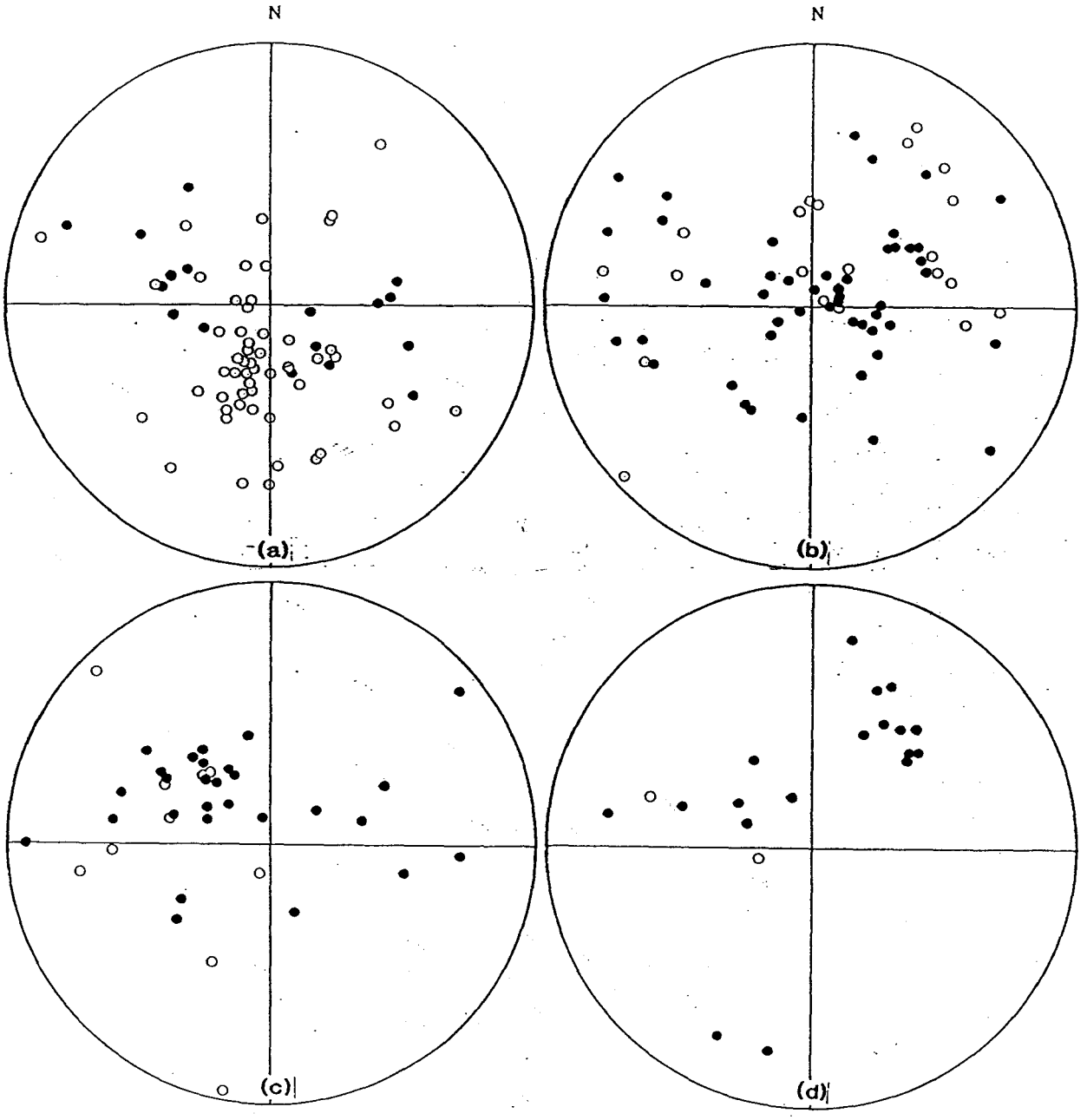
N
N
(a)
(b)
(c)
(d)

from zone IV can be distinguished into two groups (Fig. 4.35d). One group is seen in the northwestern quadrant of the stereonet. These directions are obtained from site AB21 and AB22 specimens and seem to resemble the zone III characteristic directions. The other group seen in the northeastern quadrant is obtained from the site AB23 specimens. These directions are well grouped at sample and site level and are characteristic of the site AB23 specimens only. Few scattered reversed polarities are also seen from zone IV specimens.

These clusters of stable directions from different zones appear after demagnetization. Most of the magnetizations are single component and after demagnetization they remain stable close to the NRM directions. There are some specimens which show unstable behavior i.e., they seem to be moving from one point to another, not stabilizing at one point.

4.7 Averaging of Directions

Averaging of the stable directions was carried out at three levels i.e., sample, site and zonal levels.

At first level, Sample Mean Directions were obtained by averaging the specimen directions. 2-4 specimens were used to obtain sample averages. If the direction of a specimen disagreed with the other specimen directions from the same sample by more than 50° it was rejected. Only 1% specimen directions were rejected at this level.

At second level, Site Mean Directions were obtained by averaging the sample mean directions. 2-6 sample averages were used to obtain the site mean directions.

If the direction of a sample disagreed with the other sample directions from the same site by more than 50° it was rejected. 37% sample directions were rejected at this level.

Summary of Site Average Directions is given in table 4.1 and they are plotted on stereographic nets in figure 4.36

Finally, Zonal Mean Directions were obtained by averaging the Site Mean Directions. 3-6 site averages were used to obtain the zonal mean directions.

Summary of Zonal Average Directions and their corresponding palaeomagnetic poles is given in Table 4.2. and the zonal averages directions are plotted on stereographic nets in figure 4.37 with their respective site average directions.

Averages for sites AB6, AB7, AB8, AB11, AB14, AB18, AB20 and AB22 could not be obtained because their sample directions failed to pass the above mentioned criteria. It is interesting to note from figure 1.1 that sites AB7, AB8, AB11 and AB14 from zone II and sites AB16 and AB20 from zone III lie near the shear zone (along the PDF). The specimens from sites near the PDF mostly fail to pass the above mentioned selection criteria and hence yield no characteristic sample or site directions. However, the directions of specimens from some sites located near the shear zone e.g., AB9, AB10, AB12, AB13 and AB16 do agree on sample and site level but these directions do not agree on zonal levels. It implies that the magnetization in the shear zones have either been scattered or have been locally rotated.

Table 4.1: Summary of Site Average Directions
(Before Structural Corrections)

Site	N	Dec	Inc	F.Kappa	α_{95}
AB01	4	277.0	-54.0	4.0	53.0
AB02	3	187.0	-75.0	41.0	19.0
AB03	5	205.0	-41.0	30.0	14.0
AB04	4	188.0	-60.0	33.0	16.0
AB05	6	172.0	-57.0	10.0	23.0
AB06	-	—	—	—	—
ABM	4	147.0	-67.0	3.0	69.0
AB07	-	—	—	—	—
AB08	-	—	—	—	—
AB09	2	63.0	-30.0	30.0	47.0
AB10	3	54.0	37.0	20.0	28.0
AB11	-	—	—	—	—
AB12	3	265.0	50.0	5.0	66.0
AB13	4	106.0	49.0	9.0	33.0
AB14	-	—	—	—	—
AB15	5	306.0	46.0	34.0	13.0
AB16	4	78.0	41.0	7.0	38.0
AB17	2	284.0	38.0	31.0	46.0
AB18	-	—	—	—	—
AB19	3	320.0	52.0	74.0	14.0
AB20	-	—	—	—	-.0
AB21	4	297.0	52.0	9.0	33.0
AB22	-	—	—	—	—
AB23	6	34.0	29.0	28.0	13.0

N = No. of Samples
Dec = Declination
Inc = Inclination
k = F. Kappa (A measure of scatter of N vectors)
α_{95} = Angle of 95% probability of true mean direction

Figure 4.36: Equal area stereographic projections of site average directions for Zone I (a), Zone II (b), Zone III (c) and Zone IV (d).

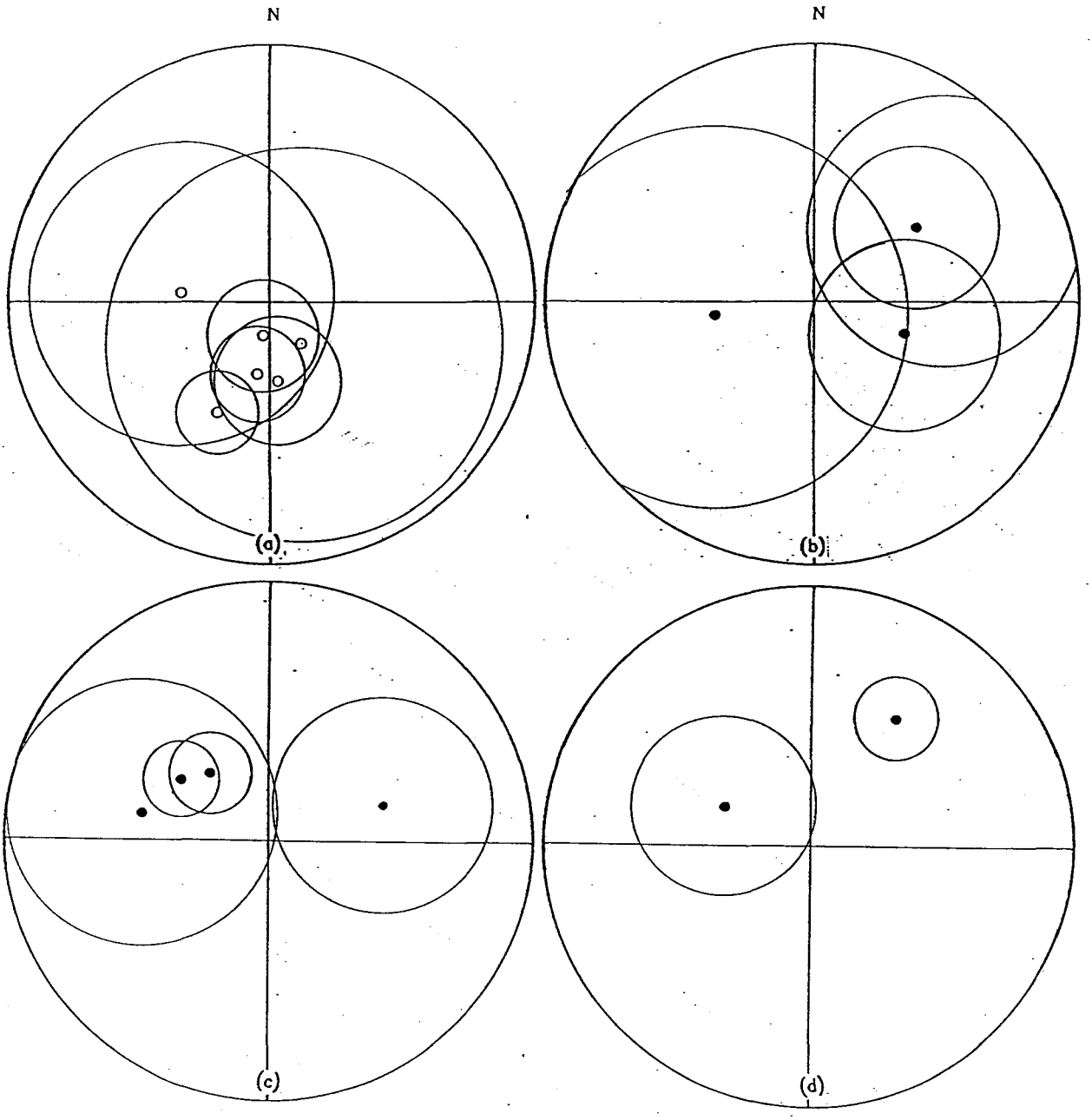
N
N
(a)
(b)
(c)
(d)

Figure 4.37: Equal area stereographic projections of zonal average directions for Zone I, Zone II, Zone III, and Zone IV with their respective site average directions.

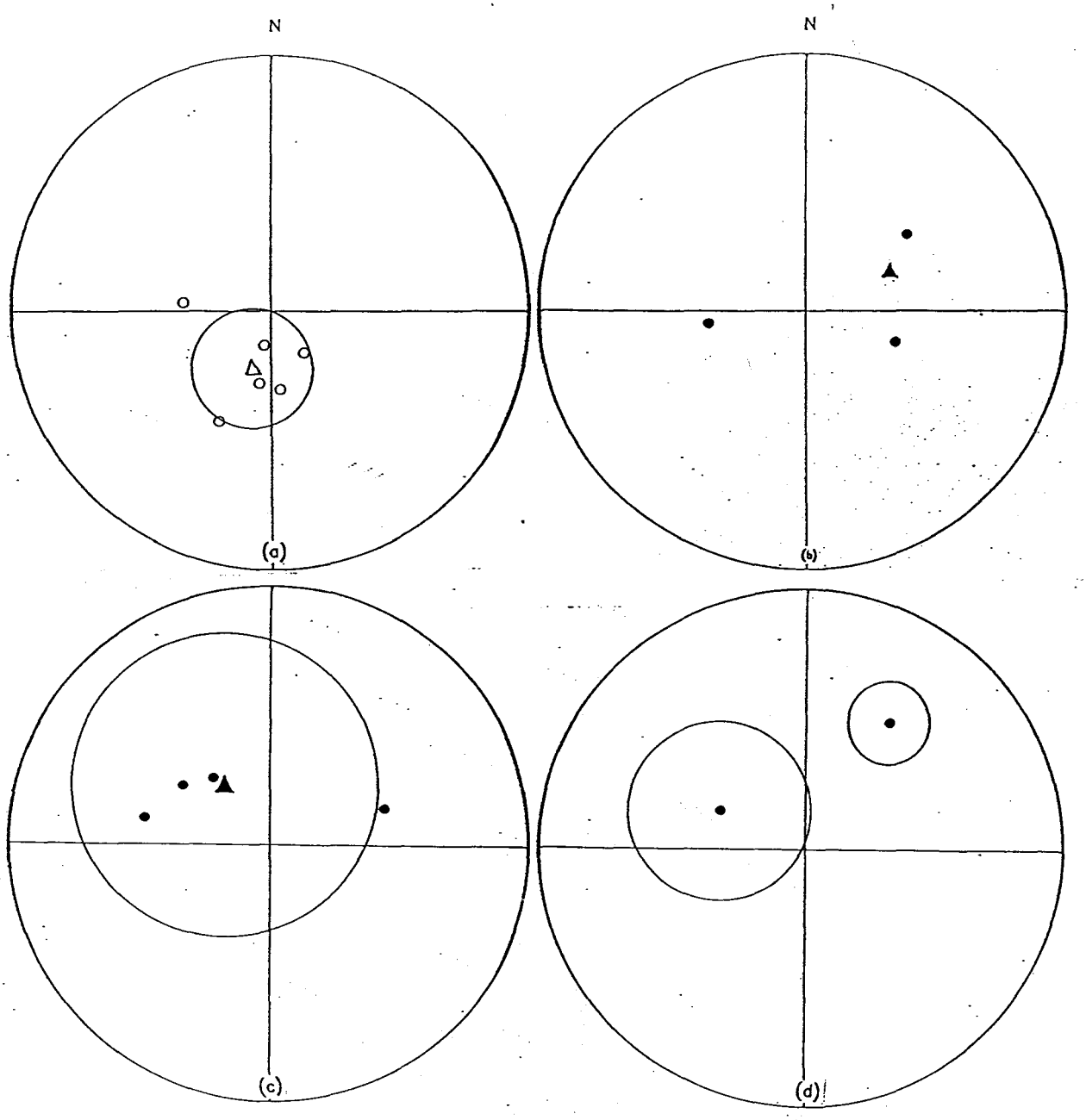
N
N
(a)
(b)
(c)
(d)

Table 4.2: Summary of Palaeomagnetic Results Before Structural Corrections.

Zone/Site	N	Dec	Inc	k	α_{95}	Lat	Long	d_p	d_m
Zone I	6	197.0	-65.0	11.0	21.0	78.0	165.0	40.0	10.0
Zone II	4	66.0	48.0	2.0	—	36.0	166.0	112.0	129.0
Zone III	3	301.0	46.0	31.0	23.0	41.0	346.0	26.0	24.0
Site AB23	6	34.0	29.0	28.0	13.0	47.0	207.0	17.0	10.0

N	=	No. of Sites (Samples) for Zones (Sites)
Dec	=	Declination
Inc	=	Inclination
k	=	F. Kappa (A measure of scatter of N vectors)
α_{95}	=	Angle of 95% probability of true mean direction
Lat	=	Ancient Latitude
Long	=	Ancient Longitude
d_p&d_m	=	Polar errors

4.8 Structural Correction of Stable Directions

The Fold test proposed by Graham, 1949 was applied and the site average directions obtained were corrected for the local strike and dip of the rocks (Collinson, 1983). Geo-information map sheets of the Ministry of Energy and Resources, Govt. of Quebec were used to obtain the local strike and dip of the sites.

Zone I mean direction after structural correction (Dec=154.0, Inc=-35.0, k=13.0, α_{95}=19.0, N=6 sites) shows some improvement in k (Fisher Kappa, a measure of the scatter of directions) and α_{95} (the angle of 95% probability of true mean direction) as compared to the Zone I uncorrected mean direction (Dec=197.0, Inc=-65.0, k=11.0, α_{95}=21.0, N=6 sites). Although this improvement is very small, it is evidence suggesting that the Zone I magnetization is pre-folding and hence, may be Archean

in age.

The rotated Zone II mean direction (Dec=68.0, Inc=52.0, k=2.0, N=4 sites) does not show any improvement in k and α_{95} compared to the unrotated Zone II mean direction (Dec=66.0, Inc=47.0, k=2.0, N=4 sites). Very low value for k and very large values for α_{95} imply that these directions are randomly distributed. Since the Zone II sites are located near the PDF zone, their magnetization may have been destroyed by shearing (Hale and Lloyd, 1989).

The rotated Zone III mean direction (Dec=211, Inc=-23, k=3.0, N=4 sites) also does not show any improvement in k and α_{95} as compared to the unrotated Zone III mean direction (Dec=323, Inc=59, k=4.0, N=4 sites). After structural corrections three sites (AB15, AB17 and AB19) from this zone are well grouped and give a zonal mean direction (Dec=213.0, Inc=-43.0, k=16.0, α_{95}=32.0, N=3 sites). Site AB16 which lies near the fault zone (see figure 1.1) gives a different magnetization direction which does not agree with the other site mean directions of this zone. The structurally corrected directions from sites AB15, AB17 and AB19 are similar to the southerly, negative directions obtained from Zone I sites in inclination and polarity, but differ significantly in declination.

The rotated mean directions from Zone IV sites shift to the southwestern quadrant with out any change in their statistics because same the structural correction was applied to all the sites.

Summary of Zonal Average Directions and their corresponding palaeomagnetic poles after structural corrections is given in Table 4.3 and the zonal average directions are plotted in figure 4.38 with their respective site average directions.

Figure 4.38: Equal area projection of structurally corrected zonal average directions for ZoneI, II, III and IV with their respective site averages. Open(closed) symbols are used for upper (lower) hemisphere directions.

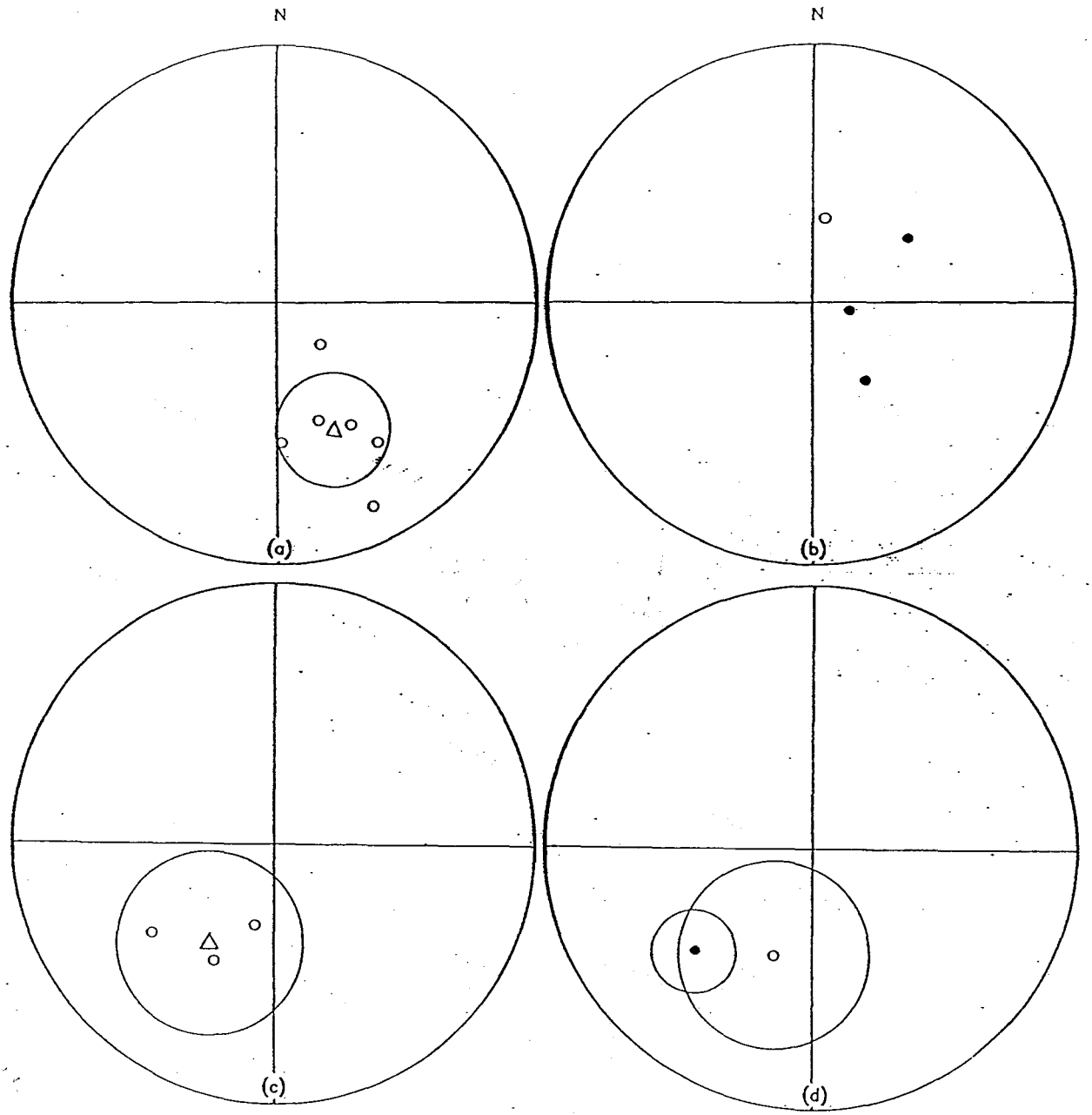
N
N
(a)
(b)
(c)
(d)

Table 4.3: Summary of Palaeomagnetic Results After Structural Corrections.

Zone/Site	N	Dec	Inc	k	α_{95}	Lat	Long	d_p	d_m
Zone I	6	154.0	-35.0	13.0	19.0	54.0	304.0	29.0	14.0
Zone II	4	68.0	52.0	2.0	—	38.0	160.0	130.0	160.0
Zone III	3	214.0	-43.0	16.0	32.0	55.0	199.0	48.0	25.0
Site AB23	6	229.0	210.0	28.0	13.0	-4.0	21.0	6.0	15.0

N	=	No. of Sites (Samples) for Zones (Sites)
Dec	=	Declination
Inc	=	Inclination
k	=	F. Kappa (A measure of scatter of N vectors)
α_{95}	=	Angle of 95% probability of true mean direction
Lat	=	Ancient Latitude
Long	=	Ancient Longitude
d_p&d_m	=	Polar errors

4.9 Palaeomagnetic Rotation

Figure 4.39 is a map showing the locations of sampling sites of zones I, II, III and IV. The site mean declination obtained after structural correction for every site is marked by the arrow. It is apparent from the map that zone I directions (sites 1-5 & M) are similar to each other lying in the southeastern direction. These appear to be rotated with respect to the zone III directions (sites 15-20) which lie in the southwestern direction.

Summary of Zonal average directions before and after structural corrections is given in Table 4.2 and Table 4.3. It is apparent from the structurally corrected (pre-folding) Zone I mean direction (D=154, I=-35, k=13.0, α_{95} =19, N=6 sites) and Zone III mean direction (D=214, I=-43, k=16.0, α_{95} =32, N=3 sites) that

Figure 4.39: Map of the area showing the direction of mean declination at each sampling site in zone I, II, III and IV.

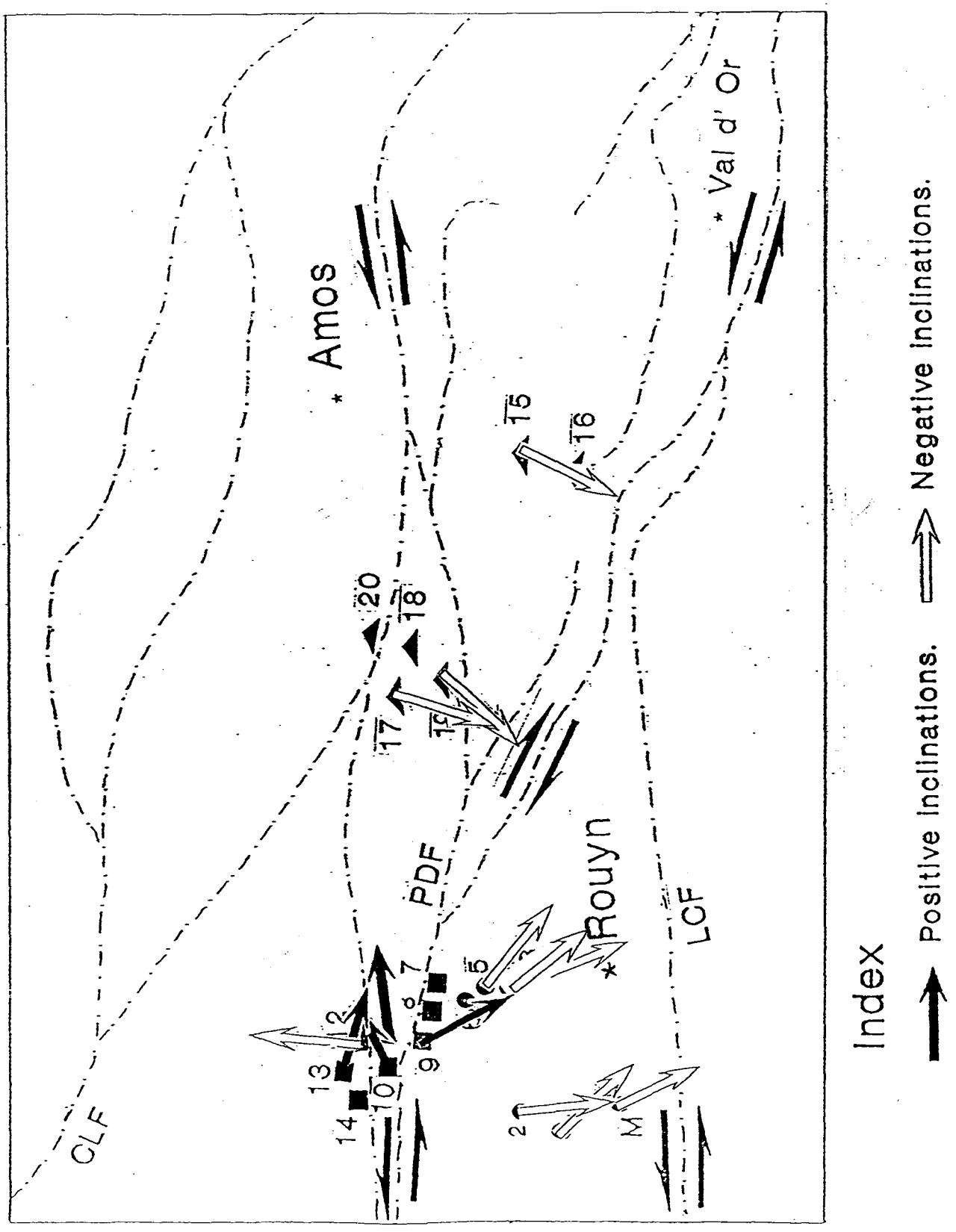
Amos
Val d' Or
Rouyn
CLF
PDF
LCF
20
18
17
15
16
5
7
2
13
14
10
9
Index
Positive Inclinations.
Negative Inclinations.

their inclinations and polarities are similar but their declinations are different. The difference between the zone I magnetization declination (154 $\pm$19°) and zone III declination (214 $\pm$32°) suggest that Rouyn-Noranda Block has rotated anti-clockwise about a vertical axis with respect to the adjacent block by approximately 60 $\pm$ 37°.

Chapter 5

DISCUSSION AND CONCLUSIONS

5.1 General Discussion

The specimens from Zone I and Zone III carry remanence which is reason-ably grouped at the sample, site and zonal levels. The specimens from Zone II carry dispersed remanences which do not agree at sample, site or zonal levels. The remanences from Zone IV specimens agree at sample and site levels but do not agree at zone level. The NRM intensities of most of the specimens are strong between 0.01 A/m and 10 A/m. The stabilities of the remanences fall in 3 categories low (MDF $<$ 10mT), medium (MDF = 10-40 mT), and high (MDF$>$ 40 mT).

Sites AB6, AB7, AB8, AB11, AB14, AB16, AB20 and AB22 which lie on the fault zones see figure 1.1 failed to yield site averages because their specimen directions were too dispersed to pass the criteria (explained in Chapter 4) set for

averaging.

Three different magnetizations were obtained from Zone I (D=197.0, I=-65.0, K=11, α_{95}=21.0, N=6 sites), Zone III (D=323.0, I=59.0, K=4, α_{95}=54.0, N=4 sites) and site AB23 in Zone IV (D=34.0, I=29.0, K=28, α_{95}=13.0, N=6 samples) before structural corrections. Zone II specimens show dispersed directions (D=66.0, I=47.0, K=2, α_{95}=—, N=4 sites). After structural corrections Zone I average direction becomes (D=154.0, I=-35.0, K=13, α_{95}=19.0, N=6 sites) and Zone III average direction becomes (D=214.0, I=-43.0, k=16, α_{95}=32.0, N=3 sites). The Zone I and Zone III directions show difference in declination of magnetization inside the Rouyn-Noranda block ($154^{+}_{-}19°$) and in the adjacent block ($214^{+}_{-}32$) suggesting that there have been a $60^{+}_{-}37°$ anti-clockwise rotation of the Rouyn-Noranda lozenge shaped block relative to the adjacent block.

Some improvement in the statistics of the Zone I mean direction after structural correction indicates that the magnetization in these rocks is pre-folding and may be Archean in age. This evidence is further strengthened by the fact that these directions are obtained from the relatively central and unstrained parts of the Abitibi greenstone belt and are present in different sampled lithologies i.e., Basalt, Gabbro and Diorite. The preservation of primary remanence in Abitibi belt have been reported earlier from Archean basalts far removed from any intrusions (Tassilo-Hirt et al., 1882 and Schutts & Dunlop, 1981), although their statistics too were not very good. Furthermore, in the present study the directions are stable, have high stability and agree reasonably well on sample and site and zonal level.

Zone II specimens show dispersed directions before and after structural corrections. The statistics (k=2, $\alpha_{95} > 50°$) of these directions before and after structural

corrections imply that they are randomly distributed.

Structurally corrected Site AB21 mean direction (D=200, I=-45, K=9, α_{95} =33) are similar to the zone III directions. Site AB23 specimens of Zone IV give a northeasterly direction (D=34, I=29, k=28, α_{95}=13) before structural correction which becomes (D=229, I=30, k=28, α_{95}=13) after structural correction. This direction is not obtained from any other site in the area and may be a locally acquired magnetization, probabily by lightening strike or by a local hydrothermal event .

Hubert et al, 1984 explained the evolution of Abitibi belt by wrench fault tectonics (Moody and Hill, 1956; Harland, 1971; Wilcox et al, 1973) model, summarized in figure 5.40. The diagram suggests that in response to the left lateral wrench fault movements between Larder Lake Cadillac fault and Porcupine Destor Faults the area has been deformed in several phases. Deformation D_1 produced by large scale movements along megashears caused stretching and shortening, deformation D_2 produced compression along Z axis (shown in figure 5.40) and resulted in the formation of reverse faults and later deformation D_3 produced a set of conjugate strike-slip faults. Hubert et al. proposed that SVZ represents allochthonous blocks of volcanic terranes that have been rotated, uplifted and eroded during wrench faulting. In a left lateral wrench zone the fault-bounded blocks are expected to rotate anti-clockwise (Wilcox et al, 1973). The apparent discrepancy between the palaeomagnetic declinations obtained from zone I and zone III specimens are consistent with this hypothesis and indicates an anti-clockwise rotation of Rouyn-Noranda block by 60 $\pm$37° relative to the adjacent blocks see figure 4.39.

The anti-clockwise rotation of Rouyn-Noranda block also suggests a right lateral

Figure 5.40: Wrench Fault Tectonics model for the evolution of southern volcanic zone (Abitibi subprovince) proposed by Hubert et al., 1984.

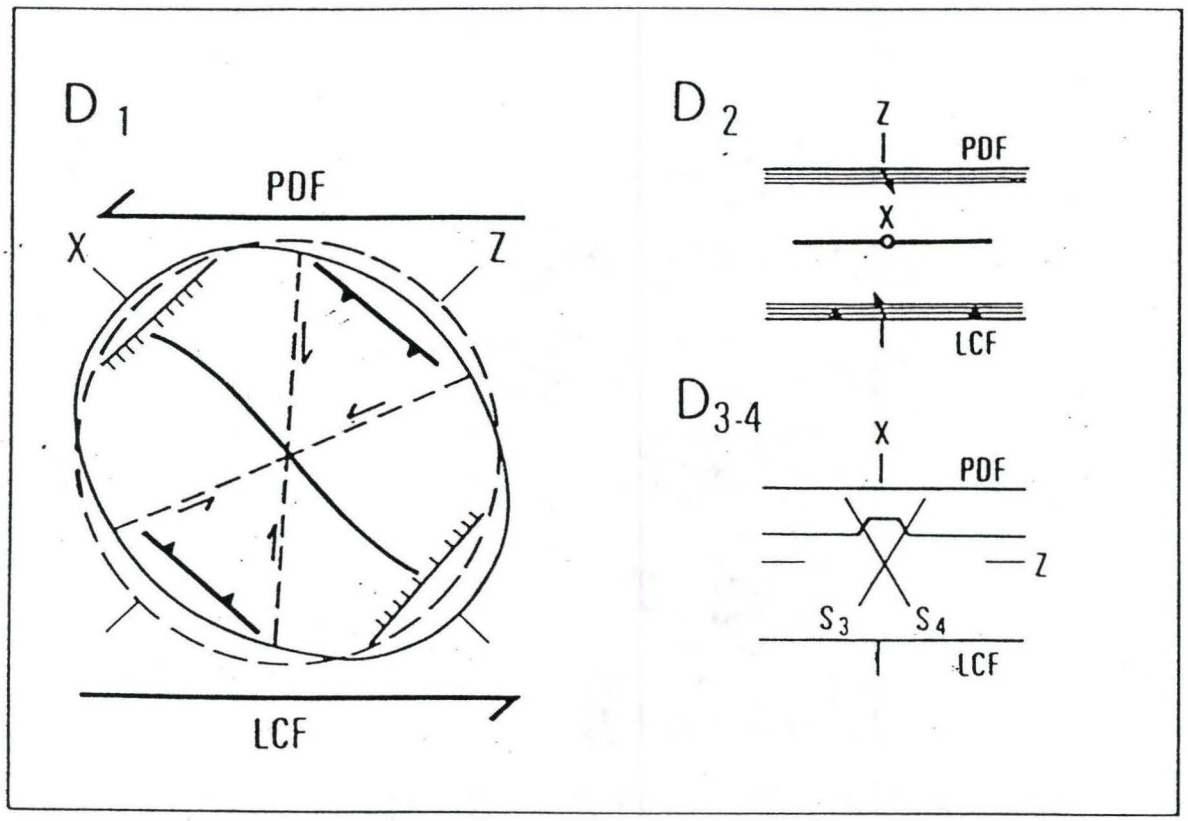
D 1
PDF
X
Z
LCF
D 2
Z
PDF
X
LCF
D3-4
X
PDF
Z
S3
S4
LCF

movement along the northwest-southeast trending faults that separate the lozenge shaped blocks in the area. This movement is in the opposite sense to that of the PDF and LCF zones.

The Archean basalt-gabbro direction obtained by Schutts and Dunlop, (1981) from western side of the present project area from the Kirkland Lake Matheson area in Ontario, (D=114.0, I=-32.0, K=15,α_{95}=11.0) differs both in declination and inclination from the characteristic direction of Rouyn-Noranda block (Zone I mean direction) but has the same polarity. The difference in declination (143-114) suggests a 29° anti- clockwise rotation of Kirkland area relative to the Rouyn-Noranda block and the difference in inclination (45-32) suggests a tilt of 13° . Earlier reported Archean gabbro (unbaked) direction (D=189.0, I=-23.0, α_{95} =17.0) and Archean lava direction (D=32.0, I=-87.0, α_{95}=6.0) by Irving and Naldrett (1977) and (D=190.0, I=-29.2, K=1.5, α_{95}=25.0) for Blake River Group by Tassilo-Hirt et al, (1982) also suggest that the declinations and inclinations in various parts of the Abitibi belt do not agree and may have been displaced relative to one another implying block rotations and tilting. However, there remains the possibility that these directions are acquired in different ages.

Since the magnetization directions in the Abitibi belt are rotated so the pole positions obtained from them are also displaced from their original positions. Therefore, the pole positions from the Abitibi belt can only be used to construct APWP for the local structural blocks and not for the North America.

5.2 Conclusions

1. Pre-folding probably Archean magnetization is preserved in the central, unstrained parts of the Abitibi Greenstone belt.
2. The remanences in the fault zones have been severely dispersed by the tectonism.
3. Declinations of primary magnetization obtained from Rouyn-Noranda structural block and the adjacent block differ by 60 $\pm$37°.
4. The discrepancy of declinations from the two adjacent zones is consistent with the "Allochthonous Collage" hypothesis proposed by Hubert et al. suggesting anti-clockwise rotation of Rouyn-Noranda block.

5.3 Suggestions For Further Work

1. The palaeomagnetic directions from the Abitibi belt are rotated/tilted along vertical/horizontal axis and their corresponding paleopoles would be displaced. Therefore the palaeopoles obtained from the Abitibi belt may not be used to make APWP for the North America.
2. The magnetization directions of samples collected near the shear zones are scattered whereas, the magnetization directions of samples collected from the unstrained parts are well grouped at sample, site and zonal level. Therefore, only the unstrained central parts of the Abitibi belt be used for paleomagnetic work.
3. Some improvement in the precision statistics shown by zone I specimens indicate that the Abitibi belt have undergone structural deformations and the

palaeomagnetic directions in the area have been folded. Therefore, detailed structural corrections are necessary to obtain the primary remanence from the Abitibi belt.

Bibliography

[1] Ade Hall, J. M., et al., 1971. "The magnetic and opaque mineralogical response of basalts to regional hydrothermal alteration." *Geophysical Journal of the Royal Astronomical Society*, 24, 137-174.

[2] Ambrose, J. W., 1941. "Clericy and La Pause map areas, Quebec." *Geological Survey of Canada*, Memoir 233.

[3] Babineau, J., 1983. "Region de LaMotte-Malartic." *Ministere de l'Energy et des Resources, Quebec:* DV 83-13, 41-42.

[4] Bannerman, H. M., 1939. "La partie centrale du canton de Destor, comte d' Abitibi." *Ministere des mines du Quebec, Quebec (Que.)*, rapport preliminaire 129.

[5] Bannerman, H. M., 1940. Region du lac Lepine, canton de Destor, comte Abitibi." *Ministere des mines du Quebec, Quebec (Que.)*, Rapport geologique 4.

[6] Beck, M. E., 1976. "Discordant paleomagnetic pole positions as evidence for regional shear in the western cordillera of North America." *American Journal*

Of Science, 276, 694.

[7] Boivin, P., 1974. "Petrographie, stratigraphie et structure de la ceinture de schistes verts" de Noranda dans les cantons de Hebecourt, de Duparquet et de Destor, Quebec, Canada. *These de doctorat, Departement des sciences exactes et naturelles de Universite de Clermont -Ferrand, Clermont, France*, 133p.

[8] Briden, J. C., 1965. "Ancient secondary magnetization in rocks."*Journal of Geophysical Research*, 70, 5205-5221.

[9] Collinson, D. W., 1965a. "Depositional remanent magnetization in sediments." *Journal of Geophysical Research*, 70, 4663-4668.

[10] Collinson, D. W., 1983. *Methods in Rock Magnetism and Palaeomagnetism. Techniques and instrumentation*, Chapman and Hall, New York, Publishers.

[11] Cox, A., 1961. "Anomalous remanent magnetization of basalt." *US Geological Survey Bulletin*, 1083-E, 131-160

[12] Dimroth et al., 1982. "Evolution of the south central part of the Archean Abitibi Belt, Quebec. Part I: Stratigraphy and Paleography model." *Canadian Journal of Earth Sciences*, 19, 1729-1758.

[13] Fisher, R. A., 1953. "Dispersion on a sphere." *Proc. R. Soc. London*, A217, 295-305.

[14] Freund, R., 1970. "Rotation of strike slip faults in Sistan, southeast Iran." *J. Geology*, 78, 188.

[15] Frith, R. A., Doig, R., 1975. "Pre-Kenoran tonalitic gneisses in the Grenville Province." *Canadian Journal of Earth Sciences*, 12, 844-849.

[16] Garfunkel, Z., 1974. "Model for the late Cenozoic history of the Mojave desert, California, and its relation to adjacent regions." *Geological Society of America Bulletin*, 85, 1931.

[17] Garfunkel, Z. V. I., Ron, H. I., 1985. "Block rotations and deformation by strike slip faults 2. The properties of a type of macroscopic discontineous deformation." *Journal of Geophysical Research*, 90, 8589-8602.

[18] Geissman, J. W. et al., 1982. "Paleomagnetism and structural history of the Ghost Range intrusive complex, central Abitibi Belt, Ontario: further evidence for the Late Archean geomagnetic field of North America." *Canadian Journal of Earth Sciences*, 19, 2085-2099.

[19] Gelinas, L., Ludden, J. N., 1984. "Rhyolitic volcanism and the geochemical evolution of an Archean central ring complex: the Blake River Group volcanics of the southern Abitibi belt, Superior Province." *Physics of the Earth and Planetary Science Interiors*, 35, 77-88.

[20] Goodwin, A. M., Ridler, R. H., 1970. "The Abitibi orogenic belt. In *Symposium on basins and geosynclines of the Canadian Shield*, A. J. Baer, ed, Geological Syrvey of Canada, paper 40-70, 1-28.

[21] Goulet, N., 1978. "Stratigraphy and structural relationships across the Cadillac -Larder lake Fault, Rouyn-Beauchastel area, Quebec. *Ministere des Richesses Naturelles du Quebec*, DP 602, 141 pp.

[22] Graham, J. W., 1949. "The stability and significance of magnetism in sedimentary rocks." *Journal of Geophysical Research*, 54, 131-167.

[23] Graham, R. B., 1954. "Parties des cantons d'Hebecourt, de duparquet et de Destor, comte d' Abitibi-Quest. *Ministere des mines du Quebec, Quebec (Que.)*, Rapport geologique 61.

[24] Griffith et. al., 1960. "The remanent magnetization of some recent varved sediments." *Proc. R. soc. London*, A256, 359-383.

[25] Gunning, H. C., 1937. "Cadillac area, Quebec." *Geological Survey of Canada*, Memoir 206, 80 p.

[26] Gunning, H. C., 1941. "Bousquet-Joannes area Quebec." *Geological Survey od Canada*, Memoir 231, 110 p.

[27] Hale, C. J., Lloyd, P., 1989. "Paleomagnetic analysis of regional and contact strains." Ontario Geoscience Research Fund Grant 342, OGRF Summary of Research, *Ontario Geological Survey Miscellaneous Paper*, 342, 199-209.

[28] Harland, W. B. 1971. "Tectonic transpression in Caledonian Spitzbhergen." *Geological Magazine*, 108, 27-42.

[29] Hubert, C. et al., 1984. "Archean wrench fault tectonics and structural evolution of the Blake River Group, Abitibi Belt, Quebec." *Canadian Journal of Earth Science*, 21, 1024-1032.

[30] Irving, E, Major, A., 1964. "Post-depositional detrital remanent magnetization in a synthetic sediment." *Sedimentology*, 3, 135-143.

[31] Irving, E., Opdyke, N. D., 1965. "The paleomagnetism of the Bloomsburg redbeds and its possible application to the tectonic history of the Appalachians." *Geophys. J. R. Astron. Soc.*, 9, 153-167.

[32] Irving, E., Naldrett, A. J., 1977. "Paleomagnetism in the Abitibi Greenstone Belt, and Abitibi and Metachewan diabase dikes: evidence of the Archean geomagnetic field." *Journal of Geology*, 85, 157-176.

[33] Irving, E., 1979. "Paleopoles and paleolatitudes of North America and speculations about displaced terrains." *Canadian Journal of Earth Sciences*, 16, 669-694.

[34] Jensen, L. S., 1975a. "Geology of Clifford and Ben Nevis Townships, District of Cochrane. *Ontario Department of Mines, Geological Report 132*, 55p.

[35] Jensen, L. S., 1975b. "Geology of Pontiac and Ossian Townships, District of Timiskaming.*Ontario Department of Mines, Geological Report 125*, 40p.

[36] Jensen, L. S., 1978a. "Geology of Thackeray and Elliott, Tannahill, and Dokis Townships, District of Cochrane, *Ontario Department of Mines, Geoscience Report 165*, 71p.

[37] Jensen, L. S., 1978b. "Archean Komatiitic and tholeiitic, calc-alkalic, and alkalic volcanic sequences in the Kirkland Lake area." *Toronto '78 Field Trip Guidebook.* A. L. Currie, W. O. Mackasey, eds.,. Geological Society of America-Geological Association of Canada, Toronto, Ontario. pp 361.

[38] Jolly, W. T., 1978. "Metamorphic history of the Archean Abitibi belt." In

metamorphism in the Canadian Shield. I. A. Fraser and W. W. Heyward), eds., *Geological Survey of Canada*, paper 16, 63-78.

[39] Jolly, W. T., 1974. "Regional metamorphic zonation as an aid in the study of Archean terrains: Abitibi region, Ontario. *Canadian Mineralogist*, 12, 499-508.

[40] Jolly, W. T., 1977. "Metamorphic history of the Archean Abitibi Belt: sample distribution and partial metamorphic zoning." In Report of activities, part A. *Geological survey of Canada*, paper 77-1A, 191-196.

[41] Kamerling, M. J., Luyendyk, B. P., 1979. "Tectonic rotation of the Santa Monica Mountains region, western Transverse Ranges, California, suggested by Paleomagnetic vectors." *Geological Society of America Bulletin*, 90, 331.

[42] Kobayashi, K., 1959. "Chemical remanent magnetization of ferromagnetic minerals and its application to rock magnetism." *J. Geomagn. Geoelectr.*, 10, 99-117.

[43] Kirschvink, J. L., 1980. "The least square line and plane and the analysis of paleomagnetic data." *Geophysical Journal of the Royal Astronomical Society*, 62, 699-718.

[44] Lamb, S. H., 1988. "Tectonic rotations about vertical axes during the last 4 Ma in part of the New Zealand plate boundary zone." *Journal of Structural Geology*, 10. No.8, 875-893.

[45] Larson, E. D., Walker, T. R., 1975. "development of chemical remanent magnetization during early stages of red-bed formation in Late Cenozoic sediments, Baja, California." *Geol. Soc. Am. Bull.*, 86, 639-650.

[46] Larson, E. et al., 1969. "Stability of remanent magnetization of igneous rocks." *Geophysical Journal of the Royal Astronomical Society*, 17, 263-292.

[47] Ludden, J. et al., 1986. "The tectonic evolution of the Abitibi greenstone belt of Canada." *Geological Magazine*, 123(2), 153-166.

[48] Luyendyk, B. P. et al., 1980. "Geometric model for Neogene crustal rotations in southern California." *Bulletin, Geological Society of America*, 91, 211-217.

[49] Martignole, J., 1984. "Some questions about Proterozoic crustal thickening: the case of the Grenville Province." *Geological Association of Canada/Mining Association of Canada Abstracts*, 9, 87.

[50] McElhinny, M. W., 1973. *Palaeomagnetism and Plate Tectonics*, Cambridge Press.

[51] McKenzie, D. P., Jackson, J. A., 1983. "The relationship between strain rates, crustal thickening, palaeomagnetism. finite strain and fault movments within a deforming zone." *Earth and Planetary Science Letters*, 65, 182 - 202.

[52] McKenzie, D. P., Jackson, J. A., 1986. "A block model of distributed deformation by faulting." *Journal of Geophysical Society of London*, 143, 349-353.

[53] McKenzie, D. P., Jackson, J. A., 1989. "The Kinematics and Dynamics of distributed deformation." *Palaeomagnetic rotations and continental deformation*, Kluwer Academic Publishers, pp 17-31.

[54] Moody, J. D., Hill, M. J., 1956. "Wrench fault tectonics." *Bulletin, Geological Society of America*, 67, 1207-1246.

[55] Nagata, T, 1961. *Rock Magnetism*, Maruzen Tokyo.

[56] Nagata, T., Kobayashi, K., 1963). "Thermochemical remanence of rocks." *Nature*, 197, 476-477.

[57] Neel, L., (1955). "Some theoretical aspects of rock magnetism." *Adv. Physics*, 4, 191-243.

[58] Nunes, P. D., Jensen, L. S., 1980. "Geochronology of the Abitibi metavolcanic belt, Timmins-Matachewan area progress report." Summary of geochronological studies 1977-1979. E. G. Pye, ed., *Ontario Geological Survey, miscellaneous paper*, 92, 40-45.

[59] O'Reilly, W., 1976). "Magnetic minerals in the crust of the earth." *Rep. Prog. Phys.*, 39, 857-908.

[60] O'Reilly, W., 1967. "The mechanism of oxidation in titano-magnetites: A magnetic study." *Mineral Magazine*, 36, 29-37.

[61] Pesonen, L. J., 1973. "The magnetic properties and paleomagnetism of some Archean volcanic rocks from the Kirkland Lake area." *M.Sc. Thesis, University of Toronto, Toronto, Ontario*, 134p.

[62] Piper, J. D. A., 1987. "Palaeomagnetism and the continental crust." John Wiley & Sons Inc., eds., NewYork, 101.

[63] Pitcher, W. S., 1983. "Granite type and tectonis environment. In *Mountain Building Processes*, K. J Hsu, ed, pp 19-40, Academic Press.

[64] Pullaiah, G., Irving, E., 1975. "Paleomagnetism of the contact aureole and late dikes of the Otto Stock, Ontario, and its application to early Proterozoic Apparent Polar Wandering." *Canadian Journal of Earth Sciences*, vol. 12, 1609-1618.

[65] Purucker, M. E., 1974. "Magnetic record of lightening strikes in sandstone." *Trans. Am. Geophys. Union* (abstract), 55, 1112.

[66] Ron, H. et al., 1984. "Block rotations by strike slip faulting, structural and palaeomagnetic evidence." *Journal of Geophysical Research*, 89, 6259 - 6270.

[67] Schutts, L. D., Dunlop, D. J., 1981. "Proterozoic magnetic overprinting of Archean rocks in the Canadian Superior Province." *Nature*, 291, 642-645.

[68] Stacey, F. D., 1962. "A generalized theory of thermo-remanence, covering the transition from single domain to multidomain grains." *Philos. Mag.*, 7, 1887-1900.

[69] Stacey, F. D., 1963. "The physical theory of rock magnetism," *Adv. Phys.*, 12, 45-133.

[70] Tassilo-Hirt, A. M. et al., 1982. "Paleomagnetism of late Archean metavolcanics and metasediments, Abitibi orogen, Canada: volcanics of the Blake River Group and sediments and volcanics of the Timiskaming Group." *Canadian Journal of Earth Sciences*, 19, 2100-2113.

[71] Trudel, P., 1979. "Le volcanisme archeen et la geologie structurale de la region de Clericy, Abitibi, Quebec. *These de Ph.D., Departement de genie mineral, Ecole Polytechnique, Montreal (Que.)*, 307p

[72] Verhoogen, J., 1959. "The origin of thermoremanent magnetization." *J. Geophys. Res.*, 64, 2441-2449.

[73] Watkins, N.D., Haggerty S. E., 1967. "Primary oxidation variation in a single lava." *Contributions to Mineralogy, Petrology*, 15, 251-271.

[74] Wilcox, R. E. et al., 1973. "Basic wrench tectonics." *American Association of Petroleum Geologists Bulletin*, 57, No. 9, 74-96.

[75] Wilson, M. E., 1962. "Rouyn-Beauchastel map area, Quebec. *Geological Survey of Canada*, Memoir 315.

[76] Zijderveld, J. D. A., 1967. "A. C. Demagnetization in rocks: Analysis of results." *Methods in paleomagnetism.* D. W. Collinson, K. M. Creer and S. K. Runcorn, eds., New York, Elsevier, 254-286.